Title
Architecture and Biogenesis of the Human Telomerase Holoenzyme

Author
Egan, Emily Denise

Publication Date
2012

Peer reviewed|Thesis/dissertation

Architecture and Biogenesis of the Human Telomerase Holoenzyme

by

Emily Denise Egan

A dissertation submitted in partial satisfaction of the

requirements for the degree of

Doctor of Philosophy

in

Molecular and Cell Biology

in the

Graduate Division

of the

University of California, Berkeley

Committee in charge:

Professor Kathleen Collins, Chair
Professor Karsten Weis
Associate Professor Jamie Cate
Assistant Professor Britt Glaunsinger
Professor Eva Harris

Spring 2012

ABSTRACT

Architecture and Biogenesis of the Human Telomerase Holoenzyme

by

Emily Denise Egan

Doctor of Philosophy in Molecular and Cell Biology

University of California, Berkeley

Professor Kathleen Collins, Chair

Telomerase adds simple sequence repeats to the ends of linear chromosomes to counteract the loss of end sequence inherent in conventional DNA replication. Telomerase is a ribonucleoprotein (RNP) whose catalytic activity arises from the cooperation of the telomerase reverse transcriptase protein (TERT) and the telomerase RNA (TER), which provides an integrated template for DNA repeat addition. TERs vary widely in sequence and structure but share a set of motifs required for TERT binding and catalytic activity. Species-specific TER motifs play essential roles in RNP biogenesis, stability, trafficking, and regulation. Human TER, or hTR, contains a motif shared with a large family of H/ACA RNAs that directs a pathway of RNP maturation.

I have investigated the RNA and RNP architecture of the hTR H/ACA domain and defined the sequence and structural elements required for RNA accumulation and RNP assembly. I have shown that, like other eukaryotic H/ACA RNAs, hTR recruits two sets of H/ACA core proteins despite a noncanonical spacing of conserved elements in its 5' H/ACA hairpin (Chapter Two). I have found that an hTR-specific BIO box motif within the 3' H/ACA loop stimulates H/ACA core RNP assembly in a manner required for hTR accumulation *in vivo* (Chapter Three). Finally, I have generated stable cell lines expressing tagged hTR and TERT to enable RNA-based and protein-based affinity purification of telomerase complexes in order to identify hTR-interacting factors and investigate telomerase multimerization (Chapter Four).

ACKNOWLEDGMENTS

Thank you to everyone who supported me during my graduate school career and made this thesis possible. I am immensely grateful to my advisor Kathleen Collins. Kathy's passion for science and her strong commitment to her students are just two of the many qualities that make her an excellent mentor. Her constant encouragement and enthusiasm inspired me to persevere and helped me to become a more confident public speaker.

I greatly appreciate the suggestions and guidance I received over the years from my thesis committee members Karsten Weis, Jamie Cate, and Britt Glaunsinger. I would also like to express my gratitude to them and to Eva Harris for their comments on this dissertation.

I have been fortunate to work with a group of talented people who have made the Collins lab an exciting and fun place to do science. Tim Errington was a patient teacher who expertly trained me during my rotation and first year. Kristin Talsky joined the lab at the same time, and I enjoyed sharing graduate school milestones and BART rides with her. Kyungah Hong has been a great asset to the lab, and I especially appreciate her efforts to keep things organized. Thanks to George Katibah and Kasper Andersen for helpful discussions and for making the RNA meeting in Japan an unforgettable experience. I would like to acknowledge Alec Sexton and Alex Wu for offering valuable scientific insights and for generously sharing reagents. In addition, I will miss their sarcastic sense of humor and unique taste in music. I also wish the best of luck to the newest members of the human telomerase team, Jacob Vogan and Dan Youmans. Finally, Bosun Min, Barbara Eckert, and Mary Couvillion have been excellent labmates and friends, offering advice on both scientific and personal matters. I could always rely on Bosun to listen when I needed to vent, and I am glad we stayed in touch after she left the lab. Barbara is the best baymate ever. She has been a great source of information, and she is one of the most caring people I have ever met. Fortunately, I do not have to say goodbye to Mary as we both move on to postdoctoral positions in Boston. I look forward to sharing the ups and downs of the coming years, and I know I will be able to count on her for ideas and feedback on my work.

Finally, I am thankful for the unwavering support of my husband and family. Even when I came home late or worked through the weekend, Colin was there for me, often with a bowl of pasta, whenever I needed him. My parents have always encouraged me, and I credit them with instilling a love of learning that has stayed with me through the years.

TABLE OF CONTENTS

CHAPTER ONE

Biogenesis of Telomerase Ribonucleoproteins

Telomerase and telomeres

The evolution of linear chromosomes in the common ancestor of eukaryotes occurred despite several challenges posed by this mode of genome organization. First, conventional primer-requiring DNA polymerases cannot copy the 3' end of a DNA template. Removal of the last RNA primer during lagging strand synthesis leads to the progressive loss of end sequence with every round of DNA replication. Second, chromosome ends resemble double-stranded DNA breaks whose recognition and repair results in chromosome fusions. Third, DNA ends are vulnerable to the destructive action of exonucleases. The solution to these challenges was to form telomeres, protective cap structures composed of repetitive DNA whose length varies from tens to thousands of base pairs. Telomeric DNA termini typically have a 3' overhang, which can invade the duplex to form a loop that sequesters the end. Single-stranded and double-stranded DNA-binding proteins coat the telomeric DNA to stabilize this structure, preserving genomic integrity (Gilson and Geli, 2007).

Telomere maintenance in most eukaryotes depends on new repeat synthesis by the specialized reverse transcriptase (RT) telomerase. Telomerase is a ribonucleoprotein (RNP) enzyme with two evolutionarily conserved subunits: the telomerase reverse transcriptase protein (TERT) and the telomerase RNA (TER), which contains an internal template that is reiteratively copied into DNA repeats. Many telomerase enzymes are capable of maintaining interaction with the DNA product during synthesis across the entire template (nucleotide addition processivity, NAP) and during multiple rounds of template copying (repeat addition processivity, RAP) (Collins, 2009). While nearly universal, a few lineages have lost telomerase and instead maintain telomeres using recombination- or transposition-based mechanisms (Biessmann and Mason, 1997; Pardue and DeBaryshe, 2011).

TERTs and the evolutionarily related retrotransposon RTs share active site motifs (Lingner et al., 1997b; Nakamura et al., 1997). In general, TERTs contain four domains: the telomerase essential N-terminal (TEN) domain, the telomerase RNA-binding domain (TRBD), the RT domain, and the C-terminal extension (CTE) (Blackburn and Collins, 2011). The TEN domain contacts single-stranded telomeric DNA and also interacts with TER. The ability of the TEN domain to bind DNA likely promotes processive telomerase activity by maintaining association with the product (Jacobs et al., 2006; Robart and Collins, 2011). The TRBD confers the specificity of interaction between TERT and TER. The RT domain active site includes the critical aspartic acid residues that coordinate magnesium ions necessary for deoxynucleotide triphosphate activation. The RT domain may also contribute to proper alignment of DNA in the active site. The C-terminal extension (CTE) contributes to processive telomerase activity in some systems (Autexier and Lue, 2006; Wyatt et al., 2010). A crystal structure of a putative TERT from the flour beetle *Tribolium castaneum*, which lacks a TEN domain, revealed that the CTE contacts the TRBD, forming a ring around a synthetic RNA-DNA hybrid (Gillis et al., 2008; Mitchell et al., 2010). It is possible that the CTE promotes processive elongation by closing this ring around the primer-template hybrid.

TERs vary greatly in their overall fold with disparate sequences and sizes ranging from

~150 nucleotides (nt) in ciliates to over 1,500 nt in some yeasts. However, several TER secondary structure elements are shared between ciliates, yeasts, and vertebrates. First is the single-stranded template, whose complement typically corresponds to 1-1.5 repeats of the telomeric DNA sequence. The 3' region of the template aligns the DNA substrate, while the 5' portion is copied. Second, a pseudoknot motif occurs adjacent to the template, with both enclosed within a domain formed by long-range base pairing of sequence at or near the 5' end. The pseudoknot is stabilized by triple-helix formation (Shefer et al., 2007; Theimer et al., 2005; Ulyanov et al., 2007). Some mutations in the pseudoknot reduce TERT binding and/or telomerase catalytic activity. However, despite its conservation, the specific function of the pseudoknot in any system remains an outstanding question. Third, a stem or hairpin 5' of the template serves as a template boundary element (TBE). The TBE acts as a steric block and/or imposes structural strain to prevent copying of non-template TER sequence into telomeric DNA. Finally, a distal stem terminus element (STE) comprising either a terminal hairpin, a hairpin within a three-way junction, or a three-way junction alone, serves to stimulate telomerase activity by providing an interaction site for the TERT TRBD. Some STE mutations reduce activity without greatly affecting TERT binding, suggesting a possible allosteric contribution such as the orientation of TERT domains during RNP assembly (Blackburn and Collins, 2011).

Cellular telomerase holoenzymes are large multisubunit complexes with a mass of 500 kiloDaltons (kDa) or more (Collins, 1999; Lingner et al., 1997a; Schnapp et al., 1998). While TERT and TER alone are capable of reconstituting telomerase catalytic activity on oligodeoxynucleotide substrates *in vitro*, many additional factors are required for telomere elongation *in vivo* (Autexier and Lue, 2006). In addition to conserved elements required for TERT binding and activity, TERs possess motifs that recruit proteins involved in RNA processing, stability, and localization. Several factors also regulate the assembly of TER and TERT and modulate telomerase catalytic activity. Finally, both telomerase- and telomere-associated factors contribute to the recruitment of the RNP to chromosome ends (Blackburn and Collins, 2011). Although the identities of telomerase holoenzyme proteins and the exact mechanisms of their functions differ between organisms, some of their biochemical roles and strategies bear striking similarities across phylogenetic groups.

In single-celled ciliates and yeasts, telomerase is essential for long-term viability, and accordingly, telomerase components are constitutively expressed. Telomere extension occurs during each cell cycle, with preferential elongation of the shortest telomeres ensuring telomere length homeostasis (Hug and Lingner, 2006). However, in multicellular organisms, the expression of some telomerase holoenzyme components and the assembly of the complex is highly restricted. In humans, telomerase activity is undetectable in most adult somatic cells except for subsets of highly proliferative hematopoietic and epithelial cells. In the absence of sufficient telomerase activity, telomeres shorten with each round of DNA replication, eventually triggering proliferative senescence or apoptosis. This process may contribute to aging phenotypes, but the restriction of telomerase activity likely serves a critical tumor suppression function. Reactivation of telomerase occurs in over 85% of human cancers, enabling the continued proliferation of tumor cells. Therefore, studies of telomerase biogenesis and regulation have potential medical applications since telomerase inhibition is an attractive therapeutic strategy (Shay and Wright, 2010).

This chapter aims to describe the shared and unique features of telomerase RNPs from ciliates, yeasts, and vertebrates, with an emphasis on pathways of telomerase RNA biogenesis and RNP assembly. Telomerase physical recruitment to, elongation of, and regulation at

telomeres involve DNA and protein dynamics that have been reviewed extensively elsewhere (Linger and Price, 2009; Palm and de Lange, 2008). Most of the work described has utilized *Tetrahymena thermophila*, *Saccharomyces cerevisiae*, *Saccharomyces pombe*, or cultured human cells. Less intensively studied, but important additional model systems include other ciliates (Collins, 1999), yeasts (Teixeira and Gilson, 2005; Yu, 2011), and vertebrates (Blasco, 2005), and also plants (Riha and Shippen, 2003).

Ciliate telomerase

Ciliate telomerase RNA structure

Ciliate TERs are the smallest to be characterized to date. The model laboratory ciliate, *Tetrahymena thermophila*, possesses a 159-nt TER (Greider and Blackburn, 1989) that includes all of the conserved motifs summarized above. The 9-nt template is positioned between a 5' TBE and a 3' pseudoknot. These motifs are enclosed by long-range base pairing of stem I. In addition to defining the template boundary, the TBE and its flanking single-stranded region provide the high-affinity TERT binding site (Autexier and Greider, 1995; Lai et al., 2002). Some mutations in the pseudoknot affect catalytic activity and telomere length maintenance, but contrary to early models suggesting conformational dynamics, a recent single-molecule fluorescence resonance energy transfer (FRET) study found that the pseudoknot is stably folded throughout the catalytic cycle (Cunningham and Collins, 2005; Gilley and Blackburn, 1999; Mihalusova et al., 2011). The STE caps terminal stem IV. Some nucleotides of loop IV contribute to TERT binding in a manner important for RNP stability, dependent on a conformational change in central stem IV (Robart et al., 2010; Stone et al., 2007). *T. thermophila* TER also includes an additional motif immediately 3' of the template termed the template recognition element (TRE) that contributes to efficient copying across the template (Cunningham and Collins, 2005; Miller and Collins, 2002).

Ciliate telomerase RNP maturation and TERT-TER assembly

T. thermophila TER is transcribed by RNA polymerase III and retains the primary transcript 3' uridine-rich termination sequence (Greider and Blackburn, 1989). This 3' tail, together with stems I and IV, form the binding site for the telomerase-specific protein p65 (O'Connor and Collins, 2006; Witkin and Collins, 2004). This La-family protein is required for TERT and TER accumulation *in vivo* as an integral subunit of the telomerase holoenzyme catalytic core. Its interaction with TER stabilizes a kink in stem IV necessary for TERT binding (Stone et al., 2007). Binding of p65 also induces additional conformational changes in stem-loop IV and beyond that promote TERT assembly and catalytic activity (Akiyama et al., 2012; Berman et al., 2010; Prathapam et al., 2005; Richards et al., 2006).

Bridging the ciliate RNP catalytic core to telomere substrates

The *T. thermophila* telomerase holoenzyme has been purified to homogeneity, enabling extensive subunit characterization. Beyond the RNP catalytic core, five associated proteins, designated p19, p45, p50, p75, and Teb1 are required for telomere maintenance *in vivo* (Min and Collins, 2009; Witkin and Collins, 2004). Four of these five proteins (p19, p45, p50, and p75) purify enzyme activity with and without high RAP. In contrast, Teb1 preferentially enriches high RAP activity (Min and Collins, 2009). Teb1 has an oligonucleotide/oligosaccharide (OB) fold architecture homologous to the large subunit of

Replication Protein A (RPA). However, Teb1 specifically recognizes telomeric repeats and is telomerase-specific. Biochemical and physical assays suggest that Teb1 association with the RNP catalytic core requires other holoenzyme proteins, which can thus be considered a telomere adaptor subcomplex (TASC) (Min and Collins, 2009). The mechanism of Teb1 stimulation of RAP may involve its ability to suppress folding of nascent product DNA and its protein-protein interactions with TASC that could influence the conformation of the catalytic core (Min and Collins, 2009, 2010).

Yeast telomerase

Yeast telomerase RNA structure

Telomerase RNAs from yeasts are relatively large (over 1000 nt) with a core containing the template, TBE, and pseudoknot enclosed by long-range base pairing of stem I. In the *S. cerevisiae* TER, TLC1, the high-affinity binding site for the TERT protein, Est2p, is within this core (Livengood et al., 2002). Most of the yeast TER length derives from three long stems, or "arms," extending from the core. One of these arms occurs 5' of the template and serves as a TBE (Box et al., 2008b; Seto et al., 2003; Tzfati et al., 2000). In addition, in *Saccharomyces*, but not other yeasts, the terminal stem-loop of this arm forms a binding site for the Ku70/80 heterodimer, which is required for TLC1 accumulation and for telomerase nuclear localization and telomere recruitment (Fisher et al., 2004; Gallardo et al., 2008; Stellwagen et al., 2003). The second arm occurs between the template and the pseudoknot and contains a binding site for the regulatory protein Est1p, which is involved in recruiting another telomerase subunit, Est3p, and in targeting the enzyme to telomeres (Osterhage et al., 2006; Qi and Zakian, 2000; Seto et al., 2002).

The third TLC1 arm is the extremely long stem I, which is further extended by folding back of the 3' end. The 3' terminal hairpin contains the STE, a three-way junction motif that stimulates telomerase catalytic activity and may contact TERT in *Kluyveromyces lactis* and likely other yeasts (Brown et al., 2007). A single-stranded uridine-rich motif near the 3' end binds to Sm proteins, which contribute to the maturation and stability of the RNA (Seto et al., 1999; Tang et al., 2012). Studies of TLC1 have demonstrated that the RNA arms can be truncated substantially and still support activity *in vitro* and prevent senescence *in vivo*, suggesting that the RNA functions as a flexible scaffold for protein assembly (Zappulla et al., 2005). However, the truncated TLC1 accumulates to levels much lower than wild-type, maintains short telomeres, and confers reduced fitness (Zappulla et al., 2005).

Studies of yeast TERs have attempted to define the function of the pseudoknot. In *K. lactis* TER, some pseudoknot mutations prevent copying of the full template (Tzfati et al., 2003). Another study used fragments of TLC1 assembled with Est2p in rabbit reticulocyte lysate to determine that disruption of the pseudoknot triple helix reduces telomerase activity but not Est2p binding (Qiao and Cech, 2008). Crosslinking identified contacts between nucleotides in the triple helix and the 3' end of a DNA primer, suggesting a possible role for the pseudoknot in substrate DNA positioning (Qiao and Cech, 2008).

Yeast telomerase RNP maturation and TERT-TER assembly

Studies of telomerase biogenesis in yeast have focused predominantly on *S. cerevisiae* TLC1 and *S. pombe* TER1. Both are independently transcribed by RNA polymerase II and accumulate primarily as unpolyadenylated species with a minor fraction (~5-10%) occurring in a

polydenylated form (Chapon et al., 1997; Leonardi et al., 2008). The unpolyadenylated form is bound by TERT (Bosoy et al., 2003; Leonardi et al., 2008). However, the processing pathways that generate mature TLC1 and TER1 differ.

While previously suggested to be a precursor, recent data suggests that the polyadenylated form of TLC1 is not required for the accumulation of the unpolyadenylated mature form (Noel et al., 2012). The 3' end of the functional TLC1 transcript is produced by the Nrd1-Nab3-Sen1 pathway, which also processes the transcripts of small nuclear (sn) and small nucleolar (sno) RNAs in yeast (Noel et al., 2012). In this pathway, specific patterns of RNA polymerase II C-terminal domain phosphorylation recruit the RNA-binding proteins Nrd1p and Nab3p, which recognize sequences downstream of the mature RNA 3' end. These proteins also interact with Sen1p, an RNA and DNA helicase, which is thought to terminate transcription by unwinding the RNA-DNA hybrid in the RNA polymerase active site (Kuehner et al., 2011).

In the case of *S. pombe* TER1, the polyadenylated form does appear to serve as a precursor that is processed by a surprising mechanism involving the uncoupling of spliceosomal cleavage and exon ligation (Box et al., 2008a). An intron between the mature 3' end and the polyA site is recognized by the spliceosome, and cleavage occurs at the 5' splice site to generate the TER1 3' end. However, the mature RNA escapes ligation to the downstream exon, an outcome potentially favored by a weak 3' splice site sequence and a long distance between this site and the branch point (Box et al., 2008a). The same mechanism may generate the 3' ends of *Candida* TERs which exhibit a similar conservation of 5' splice site and branch point sequences (Gunisova et al., 2009).

TLC1 and TER1, like snRNAs, assemble with Sm proteins and acquire a 2,2,7-trimethylguanosine (TMG) cap (Leonardi et al., 2008; Seto et al., 1999). The Sm proteins (SmB, SmD, SmD2, SmD3, SmE, SmF, and SmG) form a heteroheptameric ring that binds to single-stranded uridine-rich regions in snRNAs and at the 3' ends of TLC1 and TER1, promoting their accumulation (Seto et al., 1999; Tang et al., 2012). *Kluyveromyces* and *Candida* TERs conserve this sequence element and are likely to also bind these proteins (Gunisova et al., 2009). Sm protein assembly promotes cap hypermethylation via a protein-protein interaction with the cap hypermethyltransferase Tgs1p (Mouaikel et al., 2002; Tang et al., 2012). In *S. cerevisiae*, Est2p binds to TLC1 after Sm protein association (Seto et al., 1999). In *S. pombe*, the Sm ring on TER1 is replaced by a related Lsm2-8 complex that promotes the association of the TERT protein, Trt1p, and protects the 3' end from exonuclease activity (Tang et al., 2012).

Studies of yeast TER trafficking have primarily focused on *S. cerevisiae* TLC1. TLC1 cap hypermethylation occurs in the nucleolus (Mouaikel et al., 2002; Seto et al., 1999). TMG-capped TLC1 is then exported to the cytoplasm via the Crm1 export complex and is later reimported via Mtr10p and/or Kap122p importins (Ferrezuelo et al., 2002; Gallardo et al., 2008). The findings that all three Est proteins are required for endogenous TLC1 nuclear localization and that overexpressed Est1p and Est2p localize to the nucleus suggests the possibility that these proteins bind TLC1 in the cytoplasm and facilitate its nuclear reentry as an assembled RNP (Gallardo et al., 2008; Teixeira et al., 2002). However, unlike in ciliates, the stability of yeast TERs does not require TERT. Nuclear retention of TLC1 also depends on its recruitment to telomeres, discussed in detail below (Gallardo et al., 2008).

Bridging the yeast RNP catalytic core to telomere substrates

S. cerevisiae Est1p and Est3p are required for telomere elongation *in vivo* but not for RNP catalytic core activity on DNA oligonucleotides *in vitro* (Lingner et al., 1997a). It was thus

proposed that these proteins play a role in telomere recruitment or facilitate Est2p activity on its native substrates. Est1p interacts with TLC1 and the G-strand overhang binding protein Cdc13p , which alternately forms a telomere-associated RPA-like complex called CST with Stn1p and Ten1p (Gao et al., 2007; Seto et al., 2002). Interaction between Est1p and Cdc13p suggests that Est1p could bridge telomerase and the chromosome end (Qi and Zakian, 2000). Consistent with that hypothesis, a Cdc13p-Est2p fusion protein can maintain telomeres in the absence of Est1p (Evans and Lundblad, 1999). Later studies complicated this simple recruitment model. First, Est2p is detected at telomeres by chromatin immunoprecipitation (ChIP) dependent on TLC1 throughout the cell cycle (Taggart et al., 2002). In contrast, Est1p is not detected at the telomere during G1, when its levels are low due to protein degradation involving the proteasome (Osterhage et al., 2006; Taggart et al., 2002). These findings led to a model in which the *S. cerevisiae* telomerase RNP catalytic core is physically recruited to the telomere prior to its activation for telomere elongation by events including Est1p assembly. The nature of the activation by Est1p is unclear but could involve its recruitment of Est3p, which has been demonstrated in *C. albicans* and *S. cerevisiae* (Hsu et al., 2007; Osterhage et al., 2006). Recently, it was shown that Est3p binds to the TEN domain of Est2p *in vivo*, and recombinant Est3p stimulates telomerase catalytic activity *in vitro* when added to telomerase complexes partially purified from *S. cerevisiae* cells (Talley et al., 2011). Study of Est3p orthologs in other yeasts found that interaction with the TEN domain permitted crosslinking to telomeric DNA, suggesting that TEN interaction unmasks a DNA binding activity (Yen et al., 2011).

The Ku70/80 heterodimer is best known for its role in the recognition and repair of double-stranded DNA breaks. Interestingly, Ku is also detected at non-fusing telomeres in *S. cerevisiae* (Gravel et al., 1998). ChIP studies have found that Ku is required for telomerase recruitment to telomeres during G1, and some models suggest Ku acts as a bridge by binding TLC1 and telomeric DNA simultaneously (Fisher et al., 2004). However, recent work has revealed that Ku binds DNA and RNA in a mutually exclusive manner (Pfingsten et al., 2012).

Human telomerase

Human telomerase RNA structure

The 451-nucleotide human TER is referred to as hTR based on its original identification (Feng et al., 1995). Extensive phylogenetic comparison of vertebrate TER sequences revealed several conserved regions (CRs), which include the template and pseudoknot (Chen et al., 2000). In vertebrates, the template and pseudoknot are enclosed by the P1 stem, which also serves as a TBE. Interestingly, P1 is absent from rodent TERs which possess only a few nucleotides 5' of the template, suggesting an alternative mechanism for template boundary definition, possibly involving the RNA 5' cap (Hinkley et al., 1998). The activity-stimulating STE of hTR is formed by a three-way helical junction within CR4/5. The TERT TRBD recognizes a small hairpin termed P6.1 and adjacent nucleotides within this element, and specific P6.1 loop nucleotides stimulate catalytic activity (Chen et al., 2002; Robart and Collins, 2010). Separate template-pseudoknot and CR4/5 synthetic RNAs can reconstitute activity with recombinant TERT *in vitro* (Mitchell and Collins, 2000).

Recent work using TERT and fragments of hTR assembled in rabbit reticulocyte lysate has shown that when the template is removed from hTR, the enzyme can still capture and act on a synthetic oligonucleotide RNA-DNA hybrid supplied in *trans* (Qi et al., 2012). When the pseudoknot was also removed, a low level of activity was still observed, demonstrating that this

motif is not strictly required for catalysis (Qi et al., 2012). Based on studies of the pseudoknot to date, a unifying model for its function is the positioning of the template in the active site.

In addition to the generally conserved activity-stimulating motifs, hTR contains many regions required for mature RNA biogenesis, RNP assembly, subcellular trafficking, and regulation. The 5' end of hTR is single-stranded and contains several guanosine tracts that increase hTR accumulation. These are predicted to form G-quadruplex structures recognized by the helicase DHX36 (Lattmann et al., 2011; Sexton and Collins, 2011). Because this region is missing from the 5'-truncated rodent TERs, G quadruplex formation is not essential in these species, perhaps due to increased transcription of TER.

The 3' half of vertebrate telomerase RNAs adopts a fold shared with the H/ACA family of RNAs (Chen et al., 2000; Mitchell et al., 1999a). Eukaryotic H/ACA RNAs generally function as guides for site-specific RNA pseudouridylation and form hairpin-Hinge-hairpin-ACA secondary structures containing pockets in the hairpin stems that hybridize to sequences flanking the target uridine(s). H/ACA RNAs are divided into two groups based on their localization and target RNA: snoRNAs target ribosomal (r) RNA, while small Cajal body (sca) RNAs target snRNAs (Kiss et al., 2010). Each H/ACA RNA hairpin is assembled to contain a set of four core proteins in the mature RNP: the pseudouridylase dyskerin, NOP10, NHP2, and GAR1 (Collins, 2008; Egan and Collins, 2010). As in canonical H/ACA RNAs, the H/ACA core motifs of hTR are required for its accumulation *in vivo* as a stable RNP (Fu and Collins, 2003; Mitchell et al., 1999a; Mitchell and Collins, 2000). However, no putative target sequence complementary to either of the hTR pockets has been found, suggesting that hTR does not guide pseudouridylation.

Within the 3' H/ACA loop of hTR are two additional functional motifs: the CAB box and the BIO box. The CAB box is also found in H/ACA scaRNAs where it exists in two copies, one in each hairpin loop, and directs dynamic RNP concentration in Cajal bodies through interaction with TCAB1/WDR79 (Jády et al., 2004; Richard et al., 2003; Tycowski et al., 2009; Venteicher et al., 2009). The BIO box cooperates with other 3' hairpin stem elements to promote mature hTR accumulation but is not required for the accumulation of other H/ACA RNAs (Egan and Collins, 2012; Fu and Collins, 2003).

Human telomerase RNP maturation

The RNA polymerase II-transcribed hTR primary transcript is a potentially non-polyadenylated precursor, which acquires a 5' TMG cap and is exonucleolytically processed at its 3' end to the boundary of the H/ACA motif (Feng et al., 1995; Fu and Collins, 2006; Girard et al., 2008; Mitchell et al., 1999a). In contrast to hTR, other human H/ACA RNAs are processed from intron contexts by both 5' and 3' exonuclease action and lack the hTR 5' extension from the H/ACA motif and the TMG cap (Kiss et al., 2006). The hTR 3' end formation mechanism has not been defined but is likely to involve the nuclear exosome, which has been implicated in human U3 C/D box snoRNA precursor processing (Watkins et al., 2004) and in yeast H/ACA snoRNA processing (Kim et al., 2006; Steinmetz et al., 2001). Or, hTR 3' end processing could follow an snRNA-like pathway involving the Integrator complex (Baillat et al., 2005). Both of these pathways depend on sequences downstream of the mature RNA 3' end, and yet all of the processing signals for hTR appear to be present within the mature RNA sequence (Fu and Collins, 2003). The accumulation of hTR increases when a self-cleaving ribozyme is inserted immediately downstream of the mature 3' end, suggesting 3' end maturation may limit hTR accumulation (Egan and Collins, 2012).

hTR and other H/ACA RNAs cotranscriptionally assemble with a preformed scaffold

composed of dyskerin, NHP2, NOP10, and the pre-RNP assembly factor NAF1 (Darzacq et al., 2006; Richard et al., 2006; Wang and Meier, 2004). The assembly factor/chaperone SHQ1 binds to dyskerin but is not part of the pre-RNP (Grozdanov et al., 2009), and a study of the yeast ortholog suggests SHQ1 functions as an RNA-mimic to prevent nonspecific RNA binding by dyskerin (Walbott et al., 2011). Depletion of SHQ1, dyskerin, NHP2, NOP10, or NAF1 by RNA interference compromises H/ACA snoRNA and hTR levels (Fu and Collins, 2007; Grozdanov et al., 2009; Hoareau-Aveilla et al., 2006). RNP assembly is also aided by NUFIP, which binds NHP2, and by the helicases RUVBL1 and RUVBL2 (Boulon et al., 2008). These helicases have been shown to interact with dyskerin and TERT to facilitate telomerase RNP assembly (Venteicher et al., 2008). Knockdown of NUFIP, RUVBL1, or RUVBL2 reduces hTR levels (Boulon et al., 2008; Venteicher et al., 2008).

Dyskerin recognizes the H box or ACA sequence, each of which is located 14 to 16 nucleotides 3' of the hairpin pocket apex in canonical H/ACA RNAs (Ganot et al., 1997a). Based on a crystal structures of single-hairpin archaeal H/ACA RNPs bound to substrate RNA, this conserved spacing ensures that the target uridine in positioned in the pseudouridylase active site (Duan et al., 2009; Liang et al., 2009). NOP10 bridges dyskerin to NHP2 which is predicted to bind to the upper stem of the H/ACA RNA (Li and Ye, 2006). Although hTR does not exhibit the conserved spacing of elements in its 5' H/ACA hairpin, it still assembles a set of H/ACA core proteins on this hairpin, sharing the dimeric structure that characterizes eukaryotic H/ACA RNPs (Egan and Collins, 2010).

While most pseudouridine-guide RNAs require the presence of both H/ACA-motif hairpins to cooperatively bind the NAF1-dyskerin-NOP10-NHP2 assembly scaffold, the hTR 3' hairpin exhibits strongly enhanced RNP assembly stimulated by the BIO box motif (Egan and Collins, 2012). The BIO box is required for hTR accumulation but is not conserved in other H/ACA RNAs (Fu and Collins, 2003). BIO box mutant hTR precursor is transcribed, but it is not 3' end processed and does not escape the site of transcription, suggesting that H/ACA RNP assembly is a prerequisite for transcript release and processing (Theimer et al., 2007). The unique requirement for the BIO box in hTR may reflect an increased dependence of its independently transcribed precursor on rapid RNP assembly in order to avoid degradation. The intron-encoded precursors of other human H/ACA RNAs are likely more resistant to degradation within host mRNA transcripts or excised intron lariats and thus would not require such rapid assembly.

After transcription, assembly with H/ACA core proteins, and processing, hTR is transported to Cajal bodies via the transport factors PHAX and Nopp140 (Boulon et al., 2004; Yang et al., 2000). There, the short form of hTGS1 hypermethylates the 5' cap (Fu and Collins, 2006; Girard et al., 2008). Cajal bodies are also sites of RNP remodeling, which includes the replacement of the pre-RNP assembly factor NAF1 by the mature RNP component GAR1 (Darzacq et al., 2006). Separate from these maturation processes, the RNP also concentrates in Cajal bodies by indirect association with a subset of Sm proteins and direct association with TCAB1/WDR79 via the CAB box (Fu and Collins, 2006; Tycowski et al., 2009; Venteicher et al., 2009). Knockdown of TCAB1/WDR79 does not affect hTR accumulation but does reduce RNP association with Cajal bodies and telomeres, resulting in telomere shortening in HTC75 cancer cells (Venteicher et al., 2009; Zhong et al., 2011). Expression of CAB box mutant hTR in HTC75 cells reduced the rate of telomere elongation relative to wild-type hTR, whereas the final extent of lengthening was similar in telomerase-deficient primary human fibroblasts overexpressing hTR and TERT (Fu and Collins, 2007; Venteicher et al., 2009).

Human TERT-TER assembly

The catalytic subunit TERT joins the telomerase complex after mature RNP biogenesis. The TERT TRBD contacts the CR4/5 region of hTR and both the TEN domain and TRBD also contact the template-pseudoknot (Robart and Collins, 2011). Expression of TERT only modestly increases hTR accumulation but is required for telomere localization (Tomlinson et al., 2008; Yi et al., 1999). While various nuclear subdomains have been proposed as the site of hTR-TERT assembly, a study of endogenous hTR and TERT has suggested a possible model for the trafficking of telomerase. For most of the cell cycle, hTR localizes to Cajal bodies and TERT to distinct nuclear foci. During S phase TERT enters nucleoli and hTR-containing Cajal bodies move to the nucleolar periphery. Then both hTR and TERT colocalize adjacent to Cajal bodies before associating with telomeres (Tomlinson et al., 2006).

TERT assembly with the telomerase RNP requires the folding chaperone HSP90. RNP reconstitution in rabbit reticulocyte lysate is dependent on HSP90, and treatment with geldanamycin, an HSP90 inhibitor, reduces telomerase activity and also leads to proteasome-mediated degradation of TERT *in vivo* (Forsythe et al., 2001; Holt et al., 1999; Kim et al., 2005). In addition, TERT interacts with the snRNP assembly factor SMN, and expression of a dominant negative form of SMN disrupts the localization of TERT *in vivo* and telomerase assembly *in vitro*, suggesting that SMN could play a role in telomerase RNP assembly (Bachand et al., 2002). Another potential regulator of active telomerase assembly is the DNA-dependent protein kinase-interacting protein KIP, whose overexpression increases telomerase activity and telomere length without affecting the levels of TERT mRNA or hTR (Lee et al., 2004).

Bridging the human RNP catalytic core to telomere substrates

Human telomerase recruitment to telomeres requires the TIN2 and TPP1 telomere-binding proteins (Abreu et al., 2010), which are anchored to the double-stranded region of the telomere via TRF1 and TRF2 (Palm and de Lange, 2008). TPP1 also indirectly binds to single-stranded telomeric DNA through POT1 (Palm and de Lange, 2008), but POT1 is not required for telomerase recruitment to telomeres assayed by ChIP and fluorescence *in situ* hybridization (Abreu et al., 2010). A POT1-TPP1 complex stimulates the processivity of the telomerase catalytic core *in vitro* by maintaining association with the product DNA and aiding enzyme translocation (Latrick and Cech, 2010; Wang et al., 2007). TPP1 bridges the TERT TEN domain to POT1 to enable this stimulation (Zaug et al., 2010).

Common themes in telomerase biogenesis

Despite the great divergence in pathways of telomerase RNP maturation, catalytically active holoenzyme assembly, and telomere recruitment among ciliates, yeasts, and vertebrates, some general features are shared. TERs have evolved numerous motifs whose structures and binding partners are unique to each phylogenetic group, but which possess similar functions. TERs in all three groups interact with proteins required for RNA stability: p65 in ciliates, Sm proteins in yeasts, and H/ACA proteins in vertebrates. TERs also contain shared motifs, the template-pseudoknot and STE, to mediate their interactions with TERT. While the relative affinities of these interactions differ between species, the existence of two distinct binding sites in the RNA appears to be a conserved feature that ensures the specificity of TERT-TER

interaction. Mechanisms of telomere recruitment also bear striking similarities. Teb1 and TASC bridge the *T. thermophila* telomerase catalytic core to telomere substrates much like the telomere-associated Cdc13p or TPP1 recruits the telomerase-associated Est1p or TERT in *S. cerevisiae* and human cells, respectively. Although studies of diverse organisms have revealed a great deal about telomerase biogenesis and regulation, much remains to be discovered about the complex pathways that produce this essential enzyme.

CHAPTER TWO

Specificity and Stoichiometry of Subunit Interactions in the Human Telomerase Holoenzyme Assembled *In Vivo*

Abstract

The H/ACA motif of human telomerase RNA (hTR) directs specific pathways of endogenous telomerase holoenzyme assembly, function, and regulation. Similarities between hTR and other H/ACA RNAs have been established but differences have not been explored even though unique features of hTR H/ACA RNP assembly give rise to telomerase deficiency in human disease. Here, we define hTR H/ACA RNA and RNP architecture using RNA accumulation, RNP affinity purification, and primer extension activity assays. First, we evaluate alternative folding models for the hTR H/ACA motif 5' hairpin. Second, we demonstrate an unanticipated and surprisingly general asymmetry of 5' and 3' hairpin requirements for H/ACA RNA accumulation. Third, we establish that hTR assembles not one but two sets of all four of the H/ACA RNP core proteins dyskerin, NOP10, NHP2, and GAR1. Fourth, we address a difference in predicted specificities of hTR association with the holoenzyme subunit WDR79/TCAB1. Together, these results complete the analysis of hTR elements required for active RNP biogenesis and define the interaction specificities and stoichiometries of all functionally essential human telomerase holoenzyme subunits. This study uncovers unexpected similarities but also differences between telomerase and other H/ACA RNPs that allow a unique specificity of telomerase biogenesis and regulation.

Introduction

The challenge of eukaryotic chromosome end replication is met in part by telomerase-mediated synthesis of terminal DNA repeats (Gilson and Geli, 2007). The telomerase catalytic core can be reconstituted from telomerase reverse transcriptase (TERT) and telomerase RNA (TER), which together form a specialized reverse transcriptase enzyme (Sekaran et al., 2010). Although the sequences and structures of TERs are highly divergent across eukaryotes, all TERs contain three elements important for RNP catalytic activity: an internal template for telomeric repeat synthesis, an adjacent pseudoknot, and a distantly positioned stem terminus element (Blackburn and Collins, 2010). TERs also contain motifs that mediate RNA folding, stability, localization, and regulation *in vivo* (Collins, 2009). In vertebrate cells, the TER precursor is transcribed by RNA polymerase (Pol) II. The 451 nucleotide (nt) mature human telomerase RNA (hTR) is produced by 3' end trimming and 5' end modification with a trimethylguanosine (TMG) cap (Feng et al., 1995; Fu and Collins, 2006; Jády et al., 2004; Mitchell et al., 1999a). Consistent with the requirement for a specific pathway of biogenesis, mature hTR accumulation is favored by Pol II expression contexts lacking a downstream signal for transcription-coupled mRNA or small nuclear (sn) RNA 3' end formation (Fu and Collins, 2003).

The 5' half of hTR resembles a compact ciliate TER, with the template and pseudoknot constrained by a domain-closing stem, while the 3' half adopts a fold shared by a large family of H/ACA motif small nucleolar (sno) and small Cajal body (sca) RNAs (Fig. 1A). H/ACA snoRNAs and scaRNAs function predominantly as guides for the site-specific pseudouridylation of ribosomal (r) RNA and snRNA, respectively (Matera et al., 2007). The canonical secondary structure of a eukaryotic H/ACA RNA consists of a 5' hairpin followed by a single-stranded H box (ANANNA), and then a 3' hairpin followed by a single-stranded ACA located 3 nt from the mature RNA 3' end (Henras et al., 2004). Each hairpin contains an internal loop or "pocket" that guides the selection of a modification target. Both sides of an unpaired stem pocket base pair to the target RNA such that the target uridine is extruded from the hybrid at the top of the pocket (Duan et al., 2009; Liang et al., 2009). Putative modification guide sequences of vertebrate TERs are not conserved, suggesting that TERs do not direct RNA modification. Also, while hTR is an independent transcript trimmed at its 3' end, other vertebrate H/ACA RNAs are both 5' and 3' end-processed from introns. Despite these differences, *in vivo* accumulation of hTR requires the same H box and ACA elements required for snoRNA accumulation (Mitchell et al., 1999a; Mitchell and Collins, 2000). By directing a specific pathway of primary transcript maturation and RNP biogenesis, the hTR H/ACA motif provides a mechanism for efficient assembly of a biologically stable telomerase RNP.

Canonical H/ACA RNAs share the RNP core proteins Cbf5/NAP57/dyskerin (the pseudouridine synthase), NOP10, NHP2, and GAR1 (Reichow et al., 2007). The heterotrimer of dyskerin, NOP10, and NHP2 is deposited onto each hairpin unit of the H/ACA motif in a highly chaperoned biogenesis process (Matera et al., 2007). Cotranscriptional association of the heterotrimer is followed by an exchange of biogenesis factors for the fourth core subunit GAR1 to produce a biologically functional RNP (Darzacq et al., 2006). All four H/ACA RNP proteins copurify hTR as well as other H/ACA RNAs. The three core heterotrimer proteins can be detected by mass spectrometry of purified human telomerase holoenzyme (Fu and Collins, 2007), although one report has suggested that holoenzyme includes only dyskerin, hTR, and TERT (Cohen et al., 2007). Recent structures of reconstituted archaeal single-stem RNPs with Cbf5, Nop10, and the NHP2-related protein L7Ae indicate that Cbf5 contacts a large surface of

RNA from the 3' ACA through the hairpin lower stem and pocket, accounting for the conserved and catalytically essential 14-16 nt spacing of the ACA (or H box) and the top of the hairpin pocket (Duan et al., 2009; Liang et al., 2009; Ye, 2007). Biochemical assays and structural models of the eukaryotic H/ACA proteins suggest a conserved positioning of dyskerin and the interacting NOP10 subunit, with the other face of NOP10 binding to NHP2 to place it in the vicinity of the upper stem (Reichow et al., 2007).

The human H/ACA snoRNA and scaRNA subfamilies of modification guide RNAs differ in their targets (rRNAs versus snRNAs) and by the presence of a motif in the terminal loop of their 5' and 3' hairpins termed the Cajal body or CAB box (ugAG, where lower case letters indicate reduced sequence conservation). Many RNAs including hTR transit nuclear Cajal bodies during biogenesis, but some including H/ACA scaRNAs concentrate in Cajal bodies as a steady-state distribution (Matera and Shpargel, 2006). Cajal body localization of H/ACA scaRNAs is dependent on the CAB boxes in each hairpin stem (Richard et al., 2003). Most vertebrate TERs have a CAB box located in the 3' hairpin of the H/ACA motif (Jády et al., 2004; Xie et al., 2008). Dependent on this single CAB box, hTR shows cell-cycle-regulated concentration in Cajal bodies of TERT-expressing cancer cell lines (Jády et al., 2004; Jády et al., 2006; Tomlinson et al., 2008; Tomlinson et al., 2006; Zhu et al., 2004). The hTR CAB box is not essential for telomere elongation (Fu and Collins, 2007), but it may increase the rate of telomere elongation or the telomere length set-point when hTR is overexpressed in cancer cells (Cristofari et al., 2007). WDR79/TCAB1 was identified as a direct RNA binding protein dependent on a CAB box for H/ACA RNP interaction (Tycowski et al., 2009) and paradoxically as an RNA-independent interaction partner of dyskerin (Venteicher et al., 2009). Like the CAB box itself, WDR79/TCAB1 is not required for hTR accumulation or telomerase catalytic activity but it is required for hTR concentration in Cajal bodies (Venteicher et al., 2009). Long-term depletion of WDR79/TCAB1 in a human fibrosarcoma cell line reduced telomere length (Venteicher et al., 2009), suggesting that hTR Cajal body concentration promotes telomere maintenance. Given that not all cells with active telomerase have Cajal bodies, WDR79/TCAB1 may more generally promote telomere maintenance by allowing hTR to escape from a default snoRNA-like sequestration in the nucleolus.

Structural similarities between hTR and other H/ACA RNAs have been established by previous studies, but differences have not been explored. Unique features of hTR H/ACA RNP assembly are likely to underlie the telomerase-specific disease phenotypes resulting from inherited human dyskerin, NOP10, and NHP2 gene mutations (Armanios, 2009; Savage and Alter, 2008). A major potential point of difference involves the unresolved structure of the hTR H/ACA motif 5' hairpin. Previous structure/function studies of this region to investigate requirements for RNA accumulation were difficult to interpret due to mutagenesis-induced stem pairing rearrangements (Mitchell and Collins, 2000), and phylogenetic comparison did not derive a unique fold for this region due to high sequence variability among vertebrate TERs (Chen et al., 2000). The original model of the hTR H/ACA motif 5' hairpin (Mitchell et al., 1999a) and similar phylogenetic predictions (Chen et al., 2000; Podlevsky et al., 2008) all deviate from the conserved spacing of 14-16 nt that should separate the H box and the top of the pocket to form the contact surface for dyskerin. Therefore, unlike other human H/ACA snoRNAs and scaRNAs, hTR could assemble a set of core proteins only on the 3' hairpin. Indeed, the hTR 3' hairpin has been shown to support single-stem RNP assembly *in vitro* (Dragon et al., 2000) and single-stem RNP assembly has been shown to occur in trypanosomes *in vivo* (Uliel et al., 2004). On the other hand, mapping of an intron-expressed hTR H/ACA domain 5' end suggested an alternative 5'

boundary for the H/ACA motif (Theimer et al., 2007), which could fold a canonical 5' hairpin with an insertion in the pocket known to occur in some snoRNAs (see below; Fig. 1B). Because the 5' hairpin of the H/ACA motif separates two regions of hTR critical for TERT interaction and catalytic activity (Fig. 1A), alternative configurations of 5' hairpin stem pairing and pocket structure could influence telomerase holoenzyme activity.

Here we define the RNA and RNP architecture of the H/ACA domain of human telomerase using holoenzyme reconstitution *in vivo*. We find support for the original model of 5' hairpin structure and uncover an unexpected asymmetry of significance for the 5' versus 3' hairpin pockets that is shared by hTR and canonical snoRNAs. Curiously, most elements of hTR 5' hairpin structure are not important for holoenzyme catalytic activity. We next elucidate the hTR interaction stoichiometry of H/ACA RNP core proteins using a tandem affinity purification strategy. Independent of all but a minimal 5' hairpin stem and H box, two full sets of H/ACA RNP proteins assemble on each molecule of hTR. In contrast, WDR79/TCAB1 association appears single-copy, with strong dependence on the CAB box in the hTR 3' hairpin loop. These studies resolve open questions of telomerase subunit stoichiometry and reveal unexpected additional similarities as well as differences in the composition of telomerase, snoRNPs, and scaRNPs in human cells.

Materials and Methods

Cell culture, constructs, and transfection.

293T and VA13+TERT cells were cultured in DMEM with 10% FBS and transiently transfected using the calcium phosphate method (Mitchell and Collins, 2000). Expression constructs for mature hTR and the hTR-U64 chimera have been previously described (Fu and Collins, 2003). To generate pBS-U3-hTR-U64-500 and pBS-U3-hTR H/ACA-500, mature hTR sequence in pBS-U3-hTR-500 was replaced by hTR-U64 or the H/ACA-domain region of hTR (nt 203-451), respectively. H/ACA snoRNA expression constructs pBS-U3-U64-500 and pBS-U3-ACA28-500 were similarly constructed by replacing mature hTR sequence with the mature snoRNA sequence. The functionally validated structures of the U64 5' hairpin and the ACA28 5' and 3' hairpins target known modifications of human rRNA (Lestrade and Weber, 2006; Xiao et al., 2009). N-terminally tagged proteins were expressed in the backbone contexts pcDNA-Z (where Z represents tandem Protein A domains followed by a cleavage site for tobacco etch virus protease), pcDNA-F (where F represents three copies of the FLAG tag), and pcDNA-ZF. Due to extract proteolysis in the N-terminal tag region of ZF-WDR79/TCAB1, assays shown here used the extract-stable C-terminal FZ-tagged subunit. A plasmid containing *Tetrahymena thermophila* TER under the control of the human U6 Pol III promoter was used as a control for transfection efficiency (Mitchell et al., 1999a). All constructs were verified by sequencing.

Blot detection of RNA and protein.

RNA was purified using TRIzol according to the manufacturer's protocol (Invitrogen). Northern blot detection of hTR, hTR-U64, and the recovery control was performed using an end-labeled 2'-*O*-methyl RNA oligonucleotide complementary to hTR positions 51-72 as previously described (Fu and Collins, 2003). The 5'-processed hTR H/ACA domain alone was detected using DNA oligonucleotide probes complementary to nt 305-335, 363-390, or 419-449 depending on the hTR variants analyzed. Endogenous and recombinant human snoRNAs were detected using DNA oligonucleotide probes complementary to positions 54-82 of U64 or positions 79-107 of ACA28. Immunoblots to detect tagged proteins used FLAG M2 monoclonal antibody or rabbit IgG primary antibody and were imaged using a LI-COR Odyssey system.

Telomerase activity assay.

Cell extracts prepared by freeze-thaw lysis (Mitchell and Collins, 2000) were clarified by centrifugation. Nine µg of total protein as determined by Bradford assay was used in each reaction. Assay buffer contained final concentrations of 10 mM HEPES, 50 mM Tris acetate, 5% glycerol, 40 mM NaCl, 50 mM potassium acetate, 4 mM $MgCl_2$, 1 mM EGTA, 1 mM spermidine, and 5 mM β-mercaptoethanol at pH 8.0. Reactions were initiated by the addition of 500 nM telomeric repeat primer $(G_3T_2A)_3$, 0.25 mM dTTP and dATP, 5.5 µM unlabeled dGTP, and 0.33 µM [α-^{32}P] dGTP (3000 Ci/mmol, PerkinElmer Life Sciences) and incubated at 30°C for 1 hour. The 40 µl assay volumes were supplemented with 60 µL RNase A stop solution, incubated at 37°C for 15 min, supplemented with 50 µL Proteinase K solution, and incubated again at 37°C for 15 min. Product DNA was purified by phenol-chloroform extraction and ethanol precipitation and then analyzed by denaturing acrylamide gel electrophoresis.

Affinity purification.

For tandem affinity purification of tagged dyskerin, NHP2, GAR1, TERT, and

WDR79/TCAB1, cell extracts from freeze-thaw cell lysis were diluted to ~2 mg/mL in binding buffer (20 mM HEPES at pH 8.0, 150 mM NaCl, 2 mM $MgCl_2$, 0.2 mM EGTA, 10% glycerol, 0.1% Igepal, 1 mM DTT, 0.1 mM PMSF, and 1/1000 volume of Sigma Protease Inhibitor Cocktail). A volume of 0.9 mL of diluted extract was clarified by centrifugation immediately prior to purification using 5 µL of packed resin. Rabbit IgG agarose (Sigma) or FLAG M2 antibody resin (Sigma) was washed 3 times in 1 mL of binding buffer prior to use. Samples were rotated end-over-end for 2 hours at room temperature or overnight at 4°C. Bound samples were washed twice at room temperature in 1 mL of wash buffer (binding buffer with 0.1% Triton X-100, 0.1% CHAPS, 100 ng/µL BSA, and 100 ng/µL tRNA) for 5 min each wash and then transferred to ultra-low retention tubes (Phenix) for a third wash. To elute bound protein, a final concentration of 150 ng/µL 3xFLAG peptide (Sigma) or ~30 ng/µL of the S219V variant of tobacco etch virus protease was added in a volume of 50 µL of wash buffer and rotated end-over-end for 15 min at room temperature. Supernatant was removed and the resin rinsed with another 50 µL of wash buffer. The combined 100 µL of elution supernatant was cleared of contaminating beads using Micro Bio Spin columns (Bio-Rad) and added to 5 µL of the second resin. Second-step binding was performed by end-over-end rotation for 30 min at room temperature followed by washing and elution as described above. Single-step purification of WDR79/TCAB1 was performed using Z-tagged protein with conditions described above.

Results

The hTR H/ACA motif has a noncanonical secondary structure.

The first investigation of hTR H/ACA motif structure proposed a 5' hairpin starting at position 211 (Fig. 1B, left). Consistent with studies of the yeast H/ACA snoRNAs known at that time, the hTR H box, ACA, and 3' hairpin lower stem were each found to be essential for *in vivo* accumulation (Bortolin et al., 1999; Mitchell et al., 1999a; Mitchell and Collins, 2000). Although the 5' hairpin lower stem is critical for intron-encoded snoRNA accumulation, it is not essential for accumulation of an independently transcribed yeast snoRNA (Bortolin et al., 1999). Substitutions of the predicted hTR 5' hairpin lower stem did not inhibit mature hTR accumulation, but changes in the size and accumulation level of the hTR H/ACA domain processed from the hTR primary transcript at its 5' and 3' ends suggested that mutagenesis of the 5' hairpin created alternative stem pairings (Mitchell and Collins, 2000). A full-length hTR secondary structure prediction derived by phylogenetic comparison supported the original model of H/ACA motif structure and placed the 5' hairpin at the base of a hypervariable stem (Chen et al., 2000). More recently, 5' end mapping of the 5' and 3' end-processed hTR H/ACA domain raised the prospect of an alternative 5' hairpin lower stem beginning at position 225 (Theimer et al., 2007), which could fold a hairpin structure with canonical rather than noncanonical spacing from the H box to the top of the 5' pocket (Fig. 1B, right). Notably, *in vivo* modification protection of hTR (Antal et al., 2002) is most consistent with the alternative secondary structure model.

To establish the pairing register of the hTR H/ACA motif 5' hairpin, we introduced stem disruptions and stem repair combinations in the expression context U3-hTR-500, in which a Pol II snRNA promoter drives expression of hTR and its endogenous downstream flanking 500 bp. This construct produces mature hTR and catalytically active telomerase holoenzyme that is functional for telomere elongation (Fu and Collins, 2003; Wong and Collins, 2006). Recombinant hTR was expressed by transient transfection of 293T cells, allowing a high level of recombinant RNP accumulation. Substitutions that should discriminate the original and alternative models for 5' hairpin structure were designed in blocks of two to four nt (Fig. 1B), using folding predictions to minimize the potential for formation of alternative pairings. Every experiment included an empty vector control for endogenous hTR background. RNA was harvested from cells transfected to express recombinant versions of hTR and a ciliate TER transcribed using the human U6 snRNA Pol III promoter as a transfection control (TC). Total RNA was resolved by denaturing PAGE and probed to detect the RNAs of interest. Due to partial folding during acrylamide gel electrophoresis, hTR typically migrates as doublet. In this and previous studies, substitutions in the 5' hairpin induce variability in hTR gel migration.

Single-sided substitutions of the 5' hairpin lower stem inhibited hTR accumulation, and in each case this inhibition was rescued by the compensatory combination of left-side (L) and right-side (R) changes (Fig. 1C, lanes 3-11). Compensatory combinations also rescued accumulation of the hTR H/ACA domain alone, albeit giving rise to migration heterogeneity that could reflect differences in size and/or partial folding during electrophoresis. Notably, only two of the six single-sided stem substitutions reduced recombinant hTR accumulation to near the level of endogenous hTR background (Fig. 1C, compare lanes 1, 6, and 10) while the corresponding other-side substitutions (lanes 7 and 9) or a larger substitution involving the same residues (lane 3) were permissive for some hTR accumulation. Together the results support the original model of a 5' hairpin 8 bp lower stem beginning at position 211 (Fig. 1B, left), because

compensatory mutagenesis rescued the loss of accumulation imposed by a two nt substitution at the left-side base of this stem (pairing B) or a four nt right-side substitution at the top of this stem (pairing C). Although the loss and rescue of accumulation is less dramatic, disruption and repair of the hTR H/ACA motif 5' hairpin upper stem lends modest support for formation of this element as well (Fig. 1C, lanes 12-14).

We also investigated potential formation of the alternative 5' hairpin stem beginning at position 225 (Fig. 1B, right). Despite its several attractions, the alternative model was not favored by mutagenesis results. The combination of putative compensatory left-side and right-side stem substitutions did not improve hTR accumulation (Fig. 1C, lanes 17-19). We conclude that the hTR H/ACA motif 5' hairpin can and likely does begin at position 211, although alternative foldings appear to support the accumulation of mature hTR. Also, the 5' hairpin structural requirements for full-length hTR appear more lenient than for the hTR H/ACA domain alone, suggesting that folding of the 5' hairpin region could differ in full-length hTR versus the H/ACA domain stable to 5' processing. Overall these findings establish differences between the architecture of the hTR H/ACA motif 5' hairpin and the 5' hairpins of other H/ACA RNAs.

A 5' hairpin pocket is not required for hTR accumulation.

The role of the H/ACA motif hairpin pockets in base pairing to target RNAs has been well established, but to our knowledge the significance of these pockets for canonical snoRNA accumulation and RNP assembly has not been examined. Previous studies of hTR found that sequence substitution of the 3' hairpin pocket or sequence tag insertion in the 5' pocket were both tolerated for accumulation, while a substitution intended to force pairing of the canonically positioned 3' pocket was not (Mitchell et al., 1999a; Mitchell and Collins, 2000). To directly compare the significance of the hTR 5' and 3' hairpin pockets, we first examined the impact of deleting the left-side, right-side, or left and right sides of each hairpin pocket (Fig. 1D, left; pocket residues are shown for the most recent model based on phylogenetic comparison (Podlevsky et al., 2008). None of the deletions within the 5' pocket strongly reduced hTR accumulation (Fig. 1D, lanes 3-5). Making a smaller 5' pocket by deleting all but five residues of the right-side pocket (boxed in Fig. 1D, left), without or with accompanying deletion of all left-side pocket residues (lane 7 or 8, respectively), also allowed hTR accumulation. In contrast, the corresponding perturbations of the 3' pocket reduced or eliminated hTR accumulation (Fig. 1D, 9-11).

We also tested the impact of pairing across the pocket. In the 5' pocket, converting the pocket to a 5 bp duplex (depicted by the cross-pocket lines in the illustration of Fig. 1D) was detrimental for hTR accumulation (lane 6). We note that the long 21 bp duplex created by this pocket pairing could have indirectly led to transcript degradation. Replacement of the 3' pocket with a 3 bp or 9 bp duplex was also detrimental for hTR accumulation (Fig. 1D, lanes 12-13), despite the shorter overall length of duplex that was created. In general, perturbations of pocket structure had parallel impact on the accumulation of full-length hTR and the hTR H/ACA domain alone, although accumulation of the H/ACA domain alone was less tolerant of complete 5' pocket deletion (Fig. 1D, lane 5). The combined results of hTR H/ACA motif pocket mutagenesis reveal additional asymmetry in the structural requirements for the 5' and 3' hairpins.

Holoenzyme catalytic activity is tolerant of changes in 5' hairpin structure.

The hTR H/ACA motif 5' hairpin elements separate two TERT-interacting regions of

hTR critical for catalytic activity (Mitchell and Collins, 2000). To test whether relative positioning of the two TERT-interacting regions is important for holoenzyme catalytic activity, we reconstituted hTR variants into telomerase holoenzyme by transfection of VA13 cells lacking endogenous hTR (Bryan et al., 1997). VA13+TERT cells (VA13 cells with an integrated TERT expression vector) were transfected to express hTR variants that abrogate wild-type pairing of the H/ACA motif 5' hairpin lower stem (single- or double-sided substitutions of pairing A) or upper stem (single- or double-sided substitutions of pairing D) or eliminate the 5' hairpin pocket (combined left-side and right-side pocket deletion). Telomerase activity in cell extracts was assayed by direct primer extension to monitor repeat addition processivity as well as activity overall.

Surprisingly, most H/ACA motif 5' hairpin substitutions did not affect telomerase activity: catalytic activity generally paralleled hTR accumulation (Fig. 2). One exception was the left-side substitution of the 5' hairpin lower stem (Fig. 2, lane 3), which could indirectly affect the folding of the adjacent template/pseudoknot region. Notably, holoenzymes with disrupted pairing of the alternative 5' hairpin lower stem beginning at position 225 also retained catalytic activity (Fig. 2, lanes 4 and 6). We conclude that the relative positioning of TERT-interacting motifs across the intervening H/ACA motif 5' hairpin is not important for holoenzyme catalytic activity. Sufficient TERT interaction affinity for each of its bound hTR motifs may obviate the role of other proteins in hTR-TERT interactions.

Asymmetric 5' and 3' hairpin requirements are shared by canonical snoRNAs.

To establish some necessity of 5' hairpin structural elements for hTR accumulation, we sought to determine the maximal extent of the 5' hairpin that could be deleted. We created internal truncations of the 5' hairpin that removed the H/ACA motif upper stem (Δ1), the upper stem and pocket (Δ2), or the entire stem/pocket/stem hairpin (Δ3). Remarkably, deletions that removed the upper stem or the upper stem and pocket did not substantially affect hTR accumulation (Fig. 3A, lanes 3-4). A detectable level of hTR accumulated even with complete 5' hairpin deletion (Fig. 3A, lane 5), in contrast to the undetectable accumulation of hTR variants with substitutions in the H box or ACA expressed from the same vector (data not shown).

To determine whether the minimal 5' hairpin requirement was unique to hTR, we tested the accumulation of canonical human H/ACA snoRNAs U64 (Fig. 3B) and ACA28 (Fig. 3C) with deletions in the 5' or 3' hairpin. Surprisingly, for both of these snoRNAs, combined deletion of the 5' pocket right-side and left-side residues did not reduce accumulation (Figs. 3B and 3C, lane 5). Deletion of either pocket side alone had a partially inhibitory impact, perhaps resulting from induced misfolding (Figs. 3B and 3C, lanes 3-4). Remarkably, deletions of the entire 5' hairpin upper stem and pocket were permissive for snoRNA accumulation (Figs. 3B and 3C, lane 9). In contrast to the 5' hairpin pocket, any perturbation of the 3' hairpin pocket was strongly inhibitory (Figs. 3B and 3C, lanes 6-8). These unexpected findings suggest that although hTR has a uniquely divergent 5' hairpin structure, there are not fundamental differences between hTR and canonical H/ACA snoRNAs in the asymmetry of 5' and 3' hairpin requirements for RNP assembly *in vivo*.

The hTR H/ACA motif recruits two full sets of core proteins.

Yeast H/ACA snoRNAs assemble a set of core proteins on each hairpin, as demonstrated by snoRNP gel filtration and electron microscopy (Watkins et al., 1998) and cooperative function of two hairpin units *in vivo* (Bortolin et al., 1999). The atypically large spacing between

the hTR H box and the top of the 5' hairpin pocket and the autonomy of the hTR 3' hairpin for H/ACA RNP assembly *in vitro* (Dragon et al., 2000) suggest that the hTR 5' hairpin may not assemble a typical set of H/ACA RNP proteins. To address whether one or both hTR H/ACA motif hairpins assemble core proteins *in vivo*, we exploited a tandem affinity purification strategy schematized in Fig. 4A. We transiently transfected 293T cells to express plasmids encoding hTR, the hTR-U64 chimera with the 3' half of hTR replaced by a snoRNA (Mitchell and Collins, 2000), and tagged versions of the H/ACA RNP core proteins dyskerin, NHP2, or GAR1. Tagged forms of the very small protein NOP10 accumulate poorly due to tag interference with RNP assembly (Fu and Collins, 2007), but because this subunit organizes the dykerin-NOP10-NHP2 heterotrimer, its presence can be inferred from the combination of dyskerin and NHP2. Each protein was tagged with tandem Protein A domains (Z), a triple FLAG tag (F), or the fusion of both tags (ZF). In addition to each tagged protein expressed separately, the Z- and F-tagged proteins were coexpressed (indicated by +). Plasmid concentrations were optimized to yield nearly equal amounts of each tagged form of protein, as monitored by immunoblots of cell extract (data not shown).

Affinity purification was performed using panels of four transfected cell extracts in parallel (Z, F, +, ZF). First, any Z-tagged complexes were bound to IgG resin and eluted. Next, enriched Z-tagged RNPs that also harbored an F-tag were bound to FLAG antibody resin and eluted. Tandem affinity purified RNPs were supplemented with a recombinant RNA recovery control (RC) prior to RNA extraction. Purified RNA was then resolved by denaturing PAGE and interrogated by blot hybridization. For ZF-tagged protein, tandem steps of purification will recover all RNPs assembled with even a single subunit of tagged protein, but only RNP complexes containing at least two subunits of tagged protein will be recovered by tandem steps of purification from extract with the combination of Z- and F-tagged protein (Fig. 4A). Purifications from extracts containing only Z- or F-tagged protein serve as negative controls for non-specific background. This methodology has demonstrated the monomeric nature of TERT and hTR in the catalytically active human telomerase holoenzyme (Errington et al., 2008).

Here we cotransfected the hTR-U64 chimera as an internal control for tandem purification efficiency. Because U64 is a canonical snoRNA, the chimera should assemble two sets of H/ACA core proteins. Also, because hTR-U64 shares the 5' template/pseudoknot region of hTR, the same oligonucleotide hybridization probe can be used to detect hTR and hTR-U64 simultaneously. The ratio of hTR to hTR-U64 recovered by the Z- and F-tagged protein combination relative to the ZF-tagged control provides a rigorously normalized quantification of subunit stoichiometry: only if an hTR RNP harbors at least two H/ACA protein subunits will hTR be recovered from extract containing the combination of Z- and F-tagged proteins, and only if the vast majority of hTR RNP assembles precisely two sets of H/ACA proteins will the ratio of hTR to hTR-U64 recovered by the combination of Z- and F-tagged protein versus the ZF-tagged protein be consistent.

Using tagged dyskerin and tagged NHP2 extracts (Fig. 4B, lanes 1-8), recovery of hTR and hTR-U64 by ZF-tagged protein was robust. Little if any non-specific background was detected after tandem steps of purification from the negative control extracts with Z-tagged or F-tagged protein alone. As expected if H/ACA RNP complexes assemble on both the 5' and 3' hairpins of the U64 and hTR H/ACA motif, both the hTR-U64 chimera and hTR were recovered from the extracts with coexpressed Z- and F-tagged subunits. The efficiency of RNP purification by coexpressed single-tagged subunits should be less than that obtained by the double-tagged subunit, because some RNPs will assemble with two Z-tagged subunits or two F-tagged subunits

instead of one of each. Notably, the ratio of hTR to hTR-U64 remained consistent comparing purifications with the tagged protein combination and the ZF-tagged control (Fig. 4B, compare lane 3 to 4 and lane 7 to 8). These results indicate that H/ACA RNP proteins are deposited on both stems of the hTR H/ACA motif, despite the noncanonical nature of the hTR 5' hairpin. This finding is consistent with the dependence of hTR accumulation on both the H box and the ACA (Mitchell et al., 1999a). As additional controls, we confirmed that ZF-tagged TERT but not the Z- and F-tagged TERT combination copurified hTR (Fig. 4B, lanes 11-12). TERT did not substantially enrich hTR-U64 because the chimeric RNA is missing a major motif for TERT interaction.

GAR1 differs from other core H/ACA proteins in its late assembly and its dispensability for precursor RNA processing and mature RNP stability (Reichow et al., 2007). Roles proposed for GAR1 include improving the efficiency of target RNA modification and enhancing RNP nucleolar localization. Because hTR does not guide RNA modification and only a minor percentage of hTR is stably associated with nucleoli (Mitchell et al., 1999a), there is not an obvious functional requirement for GAR1 in the telomerase holoenzyme. GAR1 contacts dyskerin directly, but this interaction is mutually exclusive with at least one other direct dyskerin binding protein (Darzacq et al., 2006). GAR1 does copurify human telomerase holoenzyme, but the stoichiometry of its association could differ from that of the dyskerin-NOP10-NHP2 heterotrimer (Fu and Collins, 2007). Therefore, we compared GAR1 purification of hTR and hTR-U64 using the tandem affinity purification strategy. As observed for the other H/ACA RNP core proteins, the combination of Z- and F-tagged GAR1 purified hTR as well as hTR-U64, and a consistent ratio of the two RNAs was obtained in purifications using the single-tag subunit combination compared to the double-tagged ZF-GAR1 (Fig. 4B, lanes 15-16). Importantly, analysis of RNPs from the first step of tandem purifications confirmed the expected RNP recoveries, and when the same panels of tagged dyskerin, NHP2, and GAR1 extracts were used in purifications with the order of tandem affinity purification steps reversed, parallel results were obtained (data not shown). All results were highly reproducible over independent transfections and purifications (data not shown). Together these affinity purification assays indicate that RNP assembly on the hTR H/ACA motif yields the canonical bipartite architecture of an H/ACA snoRNP.

Assembly of two sets of H/ACA proteins requires only a minimal 5' hairpin stem.

Because most H/ACA motif elements of the hTR 5' hairpin could be eliminated without inhibition of RNA accumulation or RNP catalytic activity, it seemed possible that one set of H/ACA proteins assembled on the 3' hairpin would be sufficient for biogenesis of a telomerase RNP. To investigate whether removing most of the 5' hairpin converted hTR to an archaeal-like single-stem ACA RNP, we applied the tandem affinity purification strategy to hTR variants lacking the 5' hairpin pocket (Fig. 1D, L+R del) or lacking all nucleotides above the lower stem (Fig. 3A, Δ2; note that this RNA migrates with different mobility depending on sample heating). These two hTR variants accumulated to a sufficient level for detection after tandem steps of affinity purification. Remarkably, both of these hTR variants assembled two subunits of dyskerin, NHP2, and GAR1 per telomerase RNP (Fig. 5, lanes 3-4, 7-8, 11-12, 15-16, 19-20, 23-24). These findings indicate that a bipartite H/ACA RNP is assembled even when the 5' hairpin lacks RNA elements thought to be necessary for scaffolding of protein-protein interactions. We conclude that there is a different specificity of RNP assembly on the two hairpins of the eukaryotic H/ACA motif.

WDR79/TCAB1 association with hTR has the stoichiometry and specificity of a CAB box interaction.

WDR79/TCAB1 was recently discovered as a direct protein-protein interaction partner of dyskerin (Venteicher et al., 2009) and as a direct RNA interaction partner of the CAB box (Tycowski et al., 2009). We therefore wondered whether one or two subunits of WDR79/TCAB1 would assemble with hTR, given that a human telomerase RNP has two subunits of dyskerin but only one CAB box. Consistent with previous studies, hTR was detected after a single step of Z- or F-tagged WDR79/TCAB1 purification on the corresponding resin (data not shown). Using the tandem affinity purification strategy described above, hTR was detected after tandem steps of purification of the double-tagged WDR79/TCAB1 (Fig. 6A, lane 8) but not after tandem steps of purification from extract with the coexpressed Z- and F-tagged subunit combination (lane 7). The same result was observed when either order of tandem purification steps was used and was reproducible for independent transfections and purifications (data not shown).

The largely single-subunit nature of WDR79/TCAB1 association with hTR predicted that its interaction would be dependent on the CAB box. Using single-step WDR79/TCAB1 affinity purification from extracts of transfected VA13+TERT cells, we compared protein association with wild-type hTR and an hTR variant with a single-nucleotide CAB box substitution sufficient to disrupt hTR concentration in Cajal bodies (Jády et al., 2004). The CAB box substitution strongly impaired but did not eliminate hTR association with WDR79/TCAB1 (Fig. 6B, lanes 5-6). Similar results were obtained using extracts from transfected 293T cells (data not shown). With or without a CAB box, it seems likely that WDR79/TCAB1 binds only to the hTR 3' hairpin loop because the loop context of the CAB box is important for Cajal body localization (Theimer et al., 2007) and the hTR 5' hairpin lacks a similarly positioned loop. Overall our studies of human telomerase holoenzyme RNA and RNP architecture support the hTR-scaffolded steps of telomerase RNP biogenesis schematized in Fig. 7.

Discussion

Unique and shared features of the hTR H/ACA motif have implications for RNP biogenesis.

Elucidation of the requirements for human telomerase RNP biogenesis will bring insights for disease therapy, because differences that distinguish hTR from H/ACA snoRNAs and scaRNAs must somehow give rise to the specificity of telomerase deficiency in patients with altered dyskerin (Mitchell et al., 1999b; Wong et al., 2004). We first suspected that our original model for hTR 5' hairpin folding was incorrect, based on the potential for a more canonical 5' hairpin that satisfied the limited amount of structural data on hTR H/ACA motif folding *in vivo* (Antal et al., 2002; Theimer et al., 2007). However, extensive mutagenesis supported the original model of noncanonical 5' hairpin secondary structure. Subsequently, the surprisingly minimal 5' hairpin structural requirements for hTR accumulation led us to suspect that the hTR H/ACA motif was unique in its RNP assembly specificity. However, our studies of two canonical human snoRNAs revealed that they shared the hTR asymmetry of 5' and 3' hairpin requirements for accumulation. Another surprise was the lack of catalytic activity dependence on 5' hairpin structure. This observation suggests that vertebrate TERT has a greater autonomy in organizing TER tertiary structure than ciliate TERT, which likewise binds two separated TER motifs but does so in a manner sensitive to the geometry of intervening stem folding by the holoenzyme protein p65 (Stone et al., 2007). Combined, these findings reveal that the noncanonical hTR H/ACA motif 5' hairpin has evolved in a manner relatively unconstrained by requirements for mature RNA accumulation, unfettered by a requirement for function as an RNA modification guide, and with few if any obligations to the telomeric-repeat synthesis activity of telomerase holoenzyme.

The general asymmetry of 5' and 3' hairpin requirements for H/ACA RNA accumulation has unexpected implications for the pathway of RNP assembly *in vivo*. Our results establish that RNP assembly on the H/ACA motif 5' hairpin does not require the extensive protein-RNA interactions evident in structures of reconstituted archaeal single-stem RNPs (Ye, 2007). In contrast, RNP assembly on the H/ACA motif 3' hairpin does appear to require this large surface of protein-RNA contact. If RNP assembly on the 5' hairpin occurs subsequent to or concerted with RNP assembly on the 3' hairpin, protein-protein interactions across the hairpins could allow the 5' hairpin RNP assembly reaction to have a reduced requirement for protein-RNA interaction. Cross-hairpin interactions could be mediated by dyskerin motifs not present in the archaeal protein ortholog, a hypothesis that would account for the reduced exchange of RNP-assembled dyskerin compared to RNP-assembled NOP10 or NHP2 (Kittur et al., 2006).

Holoenzyme proteins have distinct specificities and stoichiometries of hTR interaction.

The RNP architecture of the human telomerase holoenzyme has been hotly debated. While several studies conclude that a complex of TERT and hTR has catalytic function only with a dimer of each subunit, others studies indicate that such dimerization is neither required nor physiological (Errington et al., 2008; Sekaran et al., 2010). Also, while one study claims that the human telomerase holoenzyme contains only dyskerin, TERT, and hTR (Cohen et al., 2007), other studies establish that the human telomerase holoenzyme assembles all of the H/ACA RNP proteins (Fu and Collins, 2007). Most published models draw one set of H/ACA proteins per telomerase RNP, but we demonstrate that hTR assembles two full sets of H/ACA proteins. Our results define a human telomerase holoenzyme architecture in which each subunit of hTR assembles two sets of H/ACA core proteins as a prerequisite for biogenesis of a biologically

stable telomerase RNP (Fig. 7). A telomerase RNP can then assemble single subunits of TERT and WDR79/TCAB1 to become the holoenzyme functional for telomere maintenance (Fig. 7). Additional hTR binding proteins actively or passively distinguish telomerase RNP subpopulations with differential localization and regulation (Collins, 2008).

Less hTR was recovered with tagged WDR79/TCAB1 than with any tagged H/ACA core protein after a single step of purification or after tandem purification steps using ZF-tagged protein. This lower efficiency of purification was not due to lower tagged protein expression level, because all of the tagged WDR79/TCAB1 proteins were highly overexpressed compared to any of the tagged H/ACA core proteins (data not shown). A relatively low stoichiometry of WDR79/TCAB1 association is consistent with the single peptide of WDR79/TCAB1 detected by mass spectrometry of purified holoenzyme (D. Fu and K.C., unpublished data) and with modification rather than protection of the CAB box in the endogenous pool of telomerase RNP (Antal et al., 2002). Because WDR79/TCAB1 was identified as direct dyskerin binding protein (Venteicher et al., 2009) and because other dyskerin binding proteins that interact with the core heterotrimer trade places during RNP biogenesis and regulation (Darzacq et al., 2006), we hypothesized that WDR79/TCAB1 could promote telomerase function by displacing GAR1. In contrast to predictions of this model, GAR1 association with hTR was unaffected by overexpression of WDR79/TCAB1 or by hTR CAB box mutation (data not shown). Relatively low occupancy of hTR by WDR79/TCAB1 may have precluded our ability to detect binding competition with GAR1, but the CAB-box dependence of WDR79/TCAB1 association with hTR suggests that it may not need to compete with GAR1 for telomerase RNP interaction. It seems plausible that the single hTR CAB box results in only partial telomerase RNP occupancy with WDR79/TCAB1 *in vivo*. The maximal single-subunit stoichiometry of WDR79/TCAB1 association with hTR distinguishes it from H/ACA snoRNAs and scaRNAs, perhaps sensitizing telomerase RNP to its unique dynamic of TERT-dependent and cell-cycle-regulated partitioning between nucleoli, Cajal bodies, and nucleoplasm.

Figure 1, part 1

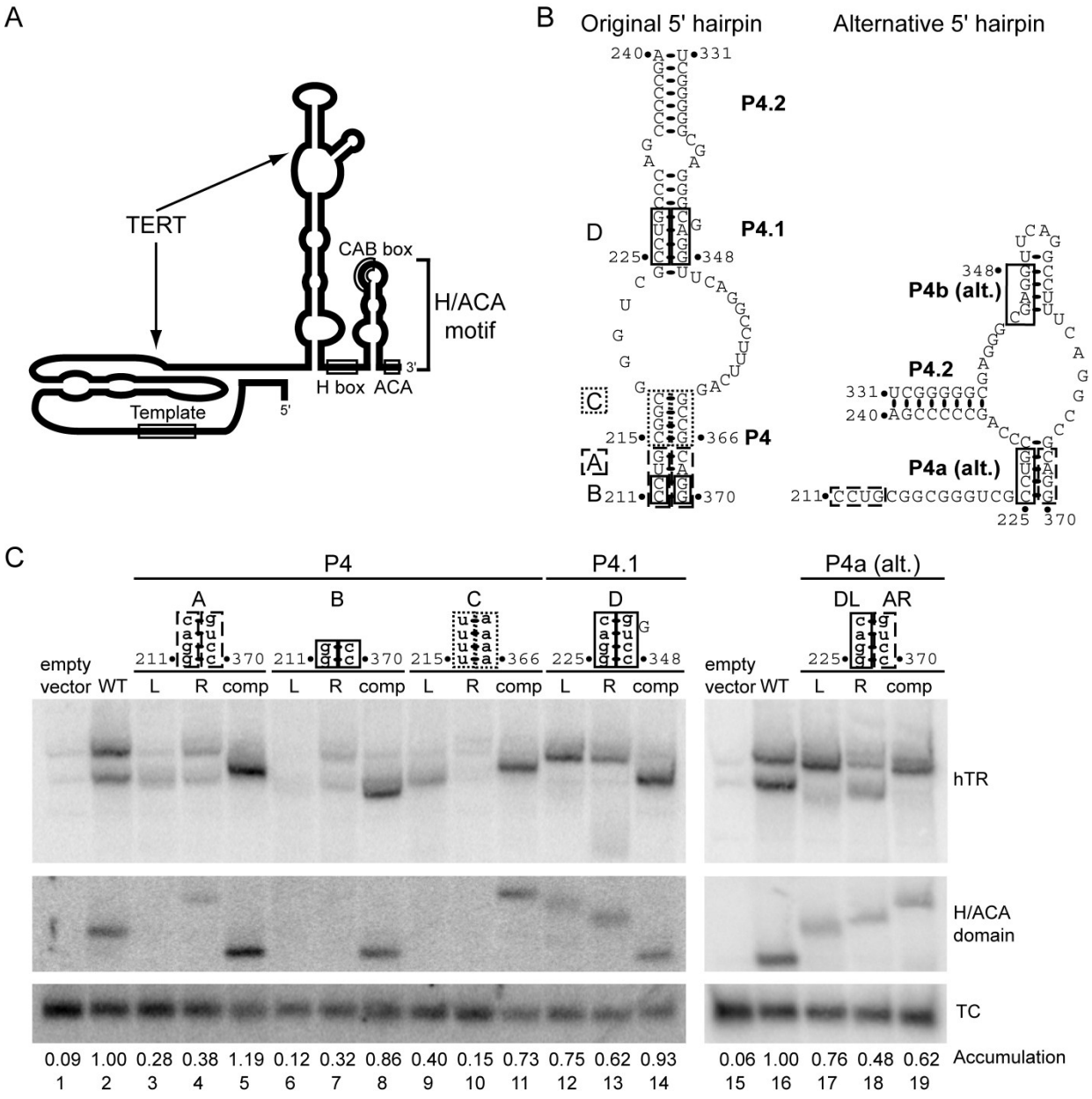

Figure 1, part 2

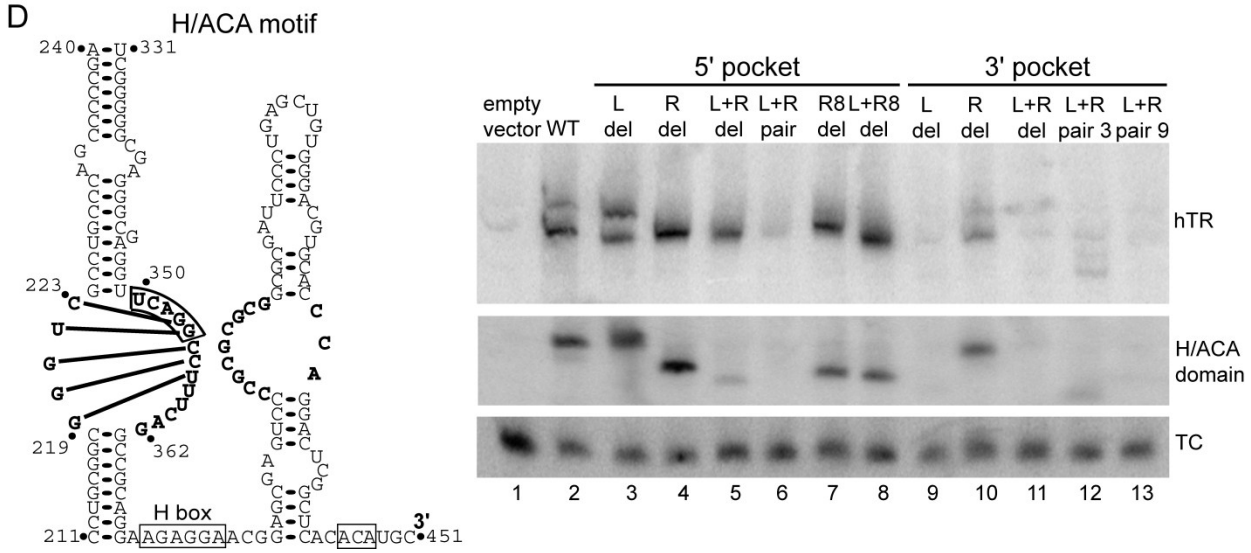

The hTR H/ACA motif 5' hairpin is noncanonical and has few structural requirements for hTR accumulation. (A) Secondary structure and primary sequence motifs of hTR are illustrated. (B) At left, the secondary structure of the originally proposed hTR H/ACA motif 5' hairpin is shown with boxes around four or two nt on each side of the putative stem pairings tested by substitution. At right is shown an alternative, more canonical secondary structure model for the H/ACA motif 5' hairpin based on a 5' domain boundary at position 225. P4, P4.1, and P4.2 are paired elements predicted by phylogenetic comparison; P4a (alt.) and P4b (alt.) are alternative pairings of the residues involved in P4 and P4.1. (C) Total RNA from transfected 293T cells was examined by blot hybridization. Empty vector lanes provide a background control for detection of endogenous hTR compared to recombinant wild-type (WT) hTR or the hTR variants indicated. Full-length hTR, the 5' processed hTR H/ACA domain, and the transfection control (TC) were detected on the same blot. In the boxed and numbered regions of hTR secondary structure taken from (B), the substituted sequences tested in (C) are specified. L and R indicate left and right side of stem pairings as illustrated. (D) Total RNA from transfected 293T cells was examined by blot hybridization. At left is shown the hTR H/ACA motif from the most recent secondary structure model based on phylogenetic comparison. Pocket sequences are highlighted in bold. L del, R del, L+R del indicate deletion of the left, right, or combined sides of the pocket. Pairings forced in the hTR variant of lane 6 are shown with connecting lines; all other pocket residues were deleted. The five right-side pocket residues retained in the hTR variants of lanes 7-8 are boxed; the other eight right-side pocket residues were deleted (R8 del).

Figure 2

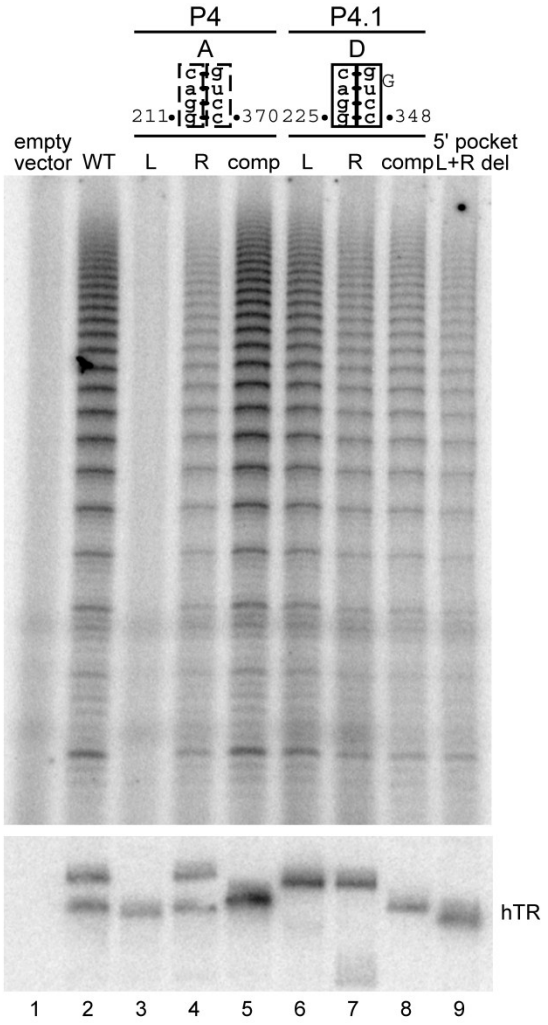

Holoenzyme catalytic activity does not require any specific paired region of the 5' hairpin stem or the 5' hairpin pocket. Direct primer extension activity assays were performed using extracts of VA13+TERT cells transfected to express the indicated hTR variants. Levels of hTR in the extracts are shown by blot hybridization; note that the hTR variant of lane 8 was slightly under-accumulated in this set.

Figure 3

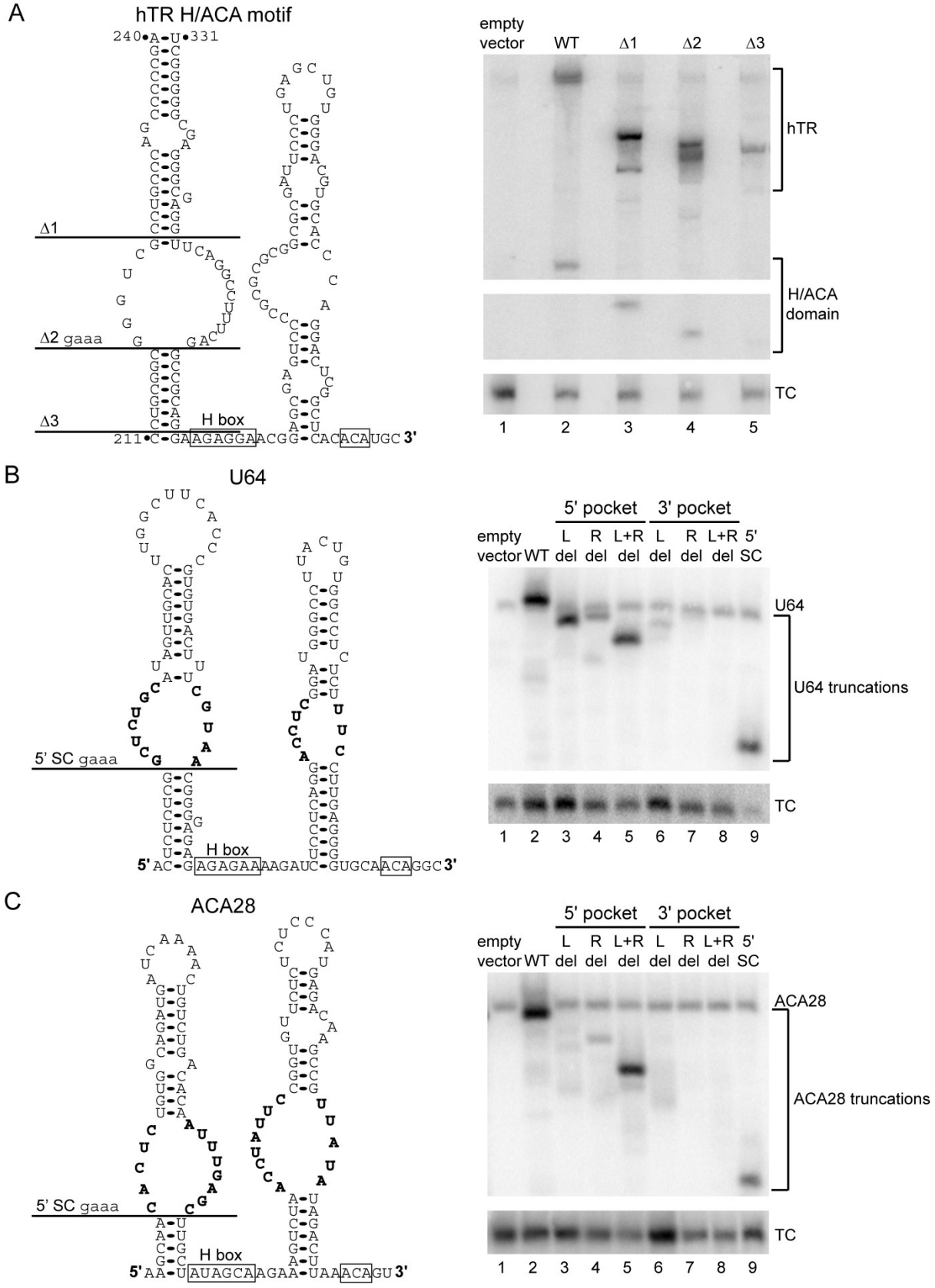
A
hTR H/ACA motif
240•A-U•331
Δ1
Δ2 gaaa
Δ3
H box
211•C-GAAGAGGAACGG-CACACAUGC 3'
empty vector
WT
Δ1
Δ2
Δ3
hTR
H/ACA domain
TC
1 2 3 4 5
B
U64
5' SC gaaa
H box
5' AC-GAGAGAAAAGAUC-GUGCAACAGGC 3'
5' pocket
3' pocket
empty vector
WT
L del
R del
L+R del
L del
R del
L+R del
5' SC
U64
U64 truncations
TC
1 2 3 4 5 6 7 8 9
C
ACA28
5' SC gaaa
H box
5' AA-UAUAGCAAGAA-UAAACAGU 3'
5' pocket
3' pocket
empty vector
WT
L del
R del
L+R del
L del
R del
L+R del
5' SC
ACA28
ACA28 truncations
TC
1 2 3 4 5 6 7 8 9

A minimal 5' hairpin stem is sufficient for accumulation of hTR and snoRNAs. Total RNA from transfected 293T cells was examined by blot hybridization. At left are shown secondary structures of the hTR H/ACA domain phylogenetic model (A), the human snoRNA U64 (B), and the human snoRNA ACA28 (C). Positions of internal deletion are indicated; only hTR Δ2 and the snoRNA 5' stem cap (SC) deletions insert a GAAA tetraloop in place of the deleted sequence. Human snoRNA pocket sequences are highlighted in bold. L del, R del, L+R del indicate deletion of the left, right, or combined left and right sides of the pocket.

Figure 4

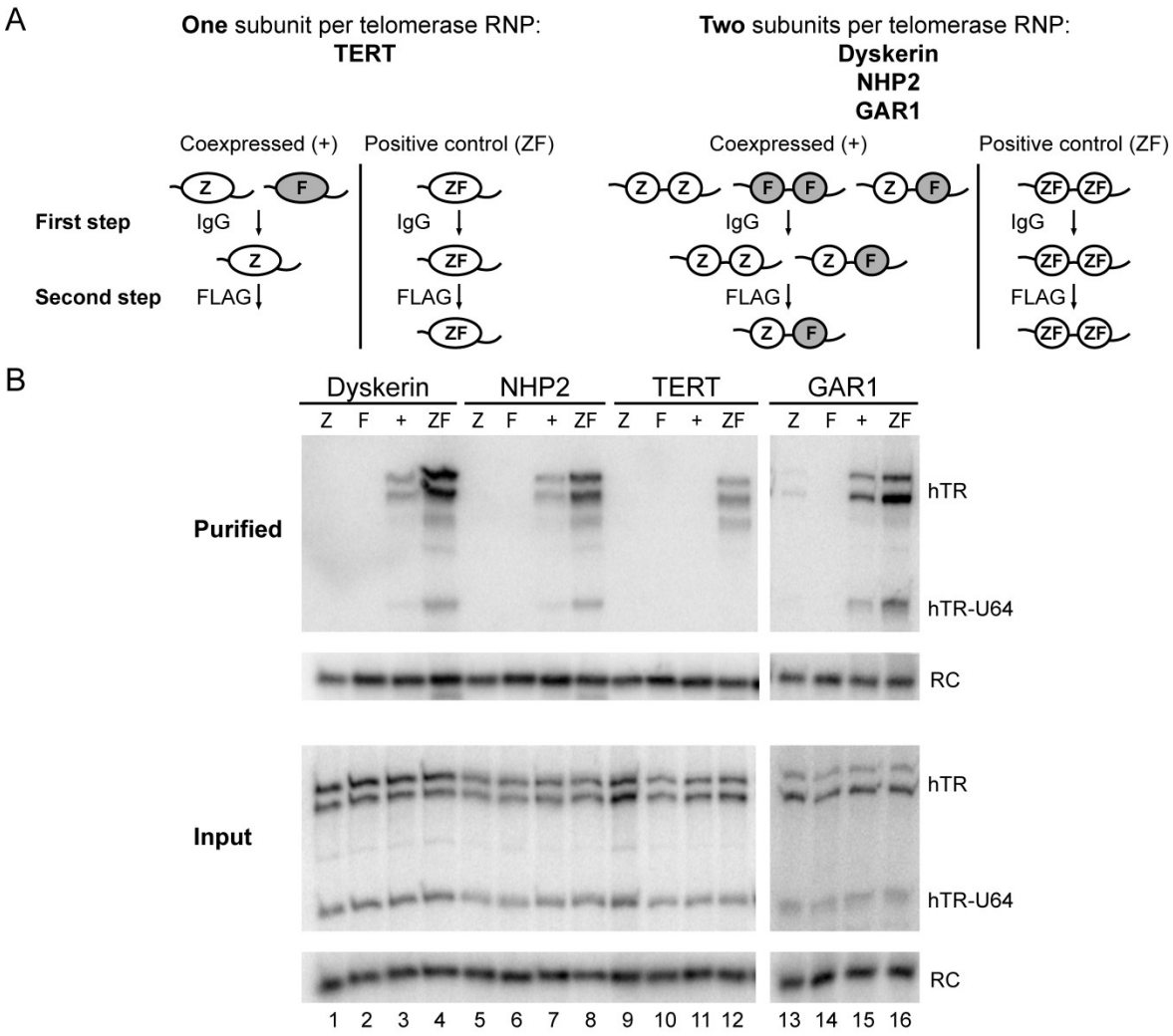

Two subunits of dyskerin, NHP2, and GAR1 assemble on each molecule of hTR. (A) Schematic of the tandem affinity purification strategy for discriminating subunit stoichiometry. (B) Extracts from 293T cells transfected to express a protein with the tag(s) indicated (Z, F, +, ZF), wild-type hTR, and the hTR-U64 chimera were subject to tandem steps of affinity purification. Input cell extracts (2%) and final purified RNP elutions (100%) were supplemented with a recombinant RNA recovery control (RC) prior to RNA extraction. Input and purified samples for the GAR1 panel were from a separate set of transfections and purifications.

Figure 5

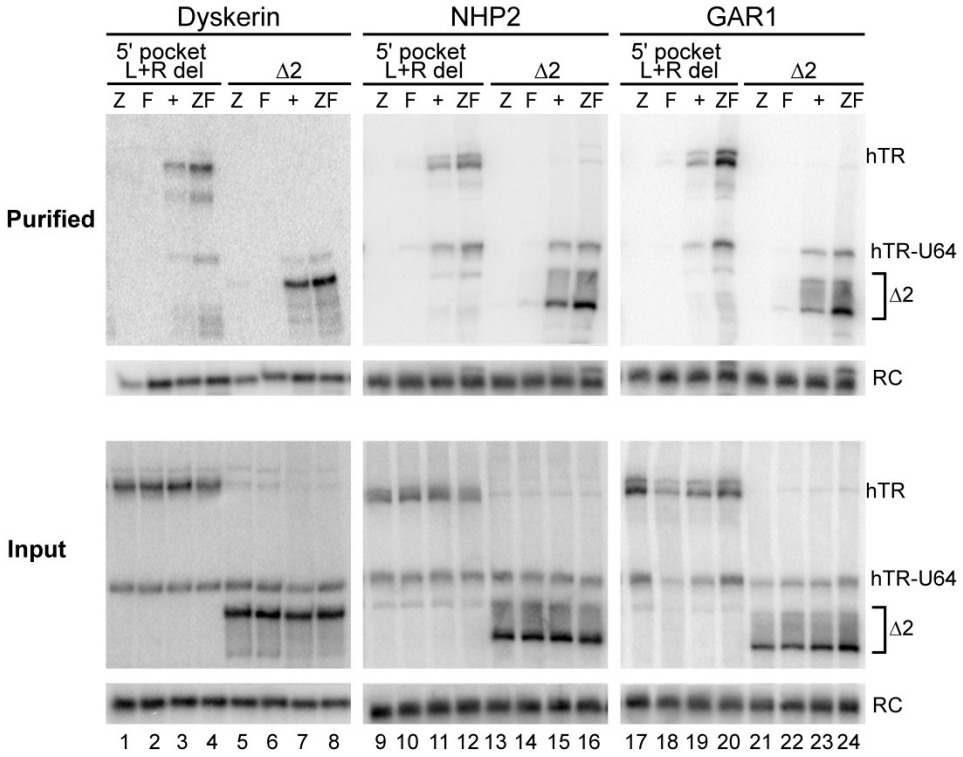

Two subunits of dyskerin, NHP2, and GAR1 assemble on hTR variants lacking consensus elements of the 5' hairpin. Extracts from 293T cells transfected to express a protein with the tag(s) indicated (Z, F, +, ZF), hTR-U64, and one of two hTR variants (5' pocket L+R del from Fig. 1D or Δ2 from Fig. 3A) were subject to tandem steps of affinity purification. RNAs in the input and purified material were analyzed as described for Fig. 4. Note that hTR Δ2 migrated with different mobility depending on sample heating. The input and purified samples of any given protein were analyzed in parallel.

Figure 6

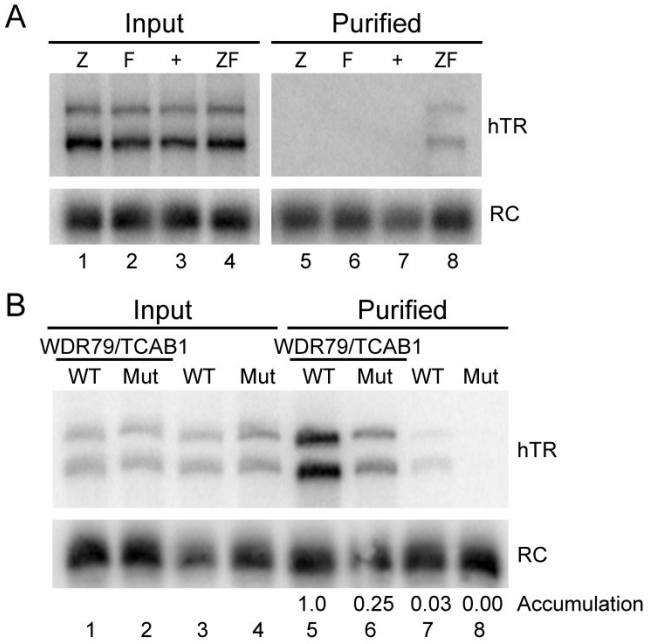

Association of WDR79/TCAB1 is influenced by the hTR CAB box. (A) Extracts from 293T cells transfected to express hTR and WDR79/TCAB1 with the tag(s) indicated (Z, F, +, ZF) were subject to tandem steps of affinity purification. RNAs in the input and purified material were analyzed as described for Fig. 4. (B) Extracts of VA13+TERT cells transfected to express either Z-tagged WDR79/TCAB1 or empty vector and either wild-type (WT) hTR or the G414C CAB-box mutant (Mut) were used for single-step affinity purification. RNAs in the input and purified material were analyzed as described above.

Figure 7

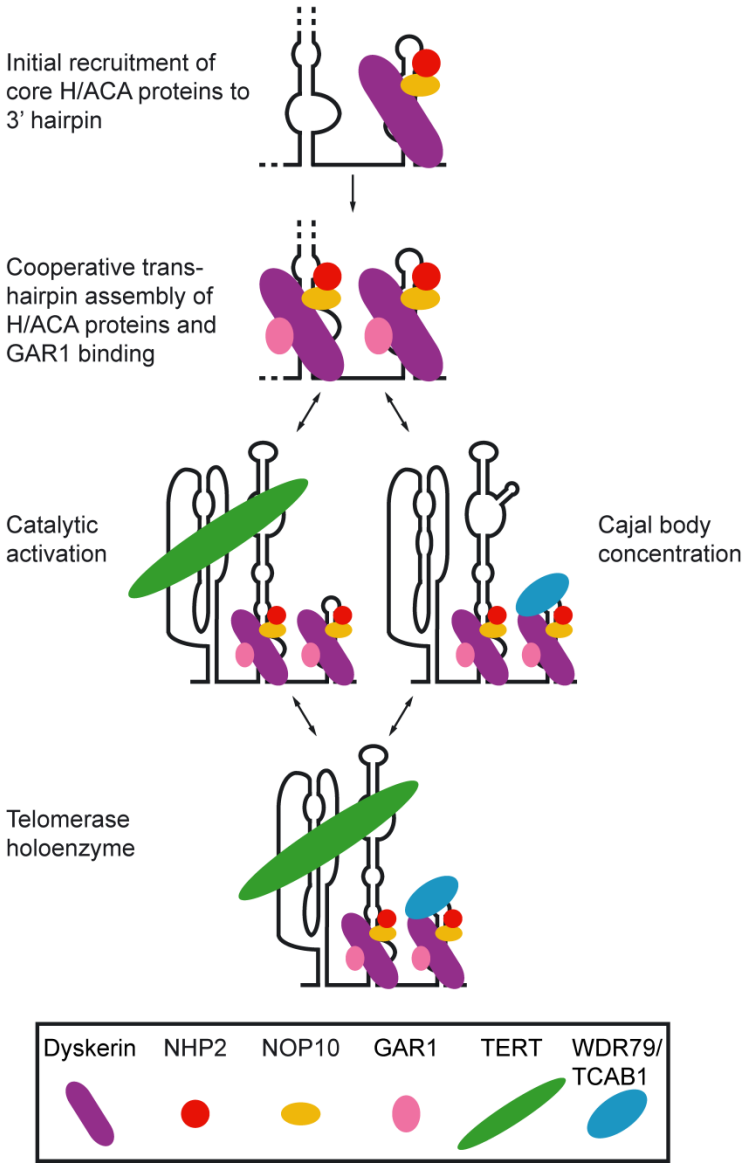

Interaction specificity and stoichiometry of telomerase holoenzyme proteins. Initial recruitment of H/ACA proteins is proposed to involve an association of dyskerin, NOP10, and NHP2 with the hTR 3' hairpin, scaffolded by extensive protein-RNA interactions. Either sequentially (as shown) or in concerted manner, there is assembly of a second H/ACA protein heterotrimer. Assembly of the second set of H/ACA proteins is proposed to have a reduced requirement for RNA interaction surface due to the formation of cross-hairpin protein-protein interaction(s). Following hTR release from the site of transcription, an exchange of biogenesis factors for GAR1 yields the mature telomerase RNP with two full sets of all four H/ACA RNP proteins. Motifs of hTR not required for stable RNP biogenesis can associate independently with TERT and WDR79/TCAB1, both of which are likely substoichiometric in the overall population of endogenous telomerase RNP.

CHAPTER THREE

An Enhanced H/ACA RNP Assembly Mechanism for Human Telomerase RNA

Abstract

The integral telomerase RNA subunit templates the synthesis of telomeric repeats. The biological accumulation of human telomerase RNA (hTR) requires hTR H/ACA domain assembly with the same proteins that assemble on other human H/ACA RNAs. Despite this shared RNP composition, hTR accumulation is particularly sensitized to disruption by disease-linked H/ACA protein variants. We show that contrary to expectation, hTR-specific sequence requirements for biological accumulation do not act at an hTR-specific step of H/ACA RNP biogenesis; instead, they enhance hTR binding to the shared, chaperone-bound scaffold of H/ACA core proteins that mediates initial RNP assembly. We recapitulate physiological H/ACA RNP assembly with a preassembled NAF1/dyskerin/NOP10/NHP2 scaffold purified from cell extract and demonstrate that distributed sequence features of the hTR 3' hairpin synergize to improve scaffold binding. Our findings reveal that the hTR H/ACA domain is distinguished from other human H/ACA RNAs not by a distinct set of RNA-protein interactions but by an increased efficiency of RNP assembly. Our findings suggest a unifying mechanism for human telomerase deficiencies associated with H/ACA protein variants.

Introduction

Incomplete genome replication by DNA-templated DNA polymerases can lead to progressive shortening of the telomeric repeats that cap eukaryotic nuclear chromosomes (O'Sullivan and Karlseder, 2010). To maintain chromosome integrity, the RNP enzyme telomerase compensates for terminal sequence loss by new repeat synthesis, for example adding tandem repeats of TTAGGG in human cells. At the catalytic core of human telomerase, a structured 451-nucleotide (nt) telomerase RNA (hTR) provides the template for repeat synthesis by telomerase reverse transcriptase (Zhang et al., 2011). Numerous proteins must associate with hTR to direct the biological specificity of precursor synthesis, processing, and RNP assembly as well as to direct mature RNP trafficking, localization, and catalytic activation (Blackburn and Collins, 2010). Improved knowledge of human telomerase RNP biogenesis and regulation should provide new strategies for enzyme activation and inhibition as disease therapies (Shay and Wright, 2010).

Human and other vertebrate telomerase RNAs, but not ciliate or yeast telomerase RNAs, have a 3' domain shared with the evolutionarily ancient H/ACA RNA family (Chen et al., 2000; Mitchell et al., 1999a). H/ACA RNAs generally function as guides for site-specific pseudouridylation of a target RNA. Eukaryotic H/ACA small nucleolar (sno) RNAs modify ribosomal RNAs, while small Cajal body (sca) RNAs modify small nuclear RNAs (Hamma and Ferre-D'Amare, 2010; Kiss et al., 2010). Eukaryotic H/ACA RNAs have a universally conserved 5’ hairpin-Hinge (H box)-3’ hairpin-ACA structure, including unpaired pockets in the hairpin stems that hybridize to target RNA sequence flanking the substrate uridine. The hairpin pockets of vertebrate telomerase RNAs show little if any phylogenetic sequence conservation (Podlevsky et al., 2008), and no complementary putative target RNA(s) have been identified. In contrast to this functional divergence, hTR and pseudouridylation guide RNAs share the cellular requirement for structural integrity of the H/ACA motif, including the H box (ANANNA) and ACA sequences, as a prerequisite for assembly of a biologically stable RNP. The 5' hairpin of the hTR H/ACA motif deviates from pseudouridylation guide RNA consensus in its atypical spacing of the apex of the 5’ hairpin pocket from the H box, but the H box and lower stem of the 5' hairpin are nonetheless critical for hTR maturation and RNP accumulation *in vivo* and the presence of a hairpin pocket is strongly stimulatory (Egan and Collins, 2010; Mitchell et al., 1999a; Mitchell and Collins, 2000). Therefore, albeit with structural deviations, the hTR H/ACA domain shares the two-hairpin secondary structure common to all eukaryotic H/ACA RNAs.

Assays of protein recruitment to an ectopic site of H/ACA RNA synthesis suggest that four proteins become rapidly associated with the RNA transcript: dyskerin, NOP10, NHP2, and NAF1 (Darzacq et al., 2006). Cotranscriptional RNP assembly protects the H/ACA RNA sequence from alternative processing or exonucleolytic degradation (Ballarino et al., 2005; Richard et al., 2006; Yang et al., 2005). The RNP subunit with pseudouridylase activity, termed dyskerin in human cells (also NAP57 or Cbf5p), binds to NOP10, which in turn binds to NHP2 to constitute the core heterotrimer (Hamma and Ferre-D'Amare, 2010; Kiss et al., 2010). Dyskerin also binds the H/ACA RNP assembly chaperone NAF1 (Fatica et al., 2002), which is exchanged after initial RNP assembly for the fourth mature RNP protein GAR1 (Darzacq et al., 2006). Reticulocyte lysate-expressed core heterotrimer proteins alone, with or without NAF1 or GAR1, can bind an H/ACA RNA (Trahan and Dragon, 2009; Wang and Meier, 2004). *In vivo* this assembly depends on NAF1 and additional H/ACA RNP biogenesis factors including the Pol II-associated protein NUFIP and RNA/RNP remodeling enzymes such as the helicase-domain

proteins RUVBL1/PONTIN and RUVBL2/REPTIN (Kiss et al., 2010). Extensive chaperoning of the H/ACA RNP assembly process may account for the technical barrier to eukaryotic core heterotrimer reconstitution as intact RNP. No high-resolution structural studies have been successful for the complete eukaryotic core heterotrimer; only structures of protein complexes lacking NHP2 have been very recently described (Li et al., 2011a; Li et al., 2011b).

Archaeal pseudouridylation guide RNAs bind dyskerin, NOP10, and an NHP2-related protein L7Ae, but unlike the eukaryotic RNAs they can autonomously assemble a single-hairpin RNP (Dennis and Omer, 2005). High-resolution structures of reconstituted single-stem archaeal RNP assemblies reveal that the archaeal ortholog of dyskerin contacts a large RNA surface spanning the ACA, lower hairpin stem, and 3' side of the pocket (Duan et al., 2009; Li, 2008; Liang et al., 2009). RNA structural requirements to maintain this contact surface rationalize the conserved 14-16 nt spacing of an H box or ACA from the apex of the preceding hairpin pocket. In contrast to dyskerin, which has an evolutionarily conserved RNA binding specificity, the RNA binding specificity of archaeal L7Ae is different from eukaryotic NHP2: L7Ae recognizes a defined kink-turn motif, while NHP2 shows weaker general RNA binding activity (Henras et al., 2001; Klein et al., 2001; Nolivos et al., 2005). Accordingly, L7Ae binds RNA dependent only on RNA sequence while the RNA binding specificity of NHP2 derives from its assembly with other eukaryotic H/ACA proteins.

All known vertebrate pseudouridylation guide RNAs are 5’- and 3’-processed from introns of host mRNAs (Kiss et al., 2010). In contrast, vertebrate telomerase RNAs are unspliced transcripts of Pol II that must be only 3'-processed to the hTR H/ACA domain boundary (Fu and Collins, 2003; Mitchell et al., 1999a; Mitchell and Collins, 2000; Theimer et al., 2007). The template-containing hTR 5’ extension is not removed and instead gains a trimethylguanosine cap added by the nuclear (short) form of the methyltransferase TGS1 (Feng et al., 1995; Girard et al., 2008; Mitchell et al., 1999a). RNP biogenesis steps required for hTR maturation but not for maturation of intron-encoded human H/ACA RNAs could account for why hTR accumulation is uniquely affected by H/ACA protein gene mutations that underlie diseases such as the bone marrow failure syndrome dyskeratosis congenita (DC). X-linked DC patient cells that express a variant dyskerin have reduced levels of hTR and prematurely short telomeres, but they show little if any general change in H/ACA snoRNAs and scaRNAs (Batista et al., 2011; Mitchell et al., 1999b; Wong and Collins, 2006). Here, we describe the mechanism by which hTR sequence features distinguish H/ACA RNP assembly on hTR from assembly of the same RNP on other human H/ACA RNAs. Instead of a difference in the pathway of RNP assembly, we find that hTR-specific *in vivo* requirements for RNP assembly act to stimulate a common, direct step of RNA-protein interaction. Our findings have implications for the specialized assembly requirements of hTR versus other H/ACA RNAs and for the mechanism of eukaryotic H/ACA RNP assembly in general.

Materials and Methods

Cell culture and expression constructs.

Human 293T and HeLa cells were cultured in DMEM with 10% fetal bovine serum and transiently transfected using the calcium phosphate method or lipofection with Lipofectamine (Invitrogen), respectively. The pBS-U3-hTR-500 and pBS-U3-hTR H/ACA-500 expression constructs for mature hTR and the hTR H/ACA domain, the snoRNA expression vectors pBS-U3-U64-500 and pBS-U3-ACA28-500, and the *Tetrahymena* TER transfection control (TC) expression construct have been previously described (Egan and Collins, 2010; Fu and Collins, 2003). Hammerhead and hepatitis δ virus self-cleavage motifs were used as previously published (Bird et al., 2005; Dower et al., 2004). Tagged proteins were expressed as N-terminal fusions in a pcDNA-ZZ-TEV (where ZZ represents two IgG-binding domains of Protein A and TEV is a tobacco etch virus protease cleavage site) or pcDNA-ZZ-TEV-calmodulin binding peptide (pcDNA-TAP) plasmid backbone. *In vitro* transcription templates were constructed by cloning DNA sequences encoding a full-length RNA or 3' hairpin into the Pvu II site of pBluescript with retention of the Pvu II site at the 3' end. The tagged RNAs harbor a *Pseudomonas* phage 7 (PP7) hairpin sequence (Chao et al., 2008) and a linker (AGUC) followed by the hTR 3' hairpin sequence. All constructs were verified by sequencing.

Blot detection of RNA and protein.

RNA was purified using TRIzol according to the manufacturer's protocol (Invitrogen). For analysis of total RNA, 10-20 μg was loaded on a 5% or 6% acrylamide, 7 M urea, 0.6X TBE gel. Northern blots were performed as previously described, using end-labeled complementary oligonucleotides as probes (Egan and Collins, 2010; Fu and Collins, 2003). The hTR H/ACA domain was detected using an end-labeled DNA probe complementary to nt 371-398; the ACA28 probe was complementary to nt 79-107, and the U64 probe was complementary to nt 54-72. Northern blots were imaged using a Typhoon Trio phosphorimaging system (GE Healthcare). Quantification of hybridization signal intensity was adjusted for background and then normalized relative to the relevant control signal in the same lane. Immunoblots to verify tagged protein expression (data not shown) used rabbit IgG primary antibody (Sigma) and were imaged using a LI-COR Odyssey system.

RNA synthesis and purification.

RNAs were generated using T7 RNA polymerase and Pvu II-digested plasmid templates. Radiolabeling was performed by incorporation of [α-^{32}P]-UTP (NEN/Perkin Elmer). RNAs were resolved by electrophoresis on a 6% acrylamide, 7 M urea, 0.6X TBE gel, excised from the gel and eluted in 0.3 M sodium acetate overnight at 37°C followed by ethanol precipitation. The concentrations of purified RNAs were determined by absorbance and their quality verified by electrophoresis and SYBR gold staining or autoradiography.

RNP assembly in extract.

RNP assembly was performed in 10 μL reactions containing ~20 μg of HeLa whole cell extract total protein obtained from freeze-thaw lysis in a final buffer of 20 mM HEPES at pH 8.0, 2 mM $MgCl_2$, 0.2 mM EGTA, 10% glycerol, 0.1% Igepal, 0.1 mM PMSF, 100 mM NaCl, 5 mM DTT, 0.25 μL of RNasin (Promega), 500 ng of yeast tRNA (Sigma), and loading dyes. Approximately 50 pg of radiolabeled RNA probe was added and reactions were incubated at

30°C for 1 hour followed by a 10 min chase with 1.5 µg of heparin. Cold competitor RNAs were preincubated at 30°C for 30 min in the presence of all components except radiolabeled RNA. RNP complexes were resolved by electrophoresis on a 5% acrylamide, 0.5X TBE gel at 4°C. Gels were dried and imaged using the Typhoon Trio.

RNP assembly and detection of radiolabeled RNA.

For affinity purification of RNPs using a tagged protein, cell extracts from freeze-thaw lysis were diluted to ~2.5 mg/mL in binding buffer (20 mM HEPES at pH 8.0, 100 mM NaCl, 2 mM $MgCl_2$, 0.2 mM EGTA, 10% glycerol, 0.1% Igepal, 1 mM DTT, and 0.1 mM PMSF). A 100-150 µL volume of diluted extract was clarified by centrifugation and adjusted to a final concentration of 5 mM DTT and supplemented with 0.5 µL of RNasin. The extract was incubated at 30°C for 20-30 min with ~5 ng of radiolabeled RNA. Then 2.5 µL of packed IgG agarose (Sigma) prewashed in 1 mL of binding buffer was added, and samples were rotated end-over-end for 1-2 hours at 4°C. Alternatively, the IgG agarose purification and RNA incubation steps were reversed, with a single wash at room temperature in 1 mL of binding buffer for 5 min and resuspension of the resin in 50 µL binding buffer plus 100 ng/µL bovine serum albumin in between. Bound RNPs were washed three times at room temperature in 1 mL of wash buffer (binding buffer with 0.1% Triton X-100 and 0.1% CHAPS) for 5 min each wash. Buffer was removed and the resin was resuspended in formamide with EDTA and loading dye then boiled for 5 min. The supernatant was loaded on a 6% acrylamide, 7 M urea, 0.6X TBE gel. Gels were dried and imaged using the Typhoon Trio.

Cellular RNP affinity purification.

For affinity purification of ZZ-tagged NHP2 RNPs assembled *in vivo*, cell extracts from freeze-thaw lysis were diluted to ~0.75 mg/mL in binding buffer as above with 150 mM NaCl. A 900 µL volume of diluted extract was clarified by centrifugation immediately prior to purification using 2.5 µL of prewashed IgG agarose. Samples were rotated end-over-end for 2 hours at 4°C then washed three times at room temperature in 1 mL of wash buffer for 5 min each wash. To elute bound RNPs, ~30 ng/µL of the S219V variant of Tobacco Etch Virus protease was added in a volume of 50 µL of elution buffer (wash buffer with 100 ng/µL bovine serum albumin and 100 ng/µL tRNA), and samples were rotated end-over-end for 30 min at room temperature.

Results

The hTR BIO box functions in collaboration with consensus elements of the H/ACA motif.

The biological accumulation of hTR but not any other studied human H/ACA RNA depends on a sequence motif in the loop of the 3' hairpin (Fig. 1A). The 3' half of this hTR loop contains the biogenesis-promoting box (the BIO box) important for mature RNA accumulation, while the 5' half of the loop contains a CAB box dispensable for RNA accumulation but required for mature RNP concentration in Cajal bodies (Fu and Collins, 2003; Jády et al., 2004; Theimer et al., 2007). Function of both the BIO box and the CAB box depends on the integrity of the adjacent stem, and disruption of this stem imposes autosomal dominant DC (Vulliamy et al., 2001). Previously assayed BIO box sequence substitutions that eliminated mature hTR accumulation either replaced the entire loop or severely disrupted loop structure by introducing additional base pairing (Fu and Collins, 2003; Theimer et al., 2007). In search of a minimal change that selectively disrupts BIO box function without altering the length of the 3' hairpin stem, we assayed additional sequence variants for their impact on mature hTR accumulation.

We expressed hTR precursor using the Pol II expression construct U3-hTR-500, which contains the U3 C/D box snoRNA promoter, mature hTR sequence, and 500 bp of downstream sequence from the endogenous locus. This construct efficiently produces 3' processed hTR that is incorporated into the biologically active telomerase holoenzyme (Fu and Collins, 2003; Wong and Collins, 2006). Total RNA was harvested from transfected human 293T cells, resolved by denaturing polyacrylamide gel electrophoresis (PAGE), and probed by northern blot to detect the accumulation of hTR and an internal loading control (LC). As demonstrated previously, the disruption of CAB box function with the substitution G414C did not inhibit mature hTR accumulation, while deletion of the 3' hairpin upper stem loop or loop replacement with a structured tetraloop reduced hTR accumulation to a level undetectable over the background of endogenous hTR in cells transfected with empty vector (Fig. 1B, lanes 1-3 and 8-9; note that mature hTR often migrates as a doublet due to partial folding). To reduce loop interaction with CAB box binding proteins for purposes of the RNP assembly assays described below, we included the G414C CAB box substitution in 'wild-type' hTR unless indicated otherwise.

Vertebrate telomerase RNAs share absolute conservation of the final loop residue that is hTR U418 (Fig. 1A) and >85% conservation of the preceding guanosine that is hTR G417 (Podlevsky et al., 2008). The NMR structure of a model hTR 3' hairpin stem loop suggests that G417 pairs with U411 (Theimer et al., 2007). Although the G417C substitution strongly reduced hTR RNP accumulation monitored by RNase protection (Theimer et al., 2007), substitution of G417 with adenosine had little impact (Fig. 1B, lane 4), perhaps because A-U base pairing would still be possible. In contrast, substitution of the absolutely conserved U418 with cytidine strongly reduced mature hTR accumulation (Fig. 1B, lane 5). The combination of these two substitutions was no more deleterious than the U418C substitution alone (Fig. 1B, lane 6). Substitution of the entire 3' hairpin loop with the U17 snoRNA 3' hairpin loop CUGUC, which contains the BIO box sequence with an extra 3' cytidine, did not provide full BIO box function (Fig. 1B, lane 7). Because the U418C substitution substantially reduced mature hTR accumulation *in vivo* without changing 3' hairpin stem or loop length, we used this substitution for BIO box disruption in subsequent studies.

Surprisingly, it has not been addressed whether the BIO box functions autonomously or in coordination with the H/ACA motif. To investigate potential positioning-dependent coordination between the BIO box and the H/ACA motif, we altered or extended 3' hairpin base

pairing in the upper stem (Fig. 1C). We found that deleting or pairing a predicted internal loop in the upper stem did not severely inhibit mature hTR accumulation (Fig. 1C, lanes 3-5). In contrast, insertion of additional base pairs in the upper stem reduced mature hTR accumulation in proportion to the increase in stem length: insertion of two base pairs only partially inhibited hTR accumulation, while the insertion of eight base pairs reduced hTR accumulation to undetectable above background (Fig. 1C, lanes 6-7). Similar inhibition of mature hTR accumulation was observed when five or eight base pairs were added to a 3' hairpin upper stem that retained the wild-type internal loop (Fig. 1C, lanes 8-9). Accumulation was not restored by insertion of eleven base pairs, which would present the BIO box on the same helical face as in wild-type hTR (Fig. 1C, lane 10). We also attempted to functionally transplant an ectopic BIO box to other positions of mature or precursor hTR without achieving a rescue of the accumulation defect imposed by U418C substitution of the native BIO box (data not shown). Together these results suggest that the physical spacing between the BIO box and the 3' hairpin pocket is critical for BIO box function.

BIO box function does not require Pol II-coupled precursor expression or 3' end formation.

The BIO box remains critical for RNA accumulation even if the noncanonical hTR H/ACA motif is swapped for a canonical H/ACA snoRNA (Fu and Collins, 2003). However, BIO box function is not required if the hTR H/ACA domain accumulates by processing from a spliced intron rather than an unspliced autonomous transcript (Theimer et al., 2007). Together these findings suggested that BIO box function is coupled to transcription context. This hypothesis has support from precedent, because transcription-coupled association of processing factors with nascent yeast H/ACA snoRNA transcripts determines their specificity of 3' end formation and processing as snoRNAs (Steinmetz et al., 2001).

To investigate whether BIO box function is dependent on hTR H/ACA domain expression as an autonomous transcript of Pol II, we compared the BIO box dependence of hTR H/ACA domain accumulation in a Pol II versus Pol III expression context (Fig. 2A). Pol III does not support the synthesis of full-length hTR due to the presence of internal polyuridine tracts (Mitchell et al., 1999a). Therefore, the U3-hTR H/ACA-500 expression vector, which includes only the hTR H/ACA domain (nt 203-451), was minimally altered to create U6-hTR H/ACA-500, which replaces the human U3 C/D-box snoRNA Pol II promoter with the human U6 small nuclear RNA Pol III promoter. The hTR H/ACA domain has been shown to be 5'- and 3'-processed from a full-length hTR transcript *in vivo* (Mitchell and Collins, 2000). As expected from previous work, BIO box mutation reduced hTR H/ACA domain accumulation from the Pol II-transcribed precursor (Fig. 2B, lanes 1-3). Unexpectedly, BIO box mutation also reduced the accumulation of a Pol III-transcribed RNA that migrates with the mobility expected for a properly 5'- and 3'-processed hTR H/ACA domain (Fig. 2B, lanes 4-5). Based on blot hybridization results (data not shown), longer RNAs produced by Pol III are likely to be polyuridine-terminated primary transcripts protected from 3' end trimming by La protein. We conclude that although the efficiency of processing is affected by transcription context, the BIO box can promote hTR H/ACA RNP accumulation independent of the transcribing polymerase and its associated factors.

Even if forced to be uncoupled from primary transcript synthesis, the BIO box could still function to recruit productive 3' end processing machinery. For example, the BIO box could promote endonucleolytic cleavage of the primary transcript to override polyadenylation-induced nuclear export or degradation. This model has the appeal of accounting for a complete lack of a

recognizable or required 3' end formation signal downstream of mature hTR at its genomic locus (Feng et al., 1995; Fu and Collins, 2003; Mitchell et al., 1999a). We tested this model by inserting a self-cleaving ribozyme (RZ) after the 3' end of mature hTR in an attempt to rescue the accumulation defect imposed by BIO box mutation (Fig. 2C). We inserted either a minimal hammerhead RZ or a hepatitis δ virus RZ, the latter of which is reported to undergo particularly rapid cotranscriptional cleavage (Fong et al., 2009). Surprisingly, although either RZ improved the accumulation of wild-type or BIO box mutant hTR, neither rescued the relative accumulation deficit imposed by BIO box disruption (Fig. 2D, compare lane 2 to lanes 3-4 and lane 5 to lanes 6-7; also lanes 2-4 to lanes 5-7). These findings suggest that the formation or persistence of a precursor 3' end can be rate-limiting for hTR accumulation, such that RZ self-cleavage and/or formation of a nuclease-resistant 2'3' cyclic phosphate promotes mature hTR production. In addition, towards understanding the role of the BIO box, the findings above indicate that the hTR requirement for a BIO box is independent of the precursor 3' end formation mechanism.

The BIO box promotes hTR 3' hairpin RNP assembly.

Instead of acting at an hTR-specific step of RNA processing, the BIO box could act at an early RNP assembly step by directly binding to a recruiting factor for H/ACA proteins. In this scenario, the hTR-specific requirement for the BIO box would derive from the need for hTR RNP assembly to compete with the more rapid degradation of its precursor relative to intron-encoded H/ACA RNA precursors, which would be protected from exonucleolytic degradation within a host mRNA transcript. Consistent with the hypothesis above, RNP assembly monitored by electrophoretic mobility shift assay (EMSA) indicated that HeLa cell extract assembled a distinct complex on the hTR H/ACA domain in addition to the complexes formed by both hTR and H/ACA snoRNAs (Dragon et al., 2000). The hTR 3' hairpin with a wild-type CAB box and BIO box (both uncharacterized at the time) could compete for RNP assembly on the entire hTR H/ACA domain (Dragon et al., 2000). We therefore used HeLa whole cell extract to determine whether the BIO box has a stimulatory role in RNP assembly on a pretranscribed RNA. We used radiolabeled hTR 3' hairpin with the internal loop of the upper stem paired to promote stable folding (variant B in Fig. 1C) and with the CAB box disruption G414C to inhibit loop binding by the proteins that mediate Cajal body localization. RNA containing only these substitutions was the 'wild-type' backbone for BIO box disruption by U418C substitution or ACA disruption by trinucleotide replacement with UGU (BIO and ACA variants, respectively).

When incubated with HeLa whole cell extract, the reference wild-type hTR 3' hairpin assembled an RNP with a discrete shift in electrophoretic mobility (Fig. 3A, lanes 1-2). This RNP assembly was sensitive to increasing salt concentration but was still detectable in the presence of 300 mM NaCl (Fig. 3A, lanes 2-4). RNPs assembled by the BIO and ACA variant RNAs migrated faster than RNPs assembled on the wild-type RNA and were nearly eliminated by only 200 mM NaCl (Fig. 3A, lanes 6-8 and 10-12). Disruption of the salt-stable RNA mobility shift by BIO box or ACA mutation suggested that the BIO box could have a role in promoting RNP assembly.

To better compare the relative RNP assembly efficiencies of the wild-type versus BIO and ACA variant RNAs, we measured the ability of unlabeled competitor RNAs to inhibit RNP assembly on the radiolabeled wild-type RNA (Fig. 3B). Varying concentrations of unlabeled competitor RNA were preincubated with whole cell extract and other buffer components before radiolabeled wild-type 3' hairpin RNA was added. Unlabeled wild-type RNA inhibited RNP assembly to half-maximum at a concentration of 0.1 ng/μL, an approximately 20-fold excess

over the limiting radiolabeled RNA (Fig. 3B, lane 4). In contrast, BIO box mutant RNA at an over 2,000-fold excess or ACA mutant RNA at an over 20,000-fold excess of was required to achieve half-maximal inhibition (Fig. 3B, lane 9 or 13). We conclude that the U418C BIO box mutation reduced hTR 3' hairpin RNP assembly efficiency significantly but to a lesser extent than mutation of the ACA motif. This parallels the impact of BIO box or ACA mutation on hTR accumulation *in vivo*.

The BIO box promotes direct H/ACA protein-RNA interaction.

The BIO box and ACA dependence of RNP assembly on a pretranscribed RNA suggested that whole cell extract reconstituted a physiological H/ACA RNP complex, but this was not conclusively established by EMSA alone. To further investigate the nature of the RNP assembled in whole cell extract, we used extracts from HeLa cells overexpressing a protein of interest N-terminally tagged by fusion to tandem IgG binding domains (the ZZ tag). All tagged proteins used here were robustly and comparably overexpressed in transfected cells, as quantified by immunoblots of whole cell extract (data not shown). After radiolabeled RNA incubation in cell extract, RNPs containing the tagged protein were recovered on IgG resin, washed, and quantified using denaturing PAGE. In this assay, the amount of recovered radiolabeled RNA indicates the success of its assembly into RNP complexes containing the protein of interest.

We first applied this approach to the H/ACA RNP proteins dyskerin, NHP2, and GAR1 (NOP10 is refractory to tagging, but since it is the bridge between dyskerin and NHP2, its presence can be inferred). To reduce extract-mediated degradation of the radiolabeled RNA during affinity purification, we tagged the hTR 3' hairpin at its 5' end with the *Pseudomonas* phage 7 (PP7) stem loop binding site for coat protein (Hogg and Collins, 2007b), which we found to stabilize the recombinant RNA in extract even without added PP7 coat protein. Dyskerin, NHP2, and GAR1 all assembled on the hTR 3' hairpin, with an efficiency reduced by BIO box mutation and abrogated entirely by ACA mutation (Fig. 4A). Cell extract containing no tagged protein was used as a specificity control (Fig. 4A, Mock lanes 13-15). Similar results were obtained using untagged hTR 3' hairpin RNAs (data not shown). We also verified that this specificity was not due enhanced degradation of the BIO and ACA variant RNAs in extract, as judged by equal recovery of radiolabeled RNAs from the unbound extract fraction following RNP affinity purification (data not shown). We conclude that the BIO box strongly stimulates H/ACA RNP assembly on the hTR 3' hairpin in whole cell extract.

We then modified the reconstitution assay, reversing the immunopurification and RNA incubation steps. The tagged protein alone and any complexes containing the tagged protein were isolated by binding to IgG resin, washed resin was incubated with radiolabeled RNA, and after removal of free RNA with additional washes, any RNP-assembled RNA was recovered and resolved by denaturing PAGE. In this assay, complexes containing tagged dyskerin or NHP2 but not GAR1 could assemble on the hTR 3' hairpin, and this assembly was reduced by BIO box mutation and eliminated by ACA mutation (Fig. 4B). Because GAR1 joins an H/ACA RNP late in its maturation, our RNP assembly assay with prepurified complexes recapitulates the physiological specificity of H/ACA RNP assembly: GAR1 should not purify an RNA-free protein complex that can load recombinant RNA, but if RNA is assembled into RNP in extract, additional maturation steps including the recruitment of GAR1 can occur.

We next examined the specificity of NAF1 interaction. Tagged NAF1 copurified the hTR 3' hairpin RNA following RNP assembly in extract (Fig. 4C, lanes 7-9), and prepurified protein

complexes with tagged NAF1 bound RNA directly (Fig. 4D, lanes 7-9). In either case, RNP formation was strongly reduced by BIO box mutation and eliminated by ACA mutation. Overall the findings above indicate that NAF1, dyskerin, NHP2, and, by extension, NOP10 form a preassembled protein complex that is capable of binding the hTR 3' hairpin. Also, at least under our extract RNP assembly conditions, the exchange of NAF1 for GAR1 remains incomplete. More surprisingly, BIO box-dependent hTR RNP reconstitution with purified, NAF1-bound core proteins suggests that the BIO box binding partner is part of this preassembled protein scaffold.

The preassembled core protein scaffold lacks other known chaperones.

Cellular biogenesis of H/ACA RNPs requires numerous factors, in addition to NAF1, that interact with dyskerin, NOP10, and/or NHP2 and assist in the RNA processing and RNP assembly steps preceding formation of a mature RNP. To evaluate whether these factors associate with RNP assembled in extract, or, of special interest, form part of the preassembled NAF1/dyskerin/NOP10/NHP2 scaffold competent for direct RNA binding, we expressed tagged versions of known H/ACA RNP biogenesis factors and assayed their hTR interaction using both reconstitution protocols. Assembly of radiolabeled hTR 3' hairpin in extract followed by RNP purification detected BIO box- and ACA-dependent interaction of two assembly chaperones: NUFIP and RUVBL2 (Fig. 4C, lanes 4-6 and 10-12). Similar assays of additional factors required for hTR biogenesis *in vivo*, including the nuclear cap methyltransferase sTGS1 (Fig. 4C, lanes 13-15), failed to detect associations with the extract-assembled hTR 3' hairpin RNP.

Notably, neither NUFIP nor RUVBL2 was part of the preformed protein scaffold competent for direct RNA binding (Fig. 4D, lanes 4-6 and 10-12). Assays of additional factors required for hTR biogenesis *in vivo*, including sTGS1 (Fig. 4D, lanes 13-15), also did not copurify the assembly-competent protein scaffold. Despite many years of investigation it remains possible that some H/ACA RNP assembly factors remain to be discovered, but the most likely explanation to account for the results above is that a scaffold containing only NAF1, dyskerin, NOP10, and NHP2 is the platform for direct binding to an H/ACA RNA precursor. Other biogenesis factors that associate with an H/ACA RNP reconstituted in cell extract are not part of this assembly-competent scaffold prior to RNA loading. Furthermore, because hTR association with the preassembled protein scaffold remains dependent on the BIO box even when the scaffold is purified from extract prior to RNP assembly, the scaffold itself provides the BIO-box-dependent RNP assembly stimulation.

No high-resolution structure of a eukaryotic core heterotrimer is available, with or without bound RNA. Of the core heterotrimer proteins, only NHP2 would be positioned suitably for direct contact with the BIO box (Hamma and Ferre-D'Amare, 2010; Kiss et al., 2010). Consistent with results from a previous study of yeast Nhp2p (Henras et al., 2001), we find that recombinant human NHP2 alone binds the hTR 3' hairpin without specificity for the BIO box (data not shown). A measurable sequence preference of NHP2 binding is likely to require its structural constraint by protein-protein interaction(s). We suggest that protein preassembly to form the NAF1/dyskerin/NOP10/NHP2 scaffold biases the conformational heterogeneity observed in recent solution structures of isolated yeast Nhp2p (Koo et al., 2011) to favor the NHP2 conformation with binding preference for the loop uridine presented by the hTR BIO box.

The preassembled core protein scaffold supports concerted two-hairpin RNP assembly.

Results above demonstrate that hTR H/ACA RNP assembly is dependent on the hTR BIO box *in vitro* as well as *in vivo*, but other human H/ACA RNAs lack this motif. To

investigate the *in vitro* RNP assembly properties of other human H/ACAs in comparison to hTR, we created a panel of one- or two-hairpin RNAs based on the validated secondary structures of the human U17, U64, and ACA28 snoRNAs (Cervelli et al., 2002; Ganot et al., 1997b; Xiao et al., 2009). U17 is the only human H/ACA RNA known to function in ribosomal RNA precursor cleavage rather than pseudouridylation, and it is the only known individually essential H/ACA RNA in yeast (Kiss et al., 2010). Like hTR, U17 has a noncanonical 5' hairpin structure and a 3' hairpin that can compete for full-length U17 RNP assembly in HeLa nuclear extract (Dragon et al., 2000).

We first assayed RNP assembly in extract for the radiolabeled two-hairpin U17, U64, and ACA28 snoRNAs and a comparably snoRNA-sized version of hTR (Fig. 5A), which lacks the 5' hairpin extension for telomerase catalytic activation (Fig. 1A). We also assayed RNP assembly on the single 3' hairpin of each snoRNA. The two-hairpin and 3' hairpin hTR and U17 RNAs each assembled an H/ACA RNP in extract, as monitored by post-assembly purification of tagged NHP2 (Fig. 5A, lanes 8-9, 11, and 13-14). In contrast, although the two-hairpin versions of U64 and ACA28 assembled an RNP, the 3' hairpin of either snoRNA alone did not (Fig. 5A, lanes 26-29). Notably, the BIO box enhanced RNP assembly even for the snoRNA-like two-hairpin version of hTR (Fig. 5A, compare lane 9 to 10 and lane 11 to 12). Parallel controls for background binding used cell extracts with no tagged protein (Fig. 5, Mock purification lanes). The isolated 5' hairpins from hTR, U17, or other snoRNAs failed to assemble an RNP (data not shown). The same results were obtained using tagged dyskerin instead of tagged NHP2 (data not shown).

We next assayed the panel of single-hairpin and two-hairpin RNAs by RNP reconstitution following protein purification. To our surprise, complexes containing tagged NHP2 (Fig. 5B) or tagged dyskerin (data not shown) that were purified prior to RNP assembly supported not only the same specificity of single-hairpin RNP assembly characterized in extract but also robust two-hairpin-dependent RNP assembly (Fig. 5B, lanes 3-4). This finding suggests that the purified, resin-immobilized NAF1/dyskerin/NOP10/NHP2 scaffold achieves concerted assembly of core proteins on two H/ACA-motif hairpins. Although we cannot exclude some potential for physical association of two separately immobilized NAF1-bound core protein complexes, the results above suggest that the preassembled scaffold for productive RNP assembly could already contain two sets of core proteins (Fig. 5C). This scaffold architecture would account for why eukaryotic H/ACA RNAs all have two hairpins, whereas archaeal RNAs that assemble directly with dyskerin/NOP10 and separately with L7Ae do not. Unfortunately, we found the RNA-binding-competent NAF1/dyskerin/NOP10/NHP2 scaffold to be unstable to stringent washes and/or extended additional purification, hampering direct physical characterization of the functional scaffold architecture.

Distributed features of the hTR 3' hairpin cooperate to promote RNP assembly.

The BIO box alone should contribute only a small fraction of the RNA binding surface for an H/ACA core protein complex, so we considered the possibility that it is necessary but not sufficient for stimulation of hTR 3' hairpin RNP assembly. We constructed a series of chimeric 3' hairpin RNAs that contained combinations of elements from hTR and ACA28 (Fig. 6). Chimeras 1 and 2 contained ACA28 sequence with the hTR 3' loop and also pocket-region sequences, including deletion of two base pairs above the pocket and insertion of two base pairs below the pocket to make the stem lengths more similar to those of hTR. In addition, in chimera 1 an adenosine was inserted in the 5' side of the upper stem and a guanosine was inserted in the

3’ side of the lower stem to make internal loop and bulge sizes identical to hTR. Efficient RNA assembly with H/ACA proteins in extract was not supported by transplant of the hTR loop and pocket sequences; instead, these chimeric RNAs showed only low, near-background purification similar to the ACA28 3’ hairpin (Fig. 6, lanes 8-11). We next transplanted the hTR 3’ hairpin loop and its atypically long lower stem into the ACA28 3’ hairpin backbone, to generate chimera 3. The combination of these two hTR elements conferred a robust and reproducible improvement of RNP assembly (Fig. 6, lane 12) that was more than provided by the loop alone (lane 14) or the undetectable RNP assembly with transplant of the lower stem alone (lane 13). Nonetheless, even the combination of loop and lower stem did not fully recapitulate the RNP assembly efficiency of the intact hTR 3’ hairpin (Fig. 6, lane 8). Consistent with the findings above, partially unpairing the 3’ hairpin lower stem to produce a more typical stem length severely reduced mature hTR accumulation *in vivo* (data not shown). An atypically long lower stem could be precluded in modification guide RNAs by competing structural requirements for biological function (see Discussion). These results suggest that multiple features of the hTR 3’ hairpin act in a synergistic manner to increase RNA interaction affinity with the preassembled NAF1-bound core protein scaffold.

Disease-associated H/ACA protein variants affect different steps of RNP assembly.

Finally, we investigated a potential connection between hTR sequence-mediated enhancement of H/ACA RNP assembly and the specificity of telomerase deficiency in DC. We overexpressed tagged disease-associated variants of dyskerin and NHP2 in HeLa cells and used the resulting whole cell extract for reconstitution assays. All of the dyskerin variants supported hTR 3’ hairpin RNP assembly in both reconstitution assays (Figs. 7A and 7B, lanes 2-9). This observation is consistent with the modest if any inhibition of RNA binding observed when dyskerin variants were assembled as core heterotrimer in reticulocyte lysate (Trahan et al., 2010; Wang and Meier, 2004). On the other hand, the NHP2 variants imposed severe defects in RNP assembly (Figs. 7A and 7B, lanes 11-13). NHP2 variants expressed by transient transfection of 293T cells showed reduced association with hTR as well as other snoRNAs (Fig. 7C), indicating that their assembly defect is not specific to hTR. These findings also parallel results from studies using reticulocyte lysate for RNP reconstitution (Trahan et al., 2010). Importantly, because NHP2 variants are expressed heterozygously in DC patient cells, they would decrease but not eliminate functional NHP2. In sum, for the overexpressed disease-linked dyskerin and NHP2 variants tested here, we did not find an RNP assembly defect specific to hTR. Instead, we suggest that in their physiological genomic contexts, DC mutations impose phenotypes by reducing the cellular level of the preassembled RNA-binding-competent H/ACA core protein scaffold. This could result in a more dramatic reduction of mature hTR than other H/ACA RNAs, due to a differentially sensitized balance of precursor RNP assembly versus degradation.

Discussion

Against our initial hypotheses for hTR BIO box function at an RNP biogenesis step that is not required for other human H/ACA RNAs, we found that the hTR BIO box influences a shared step of H/ACA RNP assembly. *In vivo* we suggest that hTR BIO box stimulation of RNP assembly tips the balance of hTR precursor protection versus exonucleolytic degradation. Degradation of a vertebrate telomerase RNA precursor may predominate over RNP assembly even in the presence of a BIO box, based on the increase in mature hTR accumulation resulting from insertion of a self-cleaving ribozyme that generates an exonuclease-resistant precursor 3' end (Fig. 2D). Because intron-encoded H/ACA RNA precursors would be less sensitive to degradation within the host pre-mRNA transcript or within a spliced intron lariat, reducing the cellular level of the initial RNP assembly scaffold could preferentially compromise mature hTR accumulation without impact on other human H/ACA RNAs. Indeed, even hTR H/ACA domain accumulation becomes independent of BIO box function when the RNA is processed from intron context (Theimer et al., 2007). We offer the unifying hypothesis that telomerase deficiency in DC patients with mutations that affect dyskerin, NOP10, or NHP2 results from reduced availability of the RNA-binding-competent H/ACA core protein scaffold. One prediction of this model is that the NAF1 promoter and/or open reading frame would be a locus of DC mutations.

Matching the two-hairpin specificity of eukaryotic H/ACA RNP assembly *in vivo*, we show that the resin-immobilized NAF1/dyskerin/NOP10/NHP2 scaffold has a two-hairpin requirement for binding pseudouridylation guide RNAs *in vitro*. Preorganization of two sets of core proteins as a NAF1-bound scaffold would account for the universality of the eukaryotic two-hairpin motif. *In vivo*, even if one of the two RNA hairpins is not biologically functional, its presence would still be required to give the second set of H/ACA proteins an RNA landing pad. This would account for why the biological accumulation of hTR depends on at least a minimal 5' hairpin stem (Egan and Collins, 2010). The preorganized, NAF1-chaperoned H/ACA core protein scaffold may have been a eukaryotic adaption to increasing transcriptome complexity, which would have obliged enhanced discrimination of H/ACA RNP assembly on transcripts encoding advantageous modification guide RNAs versus the vast diversity of other transcription products.

From a structural perspective, it is notable that H/ACA RNA hairpins sharing the same consensus bind to the same protein scaffold with different affinities. This observation echoes previous findings of non-equivalence in protein recognition of a family of related nucleic acid binding sites (Meijsing et al., 2009). Like the hTR 3' hairpin, the single U17 3' hairpin is sufficient to reconstitute as an H/ACA RNP *in vitro*. However, U17 does not share the specific sequence determinants that enhance hTR RNP assembly. U17 also does not substitute functionally for hTR H/ACA domain sequence *in vivo* (Fu and Collins, 2003). The features of the U17 3' hairpin that enhance RNP assembly could act in a distributed manner, analogous to the assembly-enhancing sequence features of the hTR 3' hairpin, or they could instead act by providing a U17-specific NAF1-RNA interaction (Trahan and Dragon, 2009).

From an evolutionary perspective, we note that although hTR and U17 gained 3' hairpin features that enhance RNP assembly, other tested snoRNAs did not. The loss of pseudouridylation guide function by hTR and U17 may have provided the tolerance for a wider range of changes in hairpin structure. On the other hand, restrained from altering the architecture of RNA-protein interactions necessary for their function, vertebrate pseudouridylation guide RNAs instead gained an RNP assembly advantage by migrating into mRNA introns. Like the

pseudouridylation guide H/ACA RNAs, U17 is intron-encoded. For any known human H/ACA RNA other than hTR, there would be no detriment to expression in an intron context because 5' and 3' processing can generate the mature RNA independent of its flanking sequence. In contrast, hTR maturation is highly context dependent because 5' processing would remove the functionally essential template. Therefore, as all other known vertebrate H/ACA RNAs migrated to genomic locations within mRNA introns, vertebrate telomerase RNAs had to remain independently transcribed genes. We suggest that this difference in the nascent RNA substrate for RNP assembly accounts for the preferential impact of disease-linked H/ACA protein variants on hTR accumulation *in vivo*.

Figure 1

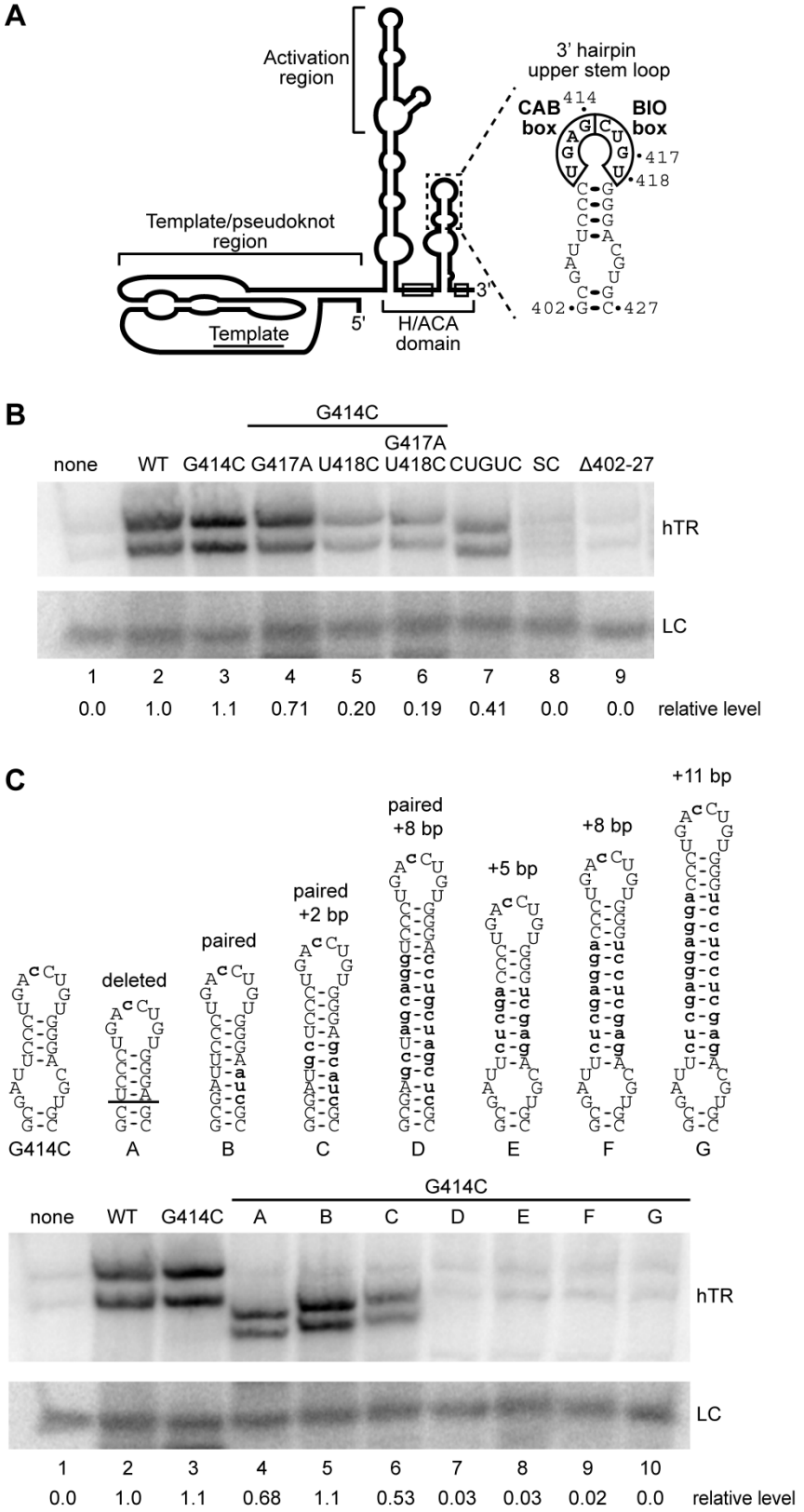
A
Activation region
3' hairpin upper stem loop
CAB box
BIO box
414
417
418
Template/pseudoknot region
3'
5'
Template
H/ACA domain
402•G•C•427
B
G414C
G417A
none
WT
G414C
G417A
U418C
U418C
CUGUC
SC
Δ402-27
hTR
LC
1 2 3 4 5 6 7 8 9
0.0 1.0 1.1 0.71 0.20 0.19 0.41 0.0 0.0
relative level
C
+11 bp
paired +8 bp
+8 bp
+5 bp
paired +2 bp
paired
deleted
G414C
A
B
C
D
E
F
G
G414C
none
WT
G414C
A
B
C
D
E
F
G
hTR
LC
1 2 3 4 5 6 7 8 9 10
0.0 1.0 1.1 0.68 1.1 0.53 0.03 0.03 0.02 0.0
relative level

The BIO box has sequence and positioning requirements for function. (A) Secondary structure of full-length hTR and primary sequence of the 3' hairpin upper stem loop. Open boxes within the H/ACA domain indicate the location of the H box and ACA (left and right boxes, respectively). (B,C) BIO box sequence and positioning requirements. Total RNA from transfected cells was examined by northern blot hybridization for recombinant wild-type (WT) hTR or the hTR variants indicated, as well as for an endogenous cross-hybridizing RNA (LC) detected in parallel on the same blot. Cells transfected with an empty expression vector provided an endogenous hTR background control (lanes labeled none). The CUGUC mutation replaces the entire loop sequence with that of the 3' hairpin loop of the human U17 snoRNA. The stem cap (SC) mutation replaces the entire loop with a GAAA tetraloop. In (C), base pairing and length of the 3' hairpin upper stem were altered as indicated by bold font and lower case lettering in the illustrations for variant stems A-G, with a line indicating the internal loop deletion in variant A. Values below the lane numbers are loading-normalized accumulation levels relative to wild-type.

Figure 2

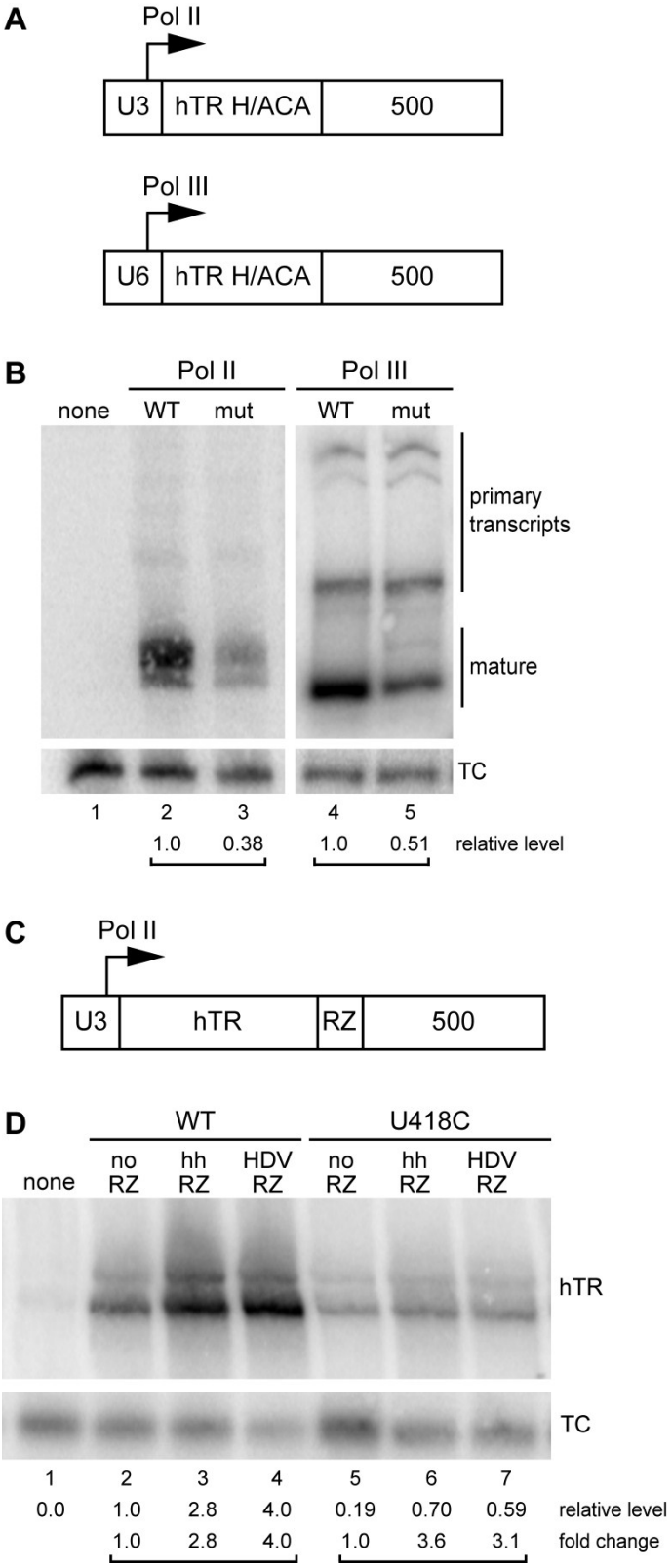
A
Pol II
U3
hTR H/ACA
500
Pol III
U6
hTR H/ACA
500
B
Pol II
Pol III
none
WT
mut
WT
mut
primary transcripts
mature
TC
1
2
3
4
5
1.0
0.38
1.0
0.51
relative level
C
Pol II
U3
hTR
RZ
500
D
WT
U418C
none
no RZ
hh RZ
HDV RZ
no RZ
hh RZ
HDV RZ
hTR
TC
1
2
3
4
5
6
7
0.0
1.0
2.8
4.0
0.19
0.70
0.59
relative level
1.0
2.8
4.0
1.0
3.6
3.1
fold change

The BIO box enhances RNP accumulation in different transcription contexts. (A,B) Construct schematics and results for BIO box function in Pol II versus Pol III expression context. The hTR H/ACA domain (nt 203-451) with a wild-type 3' hairpin loop (WT) or the CAB box/BIO box G414C/U418C double mutation (mut) were expressed using the promoter of human U3 or U6. Relative accumulation values were quantified using the signal intensities of the fastest-migrating, 3'-processed RNAs (with potential additional 5' processing of a few nt for transcripts of Pol III), first normalized to the transfection control (TC) and expressed relative to the corresponding wild-type RNA. (C,D) Schematic of hTR RZ expression constructs and RZ impact on hTR accumulation. WT or U418C hTR backbones were assayed in parallel without the RZ (lanes 2 and 5) or with the minimal hammerhead (hh) or hepatitis δ virus (HDV) RZ inserted 10 nt after the mature hTR 3' end. Accumulation values were normalized to the transfection control (TC) and expressed relative to the U3-hTR-500 construct (numbers given directly below lane numbers). Fold stimulation by ribozyme insertion was also calculated (numbers in bottom rows).

Figure 3

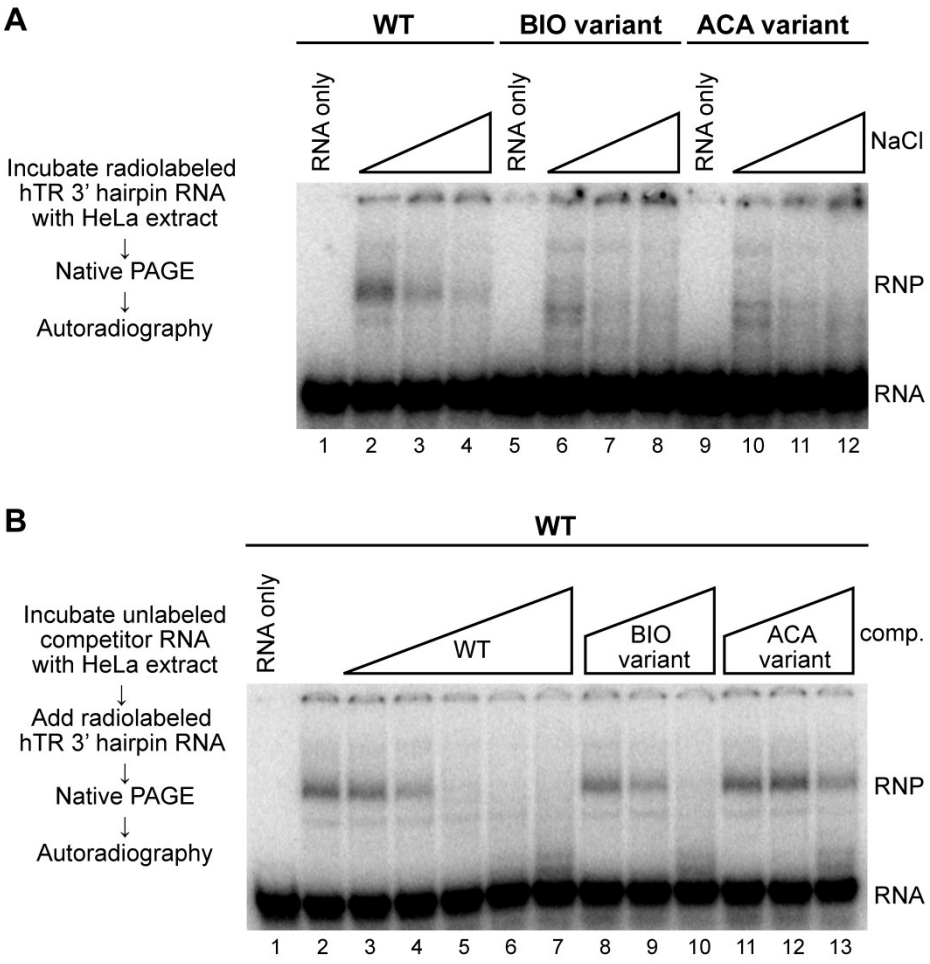

The BIO box stimulates RNP assembly on the hTR 3' hairpin. Radiolabeled hTR 3' hairpin probes were added to HeLa whole cell extract with RNP assembly monitored by EMSA. In (A), wild-type (WT) RNA corresponds to nt 381-451 of hTR variant B from Fig. 1C, in which the upper stem internal loop is paired and the CAB box is disrupted by the G414C substitution. BIO variant RNA harbors an additional U418C substitution, while ACA variant RNA has the substitution ACA446-448UGU. The concentration of NaCl was 100, 200, or 300 mM. In (B), RNP assembly on WT RNA was challenged by preaddition of unlabeled WT competitor RNA (comp.) at final concentrations of 0.01 ng/μL to 100 ng/μL or unlabeled BIO or ACA variant RNA at final concentrations of 1 ng/μL to 100 ng/μL in 10-fold steps.

Figure 4

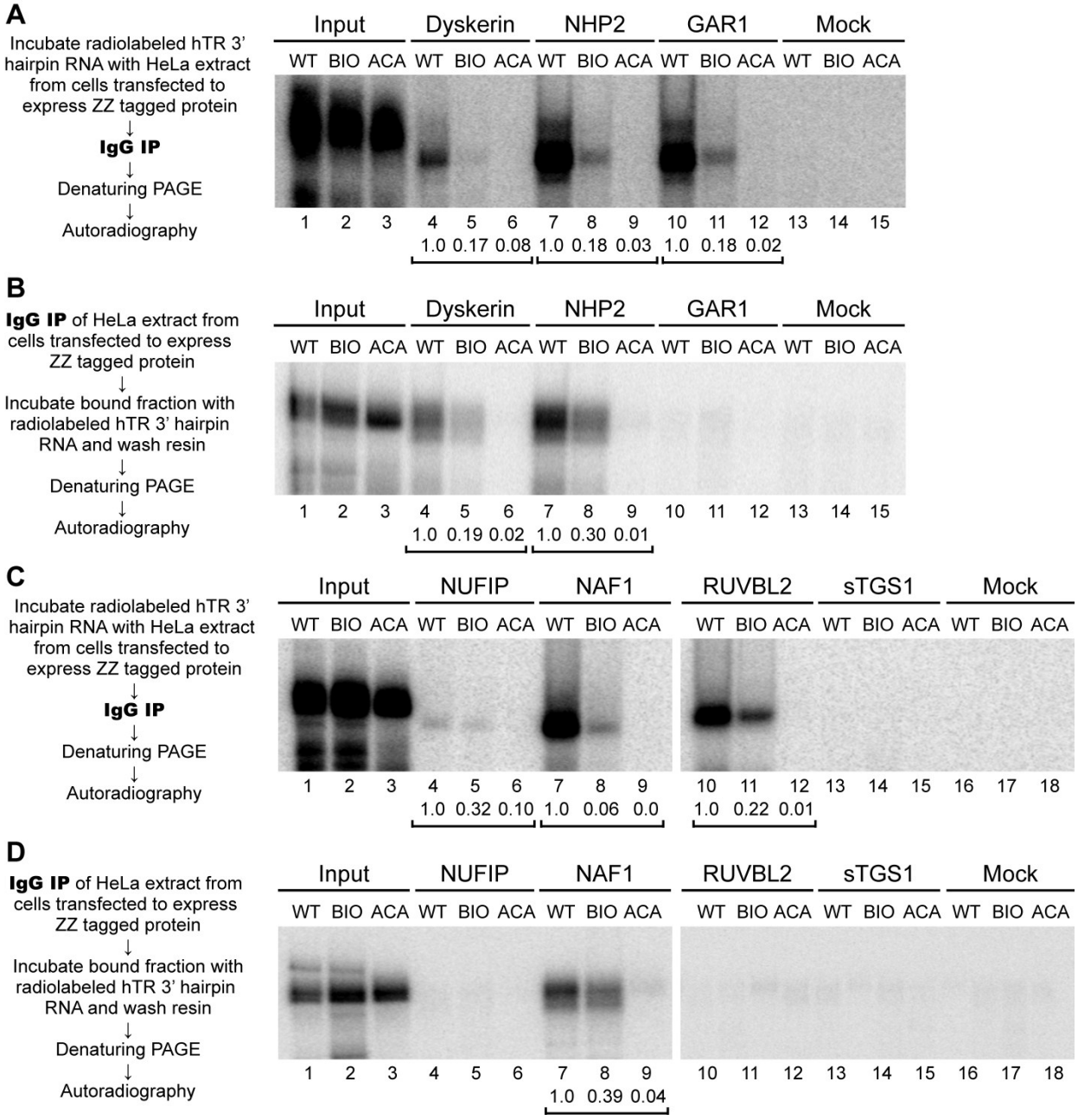

RNP assembly specificity is recapitulated with a purified protein scaffold. (A,C) HeLa whole cell extracts from cells transfected to express the indicated ZZ-tagged protein or untransfected cells (Mock) were incubated with radiolabeled PP7-tagged hTR 3' hairpin probe (WT or the BIO or ACA variant). Following RNP purification on IgG resin, bound RNA (100%) was detected relative to input RNA (2%). (B,D) Complexes containing the indicated ZZ-tagged protein were purified from whole cell extract of transfected HeLa cells prior to incubation with a radiolabeled PP7-tagged hTR 3' hairpin RNA. After washing, bound RNA (100%) was detected relative to input RNA (2%). Values below lane numbers are the input-normalized quantification of bound BIO or ACA RNA relative to WT RNA within each bracketed set.

Figure 5

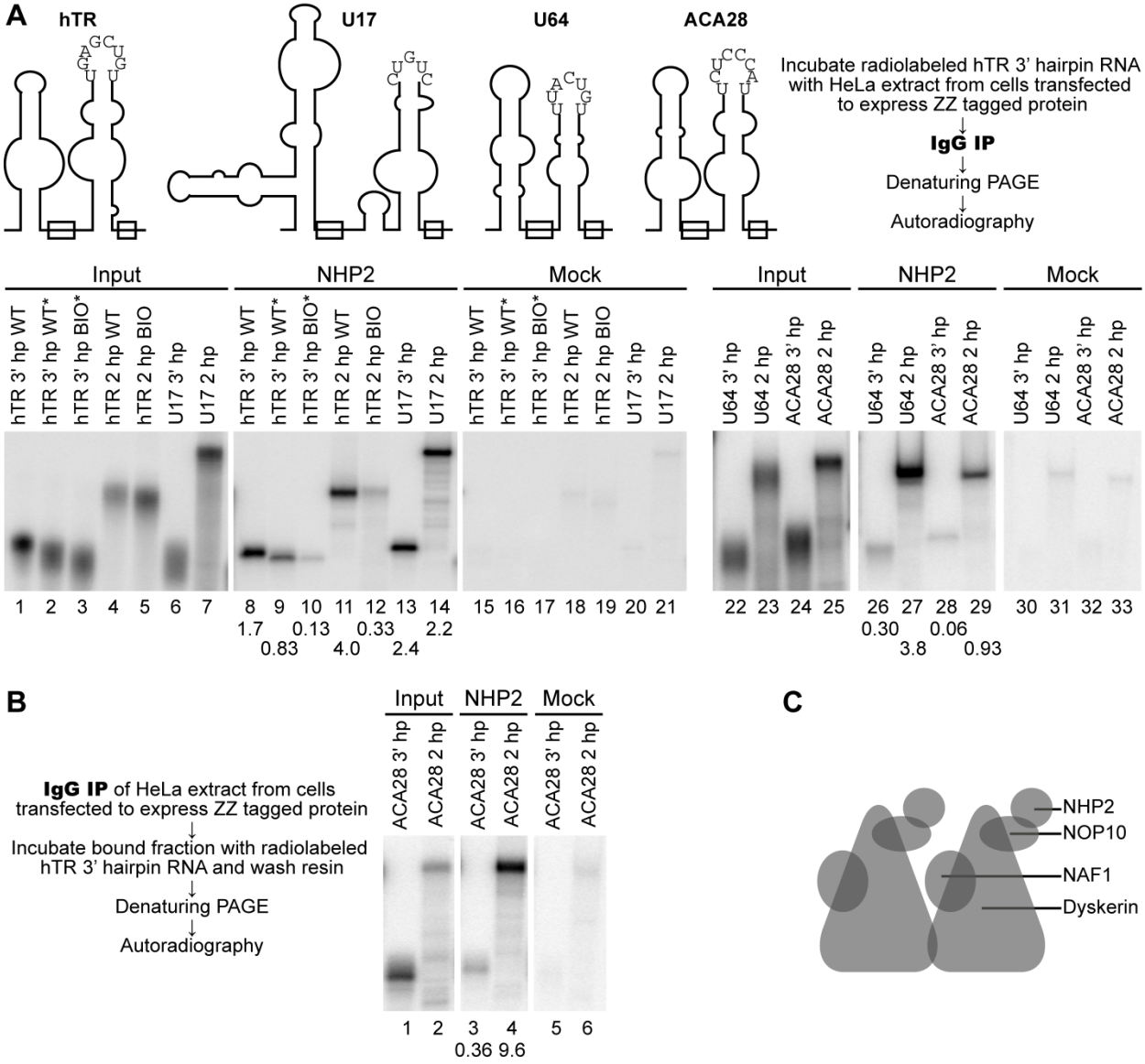

Pseudouridylation guide RNAs show concerted two-hairpin RNP assembly. (A) HeLa whole cell extracts from cells transfected to express ZZ-tagged NHP2 were incubated with radiolabeled 3' hairpin or two-hairpin hTR (WT or BIO variant), U17, U64, or ACA28. The snoRNA-sized version of hTR used as the two-hairpin RNA is depicted. An asterisk indicates RNAs in which the internal loop of the hTR 3' hairpin was paired. Following RNP purification and washing to remove unbound RNA, bound RNA (100%) was detected relative to input RNA (2%). Values below lane numbers are percent of input RNA bound. (B) Complexes containing ZZ-tagged NHP2 were immunopurified from whole cell extract prior to incubation with radiolabeled 3' hairpin or two-hairpin ACA28 RNA. Following washing to remove unbound RNA, bound RNA (100%) was detected relative to input RNA (2%). Values below lane numbers are percent of input RNA bound. (C) Model for the subunit composition of a protein scaffold competent for RNA binding. Protein interaction(s) that could putatively dimerize the core proteins are not established; for sake of illustration, contact between dyskerin subunits is suggested.

Figure 6

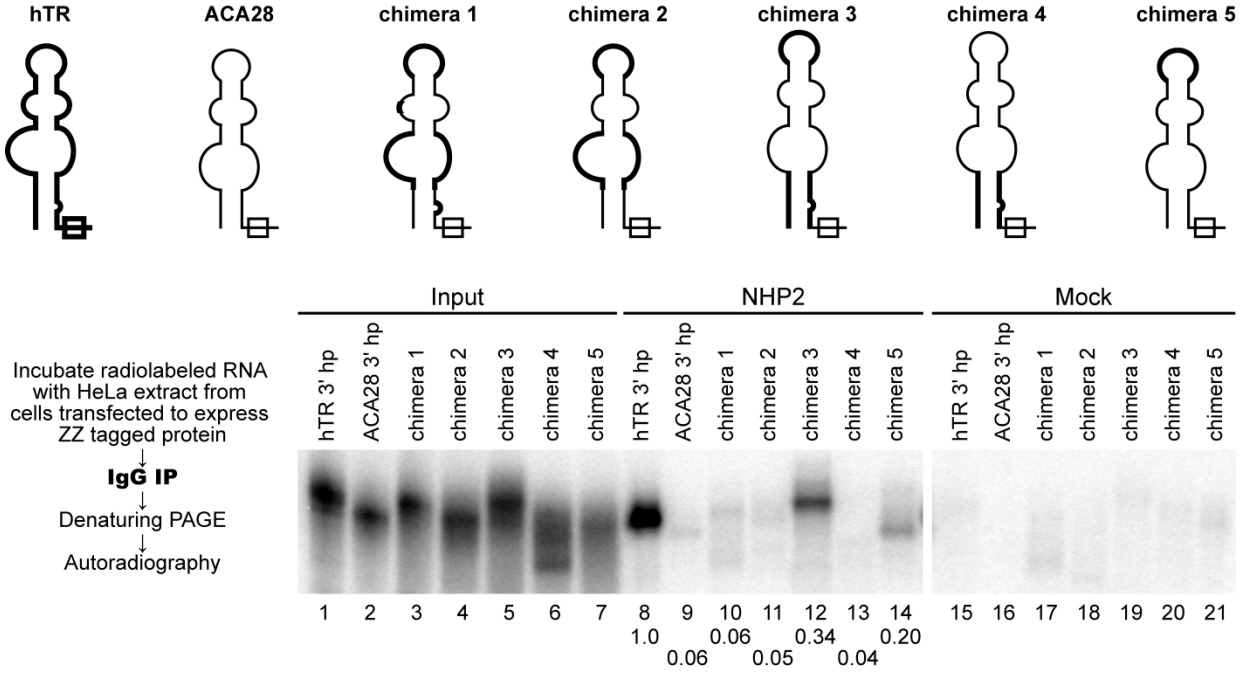

Several hTR 3' hairpin features contribute to RNP assembly enhancement. HeLa whole cell extracts from cells transfected to express ZZ-tagged NHP2 were incubated with a radiolabeled hTR 3' hairpin, ACA28 3' hairpin, or chimeric hairpin with hTR sequence in bold font. The ACA motif is boxed and a line indicates a deletion of 2 base pairs. Following RNP immunopurification and washing to remove unbound RNA, bound RNA (100%) was detected relative to input RNA (2%). Values below lane numbers are the input-normalized quantification of bound RNA relative to the hTR 3' hairpin.

Figure 7

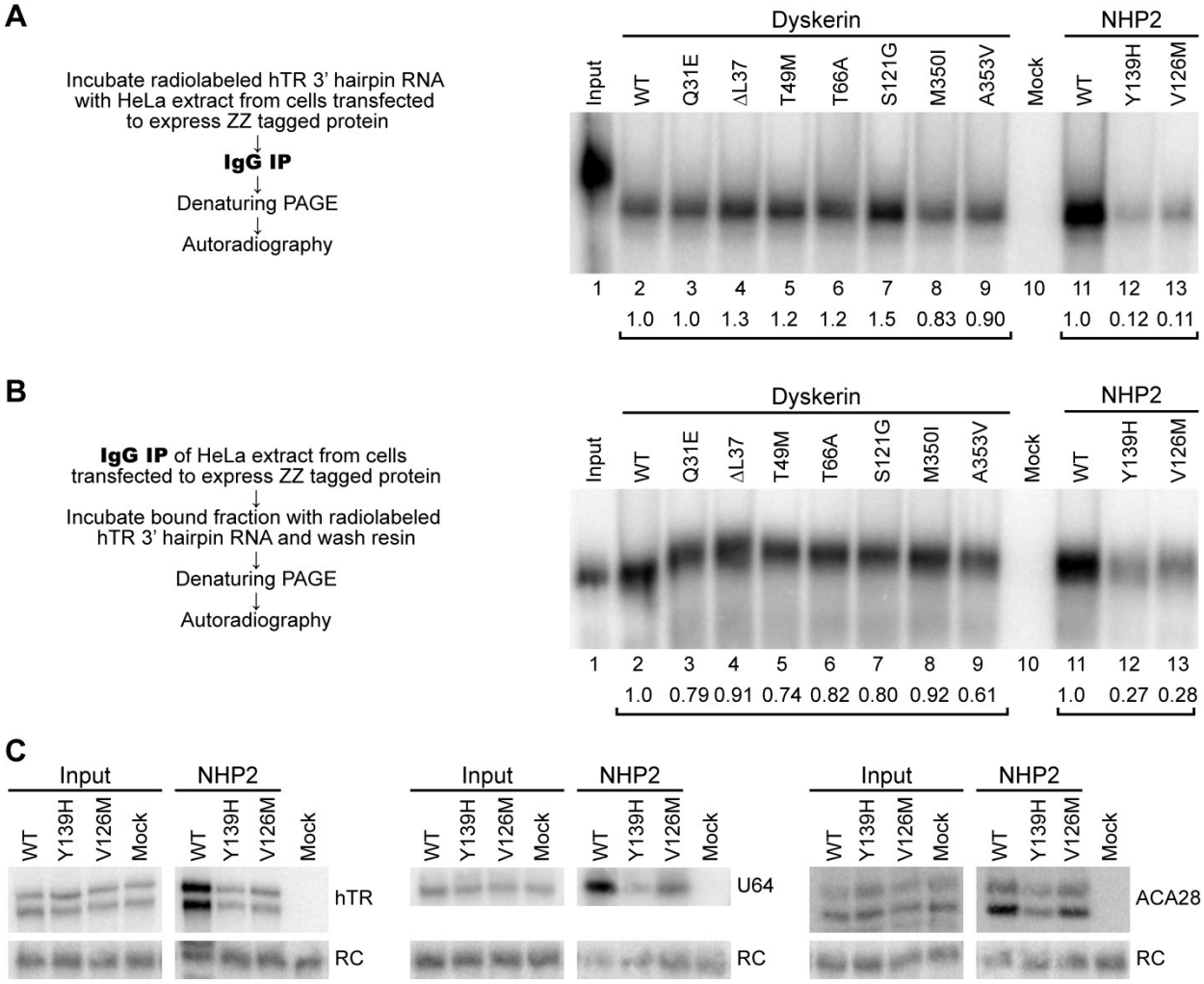

DC variants of NHP2 but not dyskerin inhibit hTR 3' hairpin RNP assembly. (A) HeLa whole cell extracts from cells transfected to express the indicated TAP-tagged dyskerin or ZZ-tagged NHP2 variant were incubated with radiolabeled PP7-tagged hTR 3' hairpin RNA. Following RNP immunopurification and washing to remove unbound RNA, bound RNA (100%) was detected relative to input RNA (2%). Values below lane numbers are the normalized quantification of bound RNA within each bracketed set. (B) Complexes containing the tagged protein with indicated variant sequence were immunopurified from whole cell extract of transfected HeLa cells prior to incubation with radiolabeled PP7-tagged hTR 3' hairpin RNA. Following washing to remove unbound RNA, bound RNA (100%) was detected relative to input RNA (2%). Values below lane numbers are the normalized quantification of bound RNA within each bracketed set. (C) Complexes containing tagged protein were immunopurified from whole cell extracts of 293T cells transfected to express the indicated ZZ-tagged NHP2 variant and H/ACA RNA. RNPs were immunopurified by binding to and elution from IgG resin. A recombinant RNA recovery control (RC) was added to input cell extracts (2%) and purified RNPs (100%) prior to RNA extraction.

CHAPTER FOUR

Analysis of Human Telomerase Interacting Factors and Multimerization Using Designed Cell Lines

Abstract

Human telomerase is a ribonucleoprotein (RNP) complex composed of the telomerase RNA, hTR, the telomerase reverse transcriptase, TERT, and several other proteins. Telomerase uses its RNA component as a template to add simple sequence repeats to linear chromosome ends, balancing the loss of repeats that results from incomplete DNA replication. In addition to motifs important for TERT-binding and catalytic activity, hTR contains elements that interact with specific protein partners essential for RNA biogenesis, RNP assembly, localization, and regulation. The telomerase holoenzyme is a large complex, and it is likely that many subunits remain to be discovered. Also, some studies suggest that this large size is the result of telomerase multimerization. Many telomerase-associated factors have been identified by affinity purification of TERT. However, hTR independently assembles a stable RNP, some components of which may dissociate before TERT assembly. Here we establish a system for the investigation of hTR-interacting proteins and telomerase RNP multimerization by RNA- and protein-based affinity purification of telomerase from stable cell lines expressing tagged hTR and TERT.

Introduction

Human telomerase is a ribonucleoprotein (RNP) enzyme that adds DNA repeats to chromosome ends to compensate for incomplete replication by conventional DNA polymerases. The repeats assemble with DNA-binding proteins to form nucleoprotein structures called telomeres that protect the chromosome end from nuclease and DNA repair activities. At the catalytic core of human telomerase is the telomerase reverse transcriptase, TERT, and the integral telomerase RNA component, hTR, which provides the template for repeat synthesis (Blackburn and Collins, 2010).

TERT can be divided into four relatively conserved domains. The telomerase N-terminal (TEN) domain associates with hTR and with DNA to promote processive synthesis (Robart and Collins, 2011). A linker region connects the TEN domain to the telomerase RNA-binding domain (TRBD) which interacts with hTR with high affinity. The reverse transcriptase (RT) domain contains the active site residues, and the C-terminal extension (CTE) contributes to processivity through unknown mechanisms (Autexier and Lue, 2006).

In addition to the template, the 451-nucleotide (nt) hTR contains several additional motifs (see Fig. 1A). Adjacent to the template is a conserved pseudoknot. The template-pseudoknot and a distal stem-loop present in a three-way junction element (the activation region) form the binding surface for TERT (Collins, 2009). The 3' half of hTR contains a motif shared with a large family of H/ACA RNAs, which function to guide pseudouridylation of ribosomal and small nuclear RNAs. H/ACA small nucleolar (sno) and small Cajal body (sca) RNAs adopt hairpin-Hinge-hairpin-ACA secondary structures containing conserved H box and ACA primary sequence elements and pockets in the hairpin stems that hybridize to sequence surrounding the target uridine(s). Each hairpin assembles with the H/ACA core proteins dyskerin, NHP2, NOP10, and GAR1. Within the 3' terminal loop of hTR and scaRNAs is an additional element called the CAB box, which directs Cajal body localization through interaction with TCAB1/WDR79 (Kiss et al., 2010).

Although hTR possesses an H/ACA domain, its biogenesis pathway differs from that of other human H/ACA RNAs. hTR is independently transcribed by RNA polymerase II as a potentially non-polyadenylated precursor that is exonucleolytically processed only at its 3' end (Feng et al., 1995; Mitchell et al., 1999a). In contrast, other human H/ACA RNAs are processed from introns by 5' and 3' exonuclease action (Kiss et al., 2006). hTR acquires a 5' trimethylguanosine cap, while other human H/ACA RNAs are uncapped (Fu and Collins, 2006; Jády et al., 2006). These unique features of hTR and its specialized function in telomere maintenance may require biogenesis factors that do not act on canonical H/ACA RNAs.

Based on glycerol gradient sedimentation, the molecular weight of the active human telomerase complex from HeLa cell extracts is ~1 megaDalton (Schnapp et al., 1998), which suggests that the RNP contains several subunits in addition to hTR, TERT, the H/ACA core proteins, and TCAB1/WDR79. Other hTR- and TERT-interacting proteins have been identified, but most appear to associate with only a fraction of the total telomerase holoenzyme population (Cohen et al., 2007; Collins, 2008; Podlevsky and Chen, 2012). It is likely that additional telomerase subunits remain to be identified, and there is also evidence that telomerase RNPs in some species may form multimers.

Several studies have suggested that human telomerase is capable of multimerization. Telomerase purified from HeLa cells under stringent chromatography conditions fractionated in glycerol gradients at ~650 kiloDaltons (kDa), and only TERT and dyskerin were detected by

mass spectrometry. This mass equals the combined mass of two TERT (127 kDa), two hTR (153 kDa), and two dyskerin (57 kDa) molecules, leading the authors to propose a dimeric structure (Cohen et al., 2007). However, comparing an RNP assembled on a highly structured RNA to globular protein standards may not accurately reflect its mass, and this highly purified and concentrated RNP may behave differently than the endogenous holoenzyme. Additional studies have attempted to define the architecture of a potentially multimeric telomerase complex and identify the subunit(s) mediating dimerization. Several groups have found that TERT can form multimers that do not require hTR *in vitro* and *in vivo* (Arai et al., 2002; Armbruster et al., 2001). Others have proposed the dimerization of hTR via intermolecular base pairing in the pseudoknot or 3' H/ACA hairpin pocket (Ly et al., 2003; Ren et al., 2003).

If telomerase complexes multimerize, an important question is whether multimerization affects telomerase activity. One influential study found that hTR variant-specific oligonucleotide affinity purification of telomerase reconstituted in insect cell lysate recovered wild-type and template mutant hTR, and the presence of mutant hTR compromised wild-type telomerase activity (Wenz et al., 2001). These results suggest that the two hTR molecules are present within a single complex and functionally interact. In another study, inactive TERT mutants or truncations complemented one another, reconstituting telomerase activity when purified from rabbit reticulocyte or human cell lysate. The functional complementation required one TERT molecule to contain a functional TEN domain and the other a CTE (Beattie et al., 2001). However, these reconstitution systems do not recapitulate all aspects of the native, *in vivo* assembled enzyme.

While there is evidence for telomerase multimerization, other studies have found that telomerase monomers exist and are fully active. Single-molecule two-color coincidence detection of hTR-TERT complexes reconstituted in rabbit reticulocyte lysate detects a 1:1 ratio (Alves et al., 2008). Coexpression of two differently tagged TERT variants in 293T cells followed by two-step affinity purification does not recover telomerase activity, suggesting that multimers do not form under these conditions (Errington et al., 2008). Similarly, purification of tagged hTR does not recover coexpressed untagged hTR (Errington et al., 2008). Finally, catalytically inactive hTR variants stably expressed in telomerase-deficient cells transduced with TERT do not exert dominant negative effects on catalytic activity or telomere extension (Errington et al., 2008). However, it remains possible that telomerase multimerizes under certain conditions, such as during a specific cell cycle stage or in a particular subcellular region such as in the Cajal body or on a telomere. Thus, whether telomerase present at endogenous levels inside cells multimerizes and, if so, whether multimerization has functional consequences, remains unclear.

RNA-based affinity purification has been successfully applied to the study of RNP complexes including spliceosomes, 7SK RNPs, Y RNPs and mRNPs (Hogg and Collins, 2007a, b; Hogg and Goff, 2010; Jurica et al., 2002). This method exploits a high-specificity, high-affinity interaction between the *Pseudomonas* phage 7 (PP7) or MS2 phage coat protein and an RNA hairpin operator element present at the 5' end of the replicase mRNA. Coat protein binding stabilizes the hairpin, which includes the Shine-Dalgarno box and start codon, and sequesters these sequences to prevent ribosome assembly and translation (Babitzke et al., 2009). RNA-based affinity purification of telomerase complexes using tagged hTR has the potential to reveal novel aspects of holoenzyme architecture and identify additional hTR-interacting proteins. Past studies of telomerase subunit composition have relied on the affinity purification of TERT (Cohen et al., 2007; Fu and Collins, 2007; Venteicher et al., 2008). However, this approach may

fail to detect some RNP subunits that do not interact directly with TERT. In addition, hTR assembles a stable RNP in the absence of TERT that may contain proteins that dissociate before TERT binding. RNA-based affinity purification of telomerase from human cells can also be used to detect telomerase multimers under conditions that are more physiological compared to heterologous reconstitution systems. Finally, affinity purification of hTR can be used to isolate complexes for structural studies, and in combination with TERT affinity purification, can selectively purify assembled telomerase RNPs rather than TERT-free RNPs or hTR-free protein complexes. In this study, we develop a set of HeLa S3 cell lines stably expressing PP7 hairpin-tagged hTR variants in the presence or absence of epitope-tagged TERT and demonstrate the successful isolation of telomerase complexes using RNA-based affinity purification.

Materials and Methods

Cell culture, constructs, transfection and retroviral integration.

Human 293T, HeLa, and HeLa S3 cells were grown on plates in DMEM with 10% fetal bovine serum. The HeLa S3 cell line was adapted to adherent growth and provided by the Rapé lab at UC Berkeley. For large-scale cultures, HeLa S3 cells were grown in suspension in a volume of 500 mL in uncoated 2 L roller bottles, which also supported some adherent growth. 293T cells were transiently transfected using the calcium phosphate method.

The mature hTR expression construct pBS-U3-hTR-500 was previously described (Fu and Collins, 2003). The hTR variant harboring the template mutations U47A, C51A, and U53A was generated by site-directed mutagenesis of pBS-U3-hTR-500. The PP7 hairpin sequence (Hogg and Collins, 2007b) was inserted at various positions in mature hTR in the pBS-U3-hTR-500 backbone and constructs were named according to the hTR nt 5' of the insertion unless otherwise noted. The PP7 5' end construct contained three tandem PP7 hairpins at the 5' end of hTR, as described previously (Errington et al., 2008). In the PP7 268 construct, nt 266-291 of hTR were replaced with the sequence CCGGCACAGAAGAUAUGGCUUCGUGCCAUC, which minimally modifies the hTR sequence to create a consensus PP7 hairpin. In the PP7 278 long construct, an AC/AG bulge and three additional base pairs (CGG/CCG) were inserted below the PP7 hairpin. The PP7 17 construct contained three additional basepairs (CGC/GCG) below the PP7 hairpin. In addition, the first G of the GG dinucleotide in the stem was changed to C with a compensatory C to G substitution to maintain pairing and the final loop nt was changed from G to A. In the PP7 6 hTR variant, nt 1-5 were repeated after the PP7 hairpin.

To create the N-terminal triple FLAG (F)-tagged PP7 coat protein (CP) *E. coli* expression construct, the sequence encoding the tandem Protein A domains (ZZ) and the tobacco etch virus protease cleavage site (TEV) of pET28a-ZZ-TEV-PP7 CP-6xHIS (Hogg and Collins, 2007b) were replaced with the triple FLAG sequence. Similarly, the triple FLAG sequence was inserted to create the ZZ-TEV-3xFLAG (ZF)-tagged PP7 coat protein construct. Recombinant coat proteins were expressed and purified as previously described (Hogg and Collins, 2007b).

To generate pBS-U3-hTR-500-box and pBS-U3-hTR-box, the 14-base pair U1 snRNA 3' box RNA processing element (box) with a 5' 10-base pair spacer was inserted after, or in place of, the 500 base pairs of endogenous downstream sequence in the pBS-U3-hTR-500 construct. The U3 C/D box snoRNA promoter sequence was replaced with the U1 promoter to generate pBS-U1-hTR-500-box and pBS-U1-hTR-box. A PP7 hairpin was inserted at position 278 in pBS-U3-hTR-box with or without the G414C CAB box mutation. In addition, the PP7 hairpin inserted at position 278 was combined with an MS2 hairpin inserted at position 17 (with the same additional base pairs as in PP7 17 construct) in the pBS-U1-hTR-box or pBS-U3-hTR-box contexts. The U3-hTR-box or U1-hTR-box portions of these constructs were then blunt-cloned into the NheI site in the 3' long terminal repeat of the retroviral vector pBABE puro. The TERT cDNA with an N-terminal ZF or ZZ-TEV-streptavidin binding peptide (ZS) tag (Keefe et al., 2001) was cloned into pBABE hygro using SnaBI and XhoI. The ΔTEN TERT truncation lacked the N-terminal 325 amino acids (Robart and Collins, 2011).

Viruses were packaged using Phoenix 293T cells. HeLa S3 cells were infected with the hTR-containing viruses. Selection with 2.5 μg/mL puromycin began 48 hours after infection and was continued for four days followed by expansion as polyclonal cultures. The hTR-expressing stable cell lines were then infected with the TERT-containing viruses. Selection with 350 μg/mL hygromycin began 48 hours after infection and was continued for one week followed by

selection with 175 μg/mL hygromycin for one week and expansion as polyclonal cultures. Population doublings were counted starting at the first post-selection split of the empty vector-infected cells.

Blot detection of RNA and protein.

RNA was purified using TRIzol according to the manufacturer's protocol (Invitrogen). For analysis of total RNA, 10-20 μg was loaded on a 5% acrylamide, 7 M urea, 0.6X TBE gel. Northern blot detection of hTR, the crossreacting endogenous RNA loading control (LC), and the recombinant RNA recovery control (RC) was performed using an end-labeled 2'-*O*-methyl RNA oligonucleotide complementary to hTR positions 51 to 72, as previously described (Fu and Collins, 2003). The hTR H/ACA domain was detected using an end-labeled probe complementary to nt 419-449. In some cases, PP7 hairpin-tagged hTR was specifically detected using probes complementary to the tag and hTR sequence flanking the insertion site. Northern blots were imaged using a Typhoon Trio phosphorimaging system (GE Healthcare). The ZF- and ZS-tagged TERT variants were detected by western blotting used rabbit IgG primary antibody (Sigma) diluted 1:10,000 and anti-rabbit AlexaFluor800 secondary antibody (Invitrogen) diluted 1:20,000 in 3% nonfat dry milk in TBS (50 mM Tris at pH 8.0, 150 mM NaCl). Tubulin was detected using mouse anti-α-tubulin primary antibody (Calbiochem) diluted 1:500 and anti-mouse AlexaFluor680 secondary antibody (Invitrogen) diluted 1:20,000 in 3% nonfat dry milk in TBS. Western blots were imaged using a LI-COR Odyssey system.

RNA-based affinity purification.

For affinity purification of PP7 hairpin-tagged hTR from transiently transfected 293T cells, cell extracts from freeze-thaw cell lysis were diluted to ~1.25 mg/mL in binding buffer (20 mM HEPES at pH 8.0, 150 mM NaCl, 2 mM $MgCl_2$, 0.2 mM EGTA, 10% glycerol, 0.1% Igepal, 1 mM DTT, and 0.1 mM PMSF). A volume of 500 μL of diluted extract was clarified by centrifugation and ~5 μg of F-tagged PP7 coat protein was added. Samples were rotated end-over-end for 2 hours at room temperature. Then 10 μL of washed anti-FLAG M2 antibody resin (Sigma) was added and samples were rotated end-over-end for 1.5 hours at room temperature. Bound samples were washed twice at room temperature in 1 mL of wash buffer (binding buffer with 0.1% Triton X-100 and 0.1% CHAPS) for 5 min each wash and then transferred to new tubes for a third wash. The same procedure was repeated using a high-salt buffer containing 20 mM HEPES at pH 8.0, 300 mM KCl, 2 mM $MgCl_2$, 1 mM EDTA, 10% glycerol, 0.1% Triton X-100, 1 mM DTT, and 0.1 mM PMSF (Cohen et al., 2007).

For affinity purification of PP7 hairpin-tagged hTR from HeLa S3 stable cell lines, 40 μL of washed anti-FLAG antibody or IgG resin (Sigma) and PP7 coat protein (~12 μg of F-tagged, ~24 μg of Z- or ZF-tagged) were combined in 500 μL of binding buffer containing 150 mM or 200 mM NaCl. Samples were rotated end-over-end for 2 hours at 4°C. Resin was rinsed in 1 mL of binding buffer before the addition of 1.5-2 mL of ~1.25 mg/mL clarified cell extract. Samples were rotated end-over-end for 2 hours at 4°C. Bound samples were washed twice at room temperature in 1 mL of binding buffer for 5 min each wash and then transferred to ultra-low retention tubes (Phenix) for a third wash (PMSF was omitted in the last wash of IgG purifications). To elute bound RNPs, a final concentration of 150 ng/μL 3xFLAG peptide (Sigma) or ~90 ng/μL of the S219V variant of TEV protease was added in a volume of 100 μL of binding buffer (without PMSF for IgG purifications) and rotated end-over-end for 30 min at room temperature. For the second purification step, 5 μL of IgG or Ni-NTA agarose (Qiagen)

was added to the first-step FLAG eluate along with 100 µL of binding buffer (containing 30 mM imidazole for Ni-NTA purifications). Samples were rotated end-over-end for 30 min at room temperature. Bound samples were washed as in the first step, except that the wash buffer for Ni-NTA purifications contained 15 mM imidazole. Bound RNPs were eluted in a volume of 15 µL with TEV protease as described above or with 500 mM imidazole for 30 min at room temperature. In large-scale purifications, ~300 µg of F-tagged PP7 coat protein and 1 mL of anti-FLAG antibody beads were combined in 12.5 mL binding buffer containing 150 mM NaCl. Samples were rotated end-over-end for 2.5 hours at 4°C. Resin was rinsed in 15 mL of binding buffer before the addition of 200 mL of ~1.25 mg/mL clarified cell extract. Samples were rotated end-over-end for 2 hours at 4°C. Bound samples were washed three times at room temperature in 25 mL of ice-cold binding buffer for 5 min each. RNPs were eluted as above in a volume of 2 mL. For the second step, 10 µL of Ni-NTA agarose was added, and samples were bound and washed as above. Bound material was eluted in batch format by two successive 30-minute incubations in 25 µL of binding buffer containing 500 mM imidazole.

Telomerase activity assay.

Anti-FLAG antibody resin-immobilized RNPs from affinity purification of PP7 hairpin-tagged hTR were rinsed in 100 µL of binding buffer without NaCl, Igepal, or protease inhibitors and then resuspended in 10 µL of the same buffer. Assay buffer contained final concentrations of 10 mM HEPES, 50 mM Tris acetate, 5% glycerol, 40 mM NaCl, 50 mM potassium acetate, 4 mM $MgCl_2$, 1 mM EGTA, 1 mM spermidine, 0.5 mM DTT, and 5 mM β-mercaptoethanol at pH 8.0. In the experiment in Fig. 1C, reactions were initiated by the addition of 500 nM telomeric repeat primer $(T_2AG_3)_3$, 0.25 mM dTTP, 0.25 mM dATP, 5.5 µM unlabeled dGTP, and 0.33 µM [α-^{32}P] dGTP (3000 Ci/mmol, PerkinElmer Life Sciences). In the experiments in Fig. 2, reactions were initiated by the addition of 500 nM WT primer T_2AG_3 or mutant primer T_3GTG, 0.25 mM dTTP, 0.25 mM dATP (wild-type only), 5.5 µM unlabeled dGTP, and 0.33 µM [α-^{32}P] dGTP. The 20 µl assays were incubated at 30°C for 1 hour then quenched with 80 µL of TE (10 mM Tris at pH 7.5, 1 mM EDTA). Product DNA was purified by phenol-chloroform extraction and ethanol precipitation and analyzed by denaturing acrylamide gel electrophoresis.

Telomere length assay.

Telomere length was measured by in-gel hybridization using a 5' end-labeled telomeric repeat oligodeoxynucleotide $(T_2AG_3)_3$ as previously described (Fu and Collins, 2007). Fragment sizes were compared to an ethidium bromide-stained DNA ladder.

Results and Discussion

RNA-based affinity purification recovers active telomerase complexes.

RNA tag insertion sites must be carefully chosen to avoid the disruption of RNA folding or RNP assembly. Guided by the secondary structure model of hTR (Chen et al., 2000), we chose several insertion sites for the PP7 hairpin tag (Fig. 1A). We transiently expressed the tagged hTR variants along with untagged TERT in 293T cells and purified RNPs using triple FLAG (F)-tagged PP7 coat protein. We then measured hTR accumulation and purification efficiency by northern blotting (Fig. 1B). We included an untagged version of hTR for the determination of relative accumulation levels and to control for nonspecific binding of RNA to the anti-FLAG antibody resin (Fig. 1B, lanes 1 and 9). The first tagged hTR variant, which was used in a previous study (see below), has three PP7 hairpins inserted at the hTR 5' end. However, this RNA accumulated poorly (Fig. 1B, lane 2), potentially due to effects of the tag on transcription or 5' end processing steps such as cap hypermethylation. PP7 hairpin insertion at position 221, in the 5' H/ACA pocket, had little effect on accumulation (Fig. 1B, lane 8), but purification did not significantly enrich this RNA above the level of nonspecific background binding exhibited by untagged hTR (Fig. 1B, compare lane 16 to lane 9). This result could be due to H/ACA core proteins interfering with coat protein binding. We also inserted the tag in the 5' single-stranded region 3' of positions 6 and 17, avoiding the disruption of guanosine tracts predicted to form a G-quadruplex structure important for hTR accumulation (Sexton and Collins, 2011). For the insertion at position 6, nt 1-5 were repeated after the PP7 hairpin to restore the potential for G-quadruplex formation. For the insertion at position 17, three base pairs were added to the base of the PP7 hairpin and the sequence of the hairpin was modified to remove GG dinucleotides that could interfere with G-quadruplex formation. These tag insertions had little impact on hTR levels, but only the insertion at nt 17 allowed efficient purification (Fig. 1B, lanes 6-7 and 14-15). Finally, we made three hTR variants tagged in the activation region, outside of the area critical for TERT binding. We first modified the terminal hairpin sequence (nt 268-288) to create a consensus PP7 hairpin. This 268 variant accumulated to wild-type levels and allowed efficient purification (Fig. 1B, lanes 3 and 11). We also inserted the PP7 hairpin, or a long version with a small bulge and three base pairs added to the base of the stem, in the terminal loop 3' of position 278. These tagged RNAs accumulated to wild-type levels and were highly enriched by F-tagged PP7 coat protein purification (Fig. 1B, lanes 4-5 and 12-13).

We next verified that the telomerase complexes retained their catalytic activity when immobilized on anti-FLAG antibody resin via an interaction between the PP7 hairpin-tagged hTR and F-tagged PP7 coat protein. We performed activity assays using the same samples obtained for the northern blot in Fig. 1B. Activity paralleled the amount of hTR enrichment (compare Fig. 1B, lanes 9-16 to Fig. 1C, lanes 1-8). These results suggest that PP7 coat protein bound to hTR at the sites we tested does not interfere with telomerase catalytic activity. For future experiments, we used the tagged hTR variants with the 5' terminal hairpin modified to create a consensus PP7 hairpin (268) or the PP7 hairpin inserted at position 17 or 278.

Discrimination of monomeric versus multimeric hTR in RNPs assembled in vivo.

Many studies have suggested that telomerase complexes multimerize *in vitro* and possibly *in vivo*. Our laboratory has not found evidence for hTR or TERT multimerization using affinity purification from human cell extracts. In one such study, hTR tagged with three PP7 hairpins at the 5' end was unable to purify coexpressed untagged hTR as detected by northern

blot (Errington et al., 2008). In order to determine whether only a small fraction of telomerase complexes contain two or more hTR molecules, we took a similar approach but used our new tagged hTR variants, which accumulate to higher levels and are more efficiently purified than the one used previously. In addition, instead of northern blotting, we designed a more sensitive system that discriminates between the tagged and untagged RNAs using telomerase activity assays. We coexpressed the PP7 hairpin-tagged hTR 268 variant and an untagged version of hTR harboring three template mutations (U47A, C51A, and U53A) along with untagged TERT in 293T cells (Fig. 2A). The template mutant hTR accumulated *in vivo* and exhibited a wild-type level of activity on a cognate primer, albeit with a boundary bypass defect (data not shown). Then we purified tagged hTR using F-tagged PP7 coat protein and used the bound material in telomerase activity assays. We divided the sample in half and added either the cognate wild-type primer T_2AG_3 or the mutant primer T_3GTG to distinguish between the two hTR variants.

After purification, tagged wild-type hTR was enriched and its activity was detected using the wild-type primer (Fig. 2A, lane 1). However, this RNA did not copurify the untagged template mutant hTR, as evidenced by lack of activity using the mutant primer (Fig. 2A, lane 2). No background activity was detectable using either primer in the absence of tagged hTR expression (Fig. 2A, lanes 3 and 4). These findings were confirmed using the PP7 17 hTR variant and did not change when a high-salt buffer (see Materials and Methods) from a previous study that suggested telomerase is multimeric was used for purification (data not shown) (Cohen et al., 2007). Thus, even using a sensitive activity assay, no functional hTR multimers were detected in this experiment.

Another way to demonstrate telomerase multimerization is to observe dominant negative effects when wild-type and a catalytically inactive, but TERT-binding competent, mutant are coexpressed. Mutations in the template region of hTR can change the sequence of telomeric repeats with negative effects on telomerase function. Consistent with this finding, our hTR variants exhibited minimal activity on non-cognate primers (data not shown). Previous studies have found evidence either for or against potential hTR multimers influencing one another's activity (Rivera and Blackburn, 2004; Wenz et al., 2001). Our laboratory has demonstrated that hTR variants with mutations in the template region do not compromise wild-type telomerase activity in telomere maintenance when stably coexpressed *in vivo* (Errington et al., 2008). We sought to extend this finding using our sensitized *in vitro* assay. Increasing amounts of template mutant hTR were expressed in the presence of PP7 hairpin-tagged wild-type hTR in 293T cells. Then tagged hTR-containing RNPs were purified using F-tagged PP7 coat protein and their activity on wild-type or mutant primer was measured. As shown in Fig. 2B, coexpressed template mutant hTR did not exert a dominant negative effect on the activity of purified PP7 hairpin-tagged wild-type hTR; activity was proportional to the amount of tagged hTR purified (Fig. 2B, lanes 1, 3 and 5 and data not shown). A low level of activity from the untagged template mutant hTR distinguished by its atypical product ladder profile was detected even in the absence of tagged hTR, suggesting it resulted from nonspecific binding of the untagged RNA to the anti-FLAG antibody resin (Fig. 2B, lanes 2 and 8). Using the alternative buffer described above did not change these results (data not shown). These findings further demonstrate that human telomerase assembled *in vivo* does not form functional multimers under these conditions.

Stable expression of tagged hTR and TERT variants affects telomere length.

It is possible that transient expression of telomerase components does not recapitulate important aspects of telomerase assembly, including its modulation by factors such as cell cycle

stage and subcellular localization. In addition, many methods to investigate telomerase architecture and identify additional subunits require more material than easily obtained by transient transfection. For these reasons, we constructed a series of stable HeLa S3 cell lines expressing tagged hTR and/or TERT.

The mature hTR transcript can be produced by a variety of RNA polymerase II promoters, but mature hTR accumulation is sensitive to the presence of 3' end processing elements. The 3' end formation signal for hTR is unknown but appears to be present within the mature RNA sequence. Insertion of a polyA site or the U1 snRNA 3' box RNA processing element and transcription terminator downstream of the mature hTR sequence greatly reduces RNA accumulation (Fu and Collins, 2003). Previous cell lines made in our laboratory have expressed hTR from an integrated U3-hTR-500 cassette. In this expression context, the U3 C/D box snoRNA promoter is followed by mature hTR and 500 bp of 3' flanking genomic sequence. Cell lines have also been generated using the U1 snRNA promoter and 3' box RNA processing element (without the downstream transcription terminator) to express hTR (Cristofari and Lingner, 2006). Before constructing our cell lines, we compared the relative amounts of hTR produced by different expression contexts in order to maximize RNA accumulation. We transiently transfected 293T cells and measured the levels of hTR by northern blotting. We found the U3 promoter yielded more hTR than the U1 promoter (Fig. 3A, compare lanes 6-7 to lanes 2-5). The presence of the U1 3' box immediately downstream modestly increased the levels of hTR expressed by both promoters relative to when the element was separated from the mature 3' end by 500 bp (Fig. 3A, compare lanes 4 and 6 to lanes 5 and 7). Based on these results, we inserted a PP7 hairpin tag at hTR position 278 in the pBS-U3-hTR-box construct and cloned the U3-hTR-box fragment into the 3' long terminal repeat of the retroviral vector pBABE puro. We also made a version with a CAB box mutation (G414C) to determine whether disrupting the localization of hTR changes its binding partners and/or multimerization state. We also combined the PP7 tag with an MS2 tag at position 17 for tandem RNA-based affinity purification. We expressed this RNA under the control of the U3 or U1 promoter.

Retroviruses packaged in Phoenix 293T cells were used to infect HeLa S3 cells adapted to adherent growth. After integration and selection, we verified the expression of the tagged RNA variants by northern blotting. The PP7 hairpin- and tandem (MP)-tagged hTR variants expressed by the U3 promoter accumulated to levels comparable to untagged endogenous hTR (Fig. 3B, lanes 3-5). However, the expression of tandem-tagged hTR by the U1 promoter was undetectable (Fig. 3B, lane 2). The mobilities of the tagged RNAs varied between experiments, likely due to sample heating and folding during gel electrophoresis. Unfortunately, purification using tagged MS2 coat protein was inefficient (data not shown) and the cell lines expressing tandem-tagged hTR were not analyzed further.

The cell lines with integrated empty vector or PP7 hairpin-tagged wild-type or CAB box mutant hTR were then infected with retroviruses containing TERT. We also infected the tagged wild-type hTR-expressing line with the corresponding empty vector. We expressed full-length TERT or a truncation lacking the TEN domain (ΔTEN) tagged with a ZS tag composed of tandem protein A domains and a streptavidin-binding peptide (SBP) separated by a tobacco etch virus (TEV) protease cleavage site. Previous studies have suggested the TEN domain could mediate TERT multimerization (Beattie et al., 2001), and this region may interact with known or yet to be discovered subunits. We also expressed full-length TERT with a ZF tag, in which SBP portion is replaced with the triple FLAG sequence. Tagged protein expression in these cell lines was monitored by western blotting (Fig. 3C).

In different cell lines, hTR and/or TERT can be limiting for telomere length set-point. In HeLa cells, a previous study suggested that both hTR and TERT limit telomere elongation (Cristofari and Lingner, 2006). To determine whether the tagged versions of hTR and TERT were biologically functional, we measured telomere length in our stable HeLa S3 cell lines. We collected cells after increasing numbers of population doublings (PD) and digested their genomic DNA with restriction enzymes that cut ubiquitously in the genome but lack a recognition site in the T_2AG_3 telomeric repeats. The DNA fragments were separated by agarose gel electrophoresis and detected by in-gel hybridization with an end-labeled telomeric probe. In the tagged hTR-expressing lines, telomeres were maintained at a short, but stable, length of approximately 4 kbp (Fig. 4D, lanes 3-6). This length was similar to that of the empty vector line (Fig. 4D, lanes 1-2), suggesting that tagged hTR expression alone had little effect on telomere elongation. In contrast, when full-length TERT was expressed in the absence or presence of tagged hTR, telomere length increased dramatically to approximately 10 kbp (Fig. 4D, lanes 9-10, 13-14, 17-18). The length in cells expressing PP7 hairpin-tagged wild-type hTR was slightly greater than in those without hTR or with CAB box mutant hTR (Fig. 4D, compare lanes 13-14 to 9-10 and 17-18), possibly reflecting a contribution of the tagged RNA to telomere lengthening dependent on its Cajal body localization. Interestingly, expression of truncated TERT decreased telomere length relative to the absence of TERT expression (Fig. 4D, compare lanes 11-12, 15-16 and 19-20 to lanes 7-8). This dominant negative effect on telomere length may be due to competition for a limiting amount of hTR or another telomerase component or could potentially result from RNP multimerization.

Tagged RNA- and protein-based purifications recover RNP complexes from stable cell lines.

In order to obtain telomerase complexes for analysis of their subunit composition and multimerization state, we tested various affinity purification schemes. We first performed IgG purifications using whole cell extract from the stable cell lines and compared the amount of PP7 hairpin-tagged hTR bound to Z-tagged PP7 coat protein versus ZS- or ZF-tagged TERT. We found that the RNA-based purification recovered more RNA than the protein-based purification (Fig. 4A, compare lane 9 to lanes 10-12). However, while the tagged TERT variants bound hTR, they exhibited a preference for endogenous untagged, rather than tagged, hTR. This finding was surprising given the robust activity of PP7 coat protein-purified telomerase complexes (Fig. 1C) and the comparable levels of tagged and untagged hTR purified by tagged TERT from transiently transfected cells (data not shown). Experiments employing transient overexpression may have failed to detect small differences in binding affinity. As expected, the ΔTEN version of TERT bound to hTR less efficiently than the full-length protein (Fig. 4A, lanes 11-12) due to the loss of TEN domain interaction with the template-pseudoknot region of hTR (Robart and Collins, 2011). The bias against tagged RNA binding by TERT will greatly decrease the yield from combined RNA- and protein-based tandem affinity purification using these cell lines. However, the fact that RNA-based affinity purification selects for hTR-containing RNPs lacking TERT may also be an advantage. The analysis of these complexes could reveal novel proteins required for hTR biogenesis and stability that are not part of TERT-containing RNPs.

We next investigated possible two-step RNA-based affinity purification schemes using tandem-tagged PP7 coat proteins. All of the PP7 coat proteins have a C-terminal 6xHIS tag for purification from *E. coli*. In addition to the Z- and F-tagged variants used in earlier experiments, we also expressed and purified a ZF-tagged coat protein. We then compared the relative efficiency of two-step purifications employing anti-FLAG antibody resin in the first step and

either IgG or Ni-NTA resin in the second step in the presence of 150 mM or 200 mM NaCl. We found that while the first step of purification was successful, only the Ni-NTA purification recovered hTR in the second step. The same results were obtained when the order of purification steps was reversed (IgG then anti-FLAG antibody) and was not due to defective binding of the ZF-tagged coat protein to either resin since one-step purifications recovered hTR (data not shown). In addition, western blotting of purification fractions showed that ZF-tagged coat protein was present in second-step eluates (data not shown). It appears that during the second binding step, the ZF-tagged coat protein or telomerase RNP undergoes a conformational change that dissociates this coat protein from the RNA. The amount of NaCl in the buffers had little effect on the first step, but the higher salt condition reduced binding to the Ni-NTA resin slightly (Fig. 4B, lanes 14-19). Two-step purifications in which IgG was followed by Ni-NTA resin also recovered hTR, but the presence of a 6xHIS tag on the TEV protease used in the first-step elution made this approach unfavorable for mass spectrometric analysis of telomerase complexes.

Based on the above results, we scaled up the tandem anti-FLAG antibody-Ni-NTA two-step purification approximately 100-fold and analyzed the protein composition of the purified complexes by SDS polyacrylamide gel electrophoresis and silver staining. Unfortunately, to minimize the elution volume in the second step, a smaller relative volume of Ni-NTA resin was used and the tagged RNPs failed to bind appreciably, based on the absence of hTR from the imidazole elution fractions (data not shown). As a result of this low recovery, no proteins specifically bound to tagged hTR were detectable (Fig. 4C). If the amount of material obtained after two-step RNA-based affinity purification is insufficient for mass spectrometry analysis, single-step purification followed by excision of specific bands may be required. Alternatively, large-scale transient transfection may be necessary to increase yield. Small-scale transient transfection of 293T cells followed by single-step RNA-based affinity purification successfully recovered high levels of overexpressed tagged hTR, but silver staining did not reveal any specifically copurifying proteins (data not shown).

In summary, in this study we have demonstrated that RNA-based affinity purification using PP7 hairpin-tagged hTR and epitope-tagged PP7 coat protein is a useful approach for the isolation of human telomerase complexes. This method can be combined with mass spectrometry to identify novel hTR-interacting proteins. In addition, the analysis of purified telomerase complexes using gel filtration, and potentially direct structural approaches such as electron microscopy, will shed light on the multimerization state of telomerase. The study of human telomerase subunit composition and holoenzyme architecture will expand our knowledge of telomerase RNP biogenesis, activity, and regulation.

Figure 1

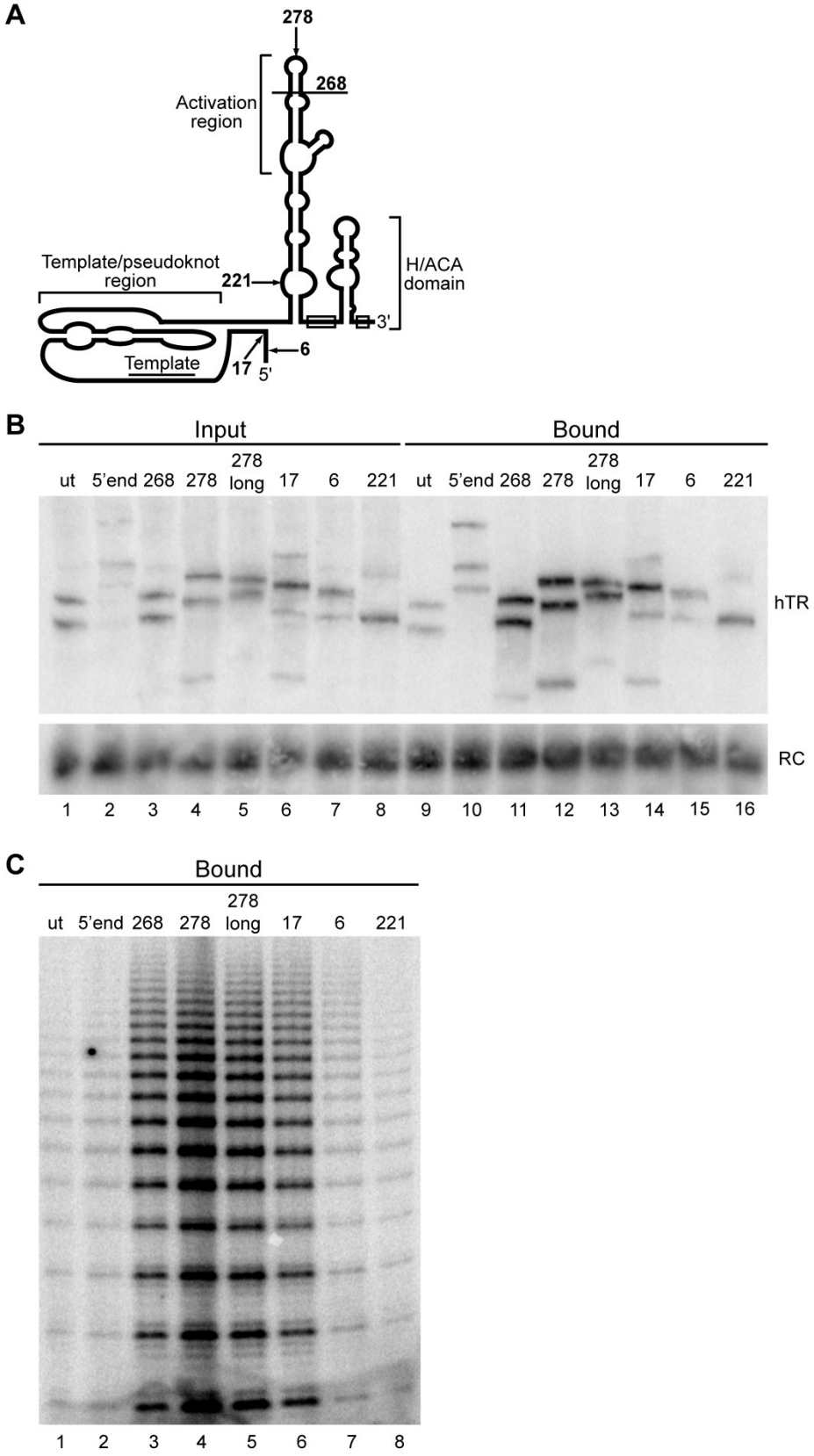
A
278
268
Activation region
Template/pseudoknot region
221
H/ACA domain
3'
6
Template
17
5'
B
Input
Bound
ut
5'end
268
278
278 long
17
6
221
hTR
RC
1 2 3 4 5 6 7 8 9 10 11 12 13 14 15 16
C
Bound
ut
5'end
268
278
278 long
17
6
221
1 2 3 4 5 6 7 8

A subset of PP7 hairpin insertions allow hTR accumulation and purification of catalytically active telomerase. (A) Secondary structure of full-length hTR. Open boxes within the H/ACA domain indicate the location of the H box and ACA (left and right boxes, respectively). Positions of PP7 hairpin tag insertions are indicated. The 268 variant minimally modifies the hTR sequence to create a consensus PP7 hairpin. (B) Extracts from 293T cells transfected to express untagged TERT and PP7 hairpin-tagged hTR variants were subjected to RNA-based affinity purification using F-tagged PP7 coat protein. Untagged (ut) hTR provides a control for nonspecific binding of RNAs to anti-FLAG antibody resin. The hTR variants and the recovery control (RC) were detected on the same blot. (C) Direct primer extension activity assays were performed using the bound material in (B).

Figure 2

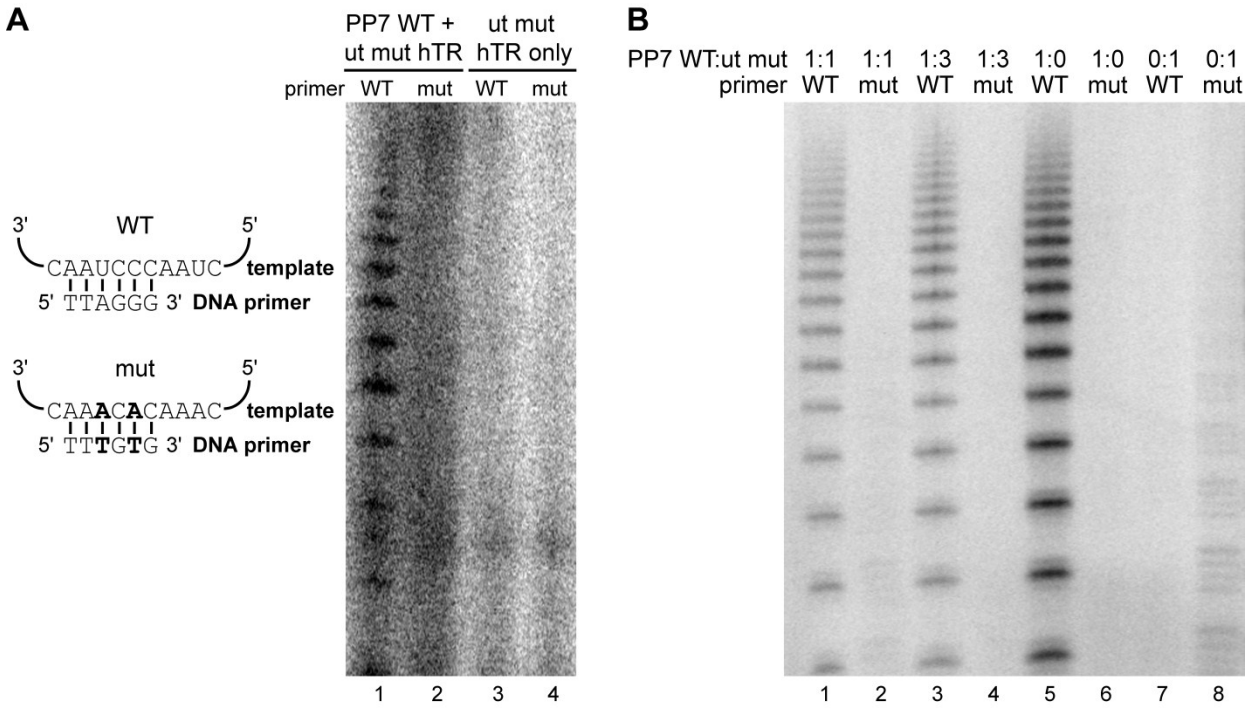

Telomerase complexes containing PP7 hairpin-tagged hTR are monomeric. (A) Diagram showing the alignment of wild-type (WT) and mutant (mut) hTR templates with cognate substrate DNA primers. Extracts from 293T cells transfected to express untagged TERT and untagged template mutant hTR with or without PP7 hairpin-tagged wild-type hTR were subjected to RNA-based affinity purification using F-tagged PP7 coat protein. Direct primer extension activity assays were performed using the bound material. (B) Extracts from 293T cells transfected to express untagged TERT and varying relative amounts of untagged template mutant hTR and PP7 hairpin-tagged wild-type hTR were subjected to RNA-based affinity purification using F-tagged PP7 coat protein. Direct primer extension activity assays were performed using the bound material.

Figure 3

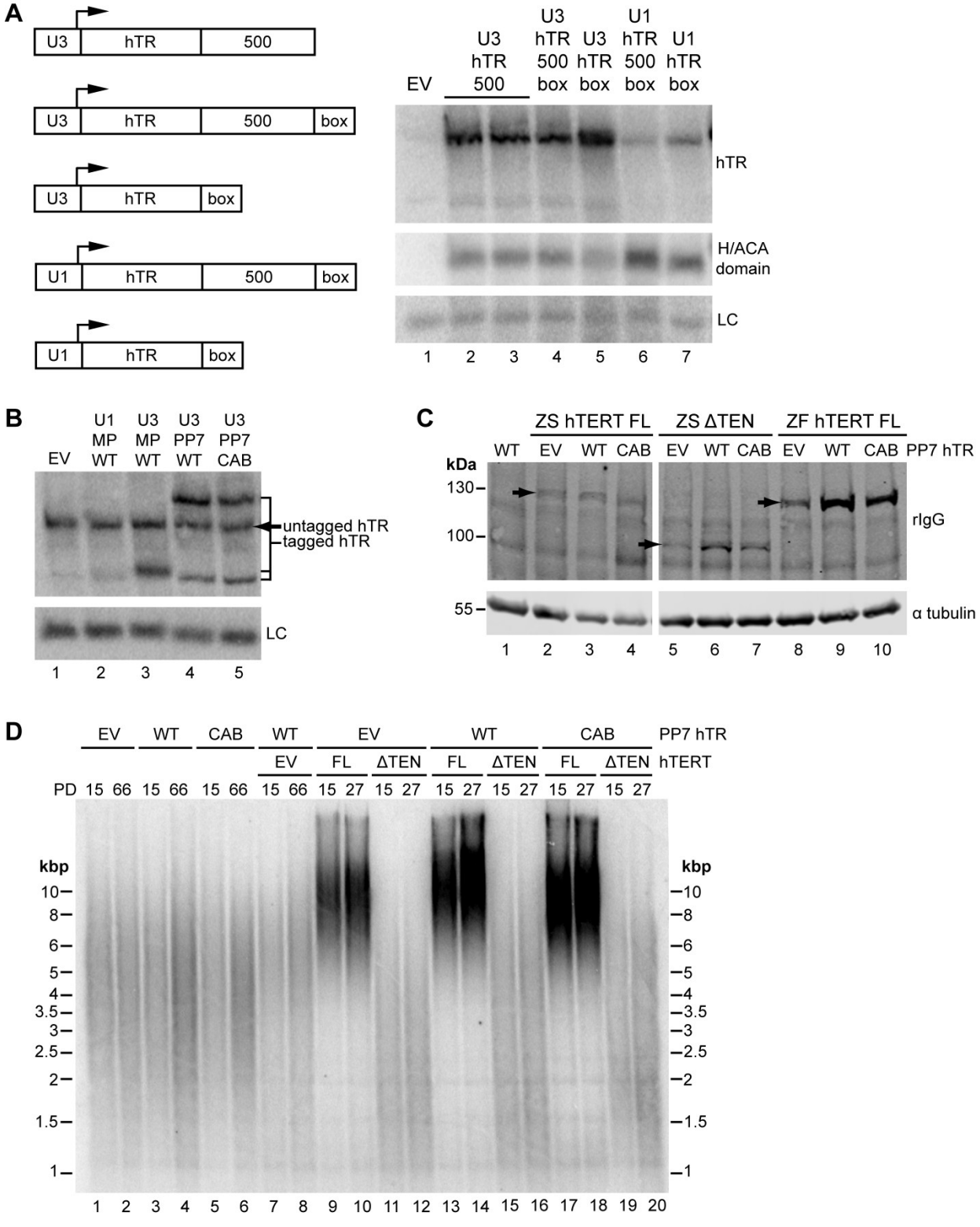
A
U3
hTR
500
box
U1
B
EV
U1 MP WT
U3 MP WT
U3 PP7 WT
U3 PP7 CAB
untagged hTR
tagged hTR
LC
C
ZS hTERT FL
ZS ΔTEN
ZF hTERT FL
WT
CAB
PP7 hTR
kDa
130
100
55
rIgG
α tubulin
D
hTERT
FL
ΔTEN
PD
15 66
15 27
kbp
10
8
6
5
4
3.5
3
2.5
2
1.5
1

Stable expression of PP7 hairpin-tagged hTR and/or epitope-tagged TERT variants affects telomere length. (A) Construct schematics and results for hTR expression from different Pol II expression contexts (U1, U1 snRNA promoter; U3, U3 snoRNA promoter; 500, 500 bp of hTR genomic 3' flanking sequence; box, U1 3' box RNA processing element). Total RNA from 293T cells transfected with an empty vector (EV) or constructs encoding hTR in different expression contexts was examined by blot hybridization. Full-length hTR and the endogenous loading control (LC) were detected on the same blot. (B) Total RNA from HeLa S3 cells stably expressing hTR with a PP7 hairpin inserted at position 278 (PP7) or a PP7 hairpin inserted at position 278 and a MS2 hairpin at position 17 (MP) was examined by blot hybridization. CAB indicates the presence of the G414C CAB box mutation. (C) Extract from HeLa S3 cells stably expressing epitope-tagged TERT (FL, full-length; ΔTEN, TEN domain truncation) with or without hTR was examined by western blotting using rIgG, which recognizes the Protein A domains (Z) of the epitope tags. The same blot was reprobed with anti-α-tubulin antibody as a loading control. (D) Genomic DNA from HeLa S3 cells stably expressing tagged hTR and or TERT was subjected to restriction enzyme digestion and telomere fragments were detected by in-gel hybridization of a telomeric DNA probe. Telomere lengths were measured relative to an ethidium bromide-stained DNA ladder.

Figure 4

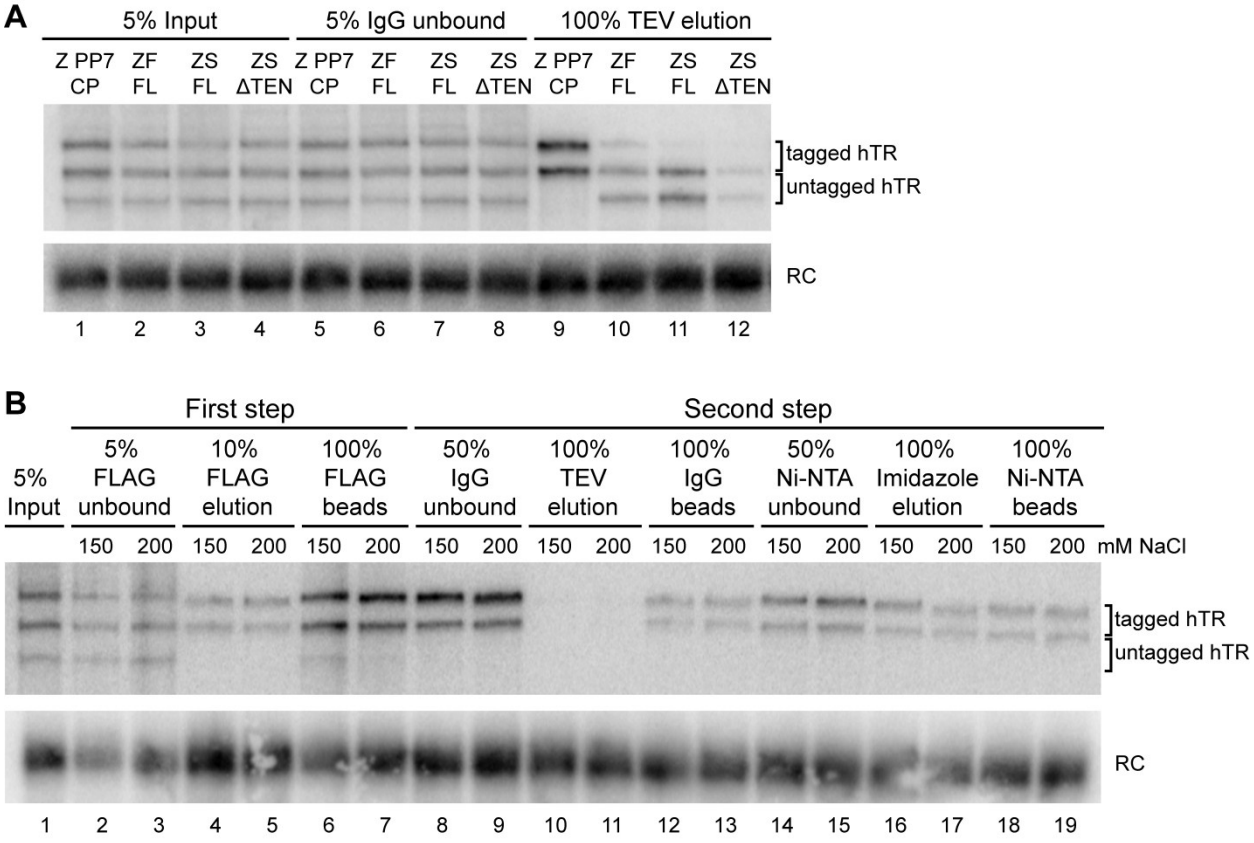
A
5% Input
5% IgG unbound
100% TEV elution
Z PP7 CP
ZF FL
ZS FL
ZS ΔTEN
tagged hTR
untagged hTR
RC
1 2 3 4 5 6 7 8 9 10 11 12
B
First step
Second step
5% Input
5% FLAG unbound
10% FLAG elution
100% FLAG beads
50% IgG unbound
100% TEV elution
100% IgG beads
50% Ni-NTA unbound
100% Imidazole elution
100% Ni-NTA beads
150 200 150 200 150 200 150 200 150 200 150 200 150 200 150 200 150 200 mM NaCl
tagged hTR
untagged hTR
RC
1 2 3 4 5 6 7 8 9 10 11 12 13 14 15 16 17 18 19
C
First step
Second step
1% FLAG elution
50% Imidazole elution
100% Ni-NTA beads
kDa
mock
PP7 hTR
200
150
120
100
85
70
60
50
40
30
25
15
1 2 3 4 5 6

RNA-based and protein-based affinity purifications recover telomerase RNPs. (A) Extracts from HeLa S3 cells stably expressing epitope-tagged TERT and/or PP7 hairpin-tagged hTR were subjected to RNA-based affinity purification using Z-tagged PP7 coat protein (CP) and IgG resin or protein-based affinity purification using IgG resin (FL, full-length TERT; ΔTEN, TEN domain truncation). (B) Extracts from HeLa S3 cells stably expressing PP7 hairpin-tagged hTR were subjected to two-step RNA- based affinity purification using ZF-tagged PP7 coat protein and anti-FLAG antibody resin followed by either IgG or Ni-NTA resin. The PP7 hairpin-tagged hTR, untagged endogenous hTR, and the recovery control (RC) were detected on the same blot. (C) Extracts from HeLa S3 cells stably expressing empty vector (mock) or PP7 hairpin-tagged hTR were subjected to two-step RNA-based affinity purification using F-tagged PP7 coat protein and anti-FLAG antibody resin followed by Ni-NTA. Proteins recovered after the first or second step of purification was resolved by SDS PAGE and detected by silver staining.

REFERENCES

Abreu, E., Aritonovska, E., Reichenbach, P., Cristofari, G., Culp, B., Terns, R.M., Lingner, J., and Terns, M.P. (2010). TIN2-tethered TPP1 recruits human telomerase to telomeres *in vivo*. Mol. Cell. Biol. *30*, 2971-2982.

Akiyama, B.M., Loper, J., Najarro, K., and Stone, M.D. (2012). The C-terminal domain of *Tetrahymena thermophila* telomerase holoenzyme protein p65 induces multiple structural changes in telomerase RNA. RNA *18*, 653-660.

Alves, D., Li, H., Codrington, R., Orte, A., Ren, X., Klenerman, D., and Balasubramanian, S. (2008). Single-molecule analysis of human telomerase monomer. Nat. Chem. Biol. *4*, 287-289.

Antal, M., Boros, E., Solymosy, F., and Kiss, T. (2002). Analysis of the structure of human telomerase RNA *in vivo*. Nucleic Acids Res. *30*, 912-920.

Arai, K., Masutomi, K., Khurts, S., Kaneko, S., Kobayashi, K., and Murakami, S. (2002). Two independent regions of human telomerase reverse transcriptase are important for its oligomerization and telomerase activity. J. Biol. Chem. *277*, 8538-8544.

Armanios, M. (2009). Syndromes of telomere shortening. Annu. Rev. Genomics Hum. Genet. *10*, 45-61.

Armbruster, B.N., Banik, S.S.R., Guo, C., Smith, A.C., and Counter, C.M. (2001). N-terminal domains of the human telomerase catalytic subunit required for enzyme activity *in vivo*. Mol. Cell. Biol. *22*, 7775-7786.

Autexier, C., and Greider, C.W. (1995). Boundary elements of the *Tetrahymena* telomerase RNA template and alignment domains. Genes Dev. *9*, 2227-2239.

Autexier, C., and Lue, N.F. (2006). The structure and function of telomerase reverse transcriptase. Annu. Rev. Biochem. *75*, 493-517.

Babitzke, P., Baker, C.S., and Romeo, T. (2009). Regulation of translation initiation by RNA binding proteins. Annu. Rev. Microbiol. *63*, 27-44.

Bachand, F., Boisvert, F.M., Cote, J., Richard, S., and Autexier, C. (2002). The product of the survival of motor neuron (SMN) gene is a human telomerase-associated protein. Mol. Biol. Cell *13*, 3192-3202.

Baillat, D., Hakimi, M.A., Naar, A.M., Shilatifard, A., Cooch, N., and Shiekhattar, R. (2005). Integrator, a multiprotein mediator of small nuclear RNA processing, associates with the C-terminal repeat of RNA polymerase II. Cell *123*, 265-276.

Ballarino, M., Morlando, M., Pagano, F., Fatica, A., and Bozzoni, I. (2005). The cotranscriptional assembly of snoRNPs controls the biosynthesis of H/ACA snoRNAs in *Saccharomyces cerevisiae*. Mol. Cell. Biol. *25*, 5396-5403.

Batista, L.F., Pech, M.F., Zhong, F.L., Nguyen, H.N., Xie, K.T., Zaug, A.J., Crary, S.M., Choi, J., Sebastiano, V., Cherry, A.*, et al.* (2011). Telomere shortening and loss of self-renewal in dyskeratosis congenita induced pluripotent stem cells. Nature *474*, 399-402.

Beattie, T.L., Zhou, W., Robinson, M.O., and Harrington, L. (2001). Functional multimerization of the human telomerase reverse transcriptase. Mol. Cell. Biol. *21*, 6151-6160.

Berman, A.J., Gooding, A.R., and Cech, T.R. (2010). *Tetrahymena* telomerase protein p65 induces conformational changes throughout telomerase RNA (TER) and rescues telomerase reverse transcriptase and TER assembly mutants. Mol. Cell. Biol. *30*, 4965-4976.

Biessmann, H., and Mason, J.M. (1997). Telomere maintenance without telomerase. Chromosoma *106*, 63-69.
Bird, G., Fong, N., Gatlin, J.C., Farabaugh, S., and Bentley, D.L. (2005). Ribozyme cleavage reveals connections between mRNA release from the site of transcription and pre-mRNA processing. Mol. Cell *20*, 747-758.
Blackburn, E.H., and Collins, K. (2010). Telomerase: An RNP enzyme synthesizes DNA. In RNA Worlds, R.F. Gesteland, J.F. Atkins, and T.R. Cech, eds. (Cold Spring Harbor: Cold Spring Harbor Laboratory Press), pp. 205-213.
Blasco, M.A. (2005). Mice with bad ends: mouse models for the study of telomeres and telomerase in cancer and aging. EMBO J. *24*, 1095-1103.
Bortolin, M.L., Ganot, P., and Kiss, T. (1999). Elements essential for accumulation and function of small nucleolar RNAs directing site-specific pseudoruidylation of ribosomal RNAs. EMBO J. *18*, 457-469.
Bosoy, D., Peng, Y., Mian, I.S., and Lue, N.F. (2003). Conserved N-terminal motifs of telomerase reverse transcriptase required for ribonucleoprotein assembly *in vivo*. J. Biol. Chem. *278*, 3882-3890.
Boulon, S., Marmier-Gourrier, N., Pradet-Balade, B., Wurth, L., Verheggen, C., Jády, B.E., Rothe, B., Pescia, C., Robert, M.C., Kiss, T.*, et al.* (2008). The Hsp90 chaperone controls the biogenesis of L7Ae RNPs through conserved machinery. J. Cell Biol. *180*, 579-595.
Boulon, S., Verheggen, C., Jady, B.E., Girard, C., Pescia, C., Paul, C., Ospina, J.K., Kiss, T., Matera, A.G., Bordonne, R.*, et al.* (2004). PHAX and CRM1 are required sequentially to transport U3 snoRNA to nucleoli. Mol. Cell *16*, 777-787.
Box, J.A., Bunch, J.T., Tang, W., and Baumann, P. (2008a). Spliceosomal cleavage generates the 3' end of telomerase RNA. Nature *456*, 910-914.
Box, J.A., Bunch, J.T., Zappulla, D.C., Glynn, E.F., and Baumann, P. (2008b). A flexible template boundary element in the RNA subunit of fission yeast telomerase. J. Biol. Chem. *283*, 24224-24233.
Brown, Y., Abraham, M., Pearl, S., Kabaha, M.M., Elboher, E., and Tzfati, Y. (2007). A critical three-way junction is conserved in budding yeast and vertebrate telomerase RNAs. Nucleic Acids Res. *35*, 6280-6289.
Bryan, T., Marusic, L., Bacchetti, S., Namba, M., and Reddel, R. (1997). The telomere lengthening mechanism in telomerase-negative immortal human cells does not involve the telomerase RNA subunit. Human Mol. Gen. *6*, 921-926.
Cervelli, M., Cecconi, F., Giorgi, M., Annesi, F., Oliverio, M., and Mariottini, P. (2002). Comparative structure analysis of vertebrate U17 small nucleolar RNA (snoRNA). J. Mol. Evol. *54*, 166-179.
Chao, J.A., Patskovsky, Y., Almo, S.C., and Singer, R.H. (2008). Structural basis for the coevolution of a viral RNA-protein complex. Nat. Struct. Mol. Biol. *15*, 103-105.
Chapon, C., Cech, T., and Zaug, A. (1997). Polyadenylation of telomerase RNA in budding yeast. RNA *3*, 1337-1351.
Chen, J.L., Blasco, M.A., and Greider, C.W. (2000). Secondary structure of vertebrate telomerase RNA. Cell *100*, 503-514.
Chen, J.L., Opperman, K.K., and Greider, C.W. (2002). A critical stem-loop structure in the CR4-CR5 domain of mammalian telomerase RNA. Nucleic Acids Res. *30*, 592-597.

Cohen, S.B., Graham, M.E., Lovrecz, G.O., Bache, N., Robinson, P.J., and Reddel, R.R. (2007). Protein composition of catalytically active human telomerase from immortal cells. Science *315*, 1850-1853.

Collins, K. (1999). Ciliate telomerase biochemistry. Annu. Rev. Biochem. *68*, 187-218.

Collins, K. (2008). Physiological assembly and activity of human telomerase complexes. Mech. Ageing Dev. *129*, 91-98.

Collins, K. (2009). Forms and functions of telomerase RNA. In Non-Protein Coding RNAs, N.G. Walter, S.A. Woodson, and R.T. Batey, eds. (Berlin: Springer-Verlag), pp. 285-301.

Cristofari, G., Adolf, E., Reichenbach, P., Sikora, K., Terns, R.M., Terns, M.P., and Lingner, J. (2007). Human telomerase RNA accumulation in Cajal bodies facilitates telomerase recruitment to telomeres and telomere elongation. Mol. Cell *27*, 882-889.

Cristofari, G., and Lingner, J. (2006). Telomere length homeostasis requires that telomerase levels are limiting. EMBO J. *25*, 565-574.

Cunningham, D.D., and Collins, K. (2005). Biological and biochemical functions of RNA in the *Tetrahymena* telomerase holoenzyme. Mol. Cell. Biol. *25*, 4442-4454.

Darzacq, X., Kittur, N., Roy, S., Shav-Tal, Y., Singer, R.H., and Meier, U.T. (2006). Stepwise RNP assembly at the site of H/ACA RNA transcription in human cells. J. Cell Biol. *173*, 207-218.

Dennis, P.P., and Omer, A. (2005). Small non-coding RNAs in Archaea. Curr. Opin. Microbiol. *8*, 685-694.

Dower, K., Kuperwasser, N., Merrikh, H., and Rosbash, M. (2004). A synthetic A tail rescues yeast nuclear accumulation of a ribozyme-terminated transcript. RNA *10*, 1888-1899.

Dragon, F., Pogacic, V., and Filipowicz, W. (2000). *In vitro* assembly of human H/ACA small nucleolar RNPs reveals unique features of U17 and telomerase RNAs. Mol. Cell. Biol. *20*, 3037-3048.

Duan, J., Li, L., Lu, J., Wang, W., and Ye, K. (2009). Structural mechanism of substrate RNA recruitment in H/ACA RNA-guided pseudouridine synthase. Mol. Cell *34*, 427-439.

Egan, E.D., and Collins, K. (2010). Specificity and stoichiometry of subunit interactions in the human telomerase holoenzyme assembled *in vivo*. Mol. Cell. Biol. *30*, 2775-2786.

Egan, E.D., and Collins, K. (2012). An enhanced H/ACA RNP assembly mechanism for human telomerase RNA. Mol. Cell. Biol. In press.

Errington, T.M., Fu, D., Wong, J.M., and Collins, K. (2008). Disease-associated human telomerase RNA variants show loss of function for telomere synthesis without dominant-negative interference. Mol. Cell. Biol. *28*, 6510-6520.

Evans, S.K., and Lundblad, V. (1999). Est1 and Cdc13 as comediators of telomerase access. Science *286*, 117-120.

Fatica, A., Dlakic, M., and Tollervey, D. (2002). Naf1p is a box H/ACA snoRNP assembly factor. RNA *8*, 1502-1514.

Feng, J., Funk, W.D., Wang, S., Weinrich, S.L., Avilion, A.A., Chiu, C., Adams, R.R., Chang, E., Allsopp, R.C., Yu, J.*, et al.* (1995). The RNA component of human telomerase. Science *269*, 1236-1241.

Ferrezuelo, F., Steiner, B., Aldea, M., and Futcher, B. (2002). Biogenesis of yeast telomerase depends on the importin Mtr10. Mol. Cell. Biol. *22*, 6046-6055.

Fisher, T.S., Taggart, A.K., and Zakian, V.A. (2004). Cell cycle-dependent regulation of yeast telomerase by Ku. Nat. Struct. Mol. Biol. *11*, 1198-1205.

Fong, N., Ohman, M., and Bentley, D.L. (2009). Fast ribozyme cleavage releases transcripts from RNA polymerase II and aborts co-transcriptional pre-mRNA processing. Nat. Struct. Mol. Biol. *16*, 916-922.

Forsythe, H.L., Jarvis, J.L., Turner, J.W., Elmore, L.W., and Holt, S.E. (2001). Stable association of hsp90 and p23, but not hsp70, with active human telomerase. J. Biol. Chem. *276*, 15571-15574.

Fu, D., and Collins, K. (2003). Distinct biogenesis pathways for human telomerase RNA and H/ACA small nucleolar RNAs. Mol. Cell *11*, 1361-1372.

Fu, D., and Collins, K. (2006). Human telomerase and Cajal body ribonucleoproteins share a unique specificity of Sm protein association. Genes Dev. *20*, 531-536.

Fu, D., and Collins, K. (2007). Purification of human telomerase complexes identifies factors involved in telomerase biogenesis and telomere length regulation. Mol. Cell *28*, 773-785.

Gallardo, F., Olivier, C., Dandjinou, A.T., Wellinger, R.J., and Chartrand, P. (2008). TLC1 RNA nucleo-cytoplasmic trafficking links telomerase biogenesis to its recruitment to telomeres. EMBO J. *27*, 748-757.

Ganot, P., Bortolin, M.-L., and Kiss, T. (1997a). Site-specific pseudouridine formation in preribosomal RNA is guided by small nucleolar RNAs. Cell *89*, 799-809.

Ganot, P., Caizergues-Ferrer, M., and Kiss, T. (1997b). The family of box ACA small nucleolar RNAs is defined by an evolutionarily conserved secondary structure and ubiquitous sequence elements essential for RNA accumulation. Genes Dev. *11*, 941-956.

Gao, H., Cervantes, R.B., Mandell, E.K., Otero, J.H., and Lundblad, V. (2007). RPA-like proteins mediate yeast telomere function. Nat. Struct. Mol. Biol. *14*, 208-214.

Gilley, D., and Blackburn, E.H. (1999). The telomerase RNA pseudoknot is critical for the stable assembly of a catalytically active ribonucleoprotein. Proc. Natl. Acad. Sci. USA *96*, 6621-6625.

Gillis, A.J., Schuller, A.P., and Skordalakes, E. (2008). Structure of the *Tribolium castaneum* telomerase catalytic subunit TERT. Nature *455*, 633-637.

Gilson, E., and Geli, V. (2007). How telomeres are replicated. Nat. Rev. Mol. Cell Biol. *8*, 825-838.

Girard, C., Verheggen, C., Neel, H., Cammas, A., Vagner, S., Soret, J., Bertrand, E., and Bordonne, R. (2008). Characterization of a short isoform of human Tgs1 hypermethylase associating with small nucleolar ribonucleoprotein core proteins and produced by limited proteolytic processing. J. Biol. Chem. *283*, 2060-2069.

Gravel, S., Larrivee, M., Labrecque, P., and Wellinger, R.J. (1998). Yeast Ku as a regulator of chromosomal DNA end structure. Science *280*, 741-744.

Greider, C.W., and Blackburn, E.H. (1989). A telomeric sequence in the RNA of *Tetrahymena* telomerase required for telomere repeat synthesis. Nature *337*, 331-337.

Grozdanov, P.N., Roy, S., Kittur, N., and Meier, U.T. (2009). SHQ1 is required prior to NAF1 for assembly of H/ACA small nucleolar and telomerase RNPs. RNA *15*, 1188-1197.

Gunisova, S., Elboher, E., Nosek, J., Gorkovoy, V., Brown, Y., Lucier, J.F., Laterreur, N., Wellinger, R.J., Tzfati, Y., and Tomaska, L. (2009). Identification and comparative analysis of telomerase RNAs from *Candida* species reveal conservation of functional elements. RNA *15*, 546-559.

Hamma, T., and Ferre-D'Amare, A.R. (2010). The box H/ACA ribonucleoprotein complex: interplay of RNA and protein structures in post-transcriptional RNA modification. J. Biol. Chem. *285*, 805-809.

Henras, A., Dez, C., Noaillac-Depeyre, J., Henry, Y., and Caizergues-Ferrer, M. (2001). Accumulation of H/ACA snoRNPs depends on the integrity of the conserved central domain of the RNA-binding protein Nhp2p. Nucleic Acids Res. *29*, 2733-2746.

Henras, A.K., Dez, C., and Henry, Y. (2004). RNA structure and function in C/D and H/ACA s(no)RNPs. Curr. Opin. Struct. Biol. *14*, 335-343.

Hinkley, C., Blasco, M., Funk, W., Feng, J., Villeponteau, B., Greider, C., and Herr, W. (1998). The mouse telomerase RNA 5'-end lies just upstream of the telomerase template sequence. Nucleic Acids Res. *26*, 532-536.

Hoareau-Aveilla, C., Bonoli, M., Caizergues-Ferrer, M., and Henry, Y. (2006). hNaf1 is required for accumulation of human box H/ACA snoRNPs, scaRNPs, and telomerase. RNA *12*, 832-840.

Hogg, J.R., and Collins, K. (2007a). Human Y5 RNA specializes a Ro ribonucleoprotein for 5S ribosomal RNA quality control. Genes Dev. *21*, 3067-3072.

Hogg, J.R., and Collins, K. (2007b). RNA-based affinity purification reveals 7SK RNPs with distinct composition and regulation. RNA *13*, 868-880.

Hogg, J.R., and Goff, S.P. (2010). Upf1 senses 3'UTR length to potentiate mRNA decay. Cell *143*, 379-389.

Holt, S.E., Aisner, D.L., Baur, J., Tesmer, V.M., Dy, M., Ouellette, M., Trager, J.B., Morin, G.B., Toft, D.O., Shay, J.W.*, et al.* (1999). Functional requirement of p23 and Hsp90 in telomerase complexes. Genes Dev. *13*, 817-826.

Hsu, M., Yu, E.Y., Singh, S.M., and Lue, N.F. (2007). Mutual dependence of *Candida albicans* Est1p and Est3p in telomerase assembly and activation. Eukaryot. Cell *6*, 1330-1338.

Hug, N., and Lingner, J. (2006). Telomere length homeostasis. Chromosoma *115*, 413-425.

Jacobs, S.A., Podell, E.R., and Cech, T.R. (2006). Crystal structure of the essential N-terminal domain of telomerase reverse transcriptase. Nat. Struct. Mol. Biol. *13*, 218-225.

Jády, B.E., Bertrand, E., and Kiss, T. (2004). Human telomerase RNA and box H/ACA scaRNAs share a common Cajal body-specific localization signal. J. Cell Biol. *164*, 647-652.

Jády, B.E., Richard, P., Bertrand, E., and Kiss, T. (2006). Cell cycle-dependent recruitment of telomerase RNA and Cajal bodies to human telomeres. Mol. Biol. Cell. *17*, 944-954.

Jurica, M.S., Licklider, L.J., Gygi, S.R., Grigorieff, N., and Moore, M.J. (2002). Purification and characterization of native spliceosomes suitable for three-dimensional structural analysis. RNA *8*, 426-439.

Keefe, A.D., Wilson, D.S., Seelig, B., and Szostak, J.W. (2001). One-step purification of recombinant proteins using a nanomolar-affinity streptavidin-binding peptide, the SBP-Tag. Protein Expr. Purif. *23*, 440-446.

Kim, J.H., Park, S.M., Kang, M.R., Oh, S.Y., Lee, T.H., Muller, M.T., and Chung, I.K. (2005). Ubiquitin ligase MKRN1 modulates telomere length homeostasis through a proteolysis of hTERT. Genes Dev. *19*, 776-781.

Kim, M., Vasiljeva, L., Rando, O.J., Zhelkovsky, A., Moore, C., and Buratowski, S. (2006). Distinct pathways for snoRNA and mRNA termination. Mol. Cell *24*, 723-734.

Kiss, T., Fayet-Lebaron, E., and Jady, B.E. (2010). Box H/ACA small ribonucleoproteins. Mol. Cell *37*, 597-606.

Kiss, T., Fayet, E., Jady, B.E., Richard, P., and Weber, M. (2006). Biogenesis and intranuclear trafficking of human box C/D and H/ACA RNPs. Cold Spring Harb. Symp. Quant. Biol. *71*, 407-417.

Kittur, N., Darzacq, X., Roy, S., Singer, R.H., and Meier, U.T. (2006). Dynamic association and localization of human H/ACA RNP proteins. RNA *12*, 2057-2062.
Klein, D.J., Schmeing, T.M., Moore, P.B., and Steitz, T.A. (2001). The kink-turn: a new RNA secondary structure motif. EMBO J. *20*, 4214-4221.
Koo, B.K., Park, C.J., Fernandez, C.F., Chim, N., Ding, Y., Chanfreau, G., and Feigon, J. (2011). Structure of H/ACA RNP protein Nhp2p reveals cis/trans isomerization of a conserved proline at the RNA and Nop10 binding interface. J. Mol. Biol. *411*, 927-942.
Kuehner, J.N., Pearson, E.L., and Moore, C. (2011). Unravelling the means to an end: RNA polymerase II transcription termination. Nat. Rev. Mol. Cell Biol. *12*, 283-294.
Lai, C.K., Miller, M.C., and Collins, K. (2002). Template boundary definition in *Tetrahymena* telomerase. Genes Dev. *16*, 415-420.
Latrick, C.M., and Cech, T.R. (2010). POT1-TPP1 enhances telomerase processivity by slowing primer dissociation and aiding translocation. EMBO J. *29*, 924-933.
Lattmann, S., Stadler, M.B., Vaughn, J.P., Akman, S.A., and Nagamine, Y. (2011). The DEAH-box RNA helicase RHAU binds an intramolecular RNA G-quadruplex in TERC and associates with telomerase holoenzyme. Nucleic Acids Res. *39*, 9390-9404.
Lee, G.E., Yu, E.Y., Cho, C.H., Lee, J., Muller, M.T., and Chung, I.K. (2004). DNA-protein kinase catalytic subunit-interacting protein KIP binds telomerase by interacting with human telomerase reverse transcriptase. J. Biol. Chem. *279*, 34750-34755.
Leonardi, J., Box, J.A., Bunch, J.T., and Baumann, P. (2008). TER1, the RNA subunit of fission yeast telomerase. Nat. Struct. Mol. Biol. *15*, 26-33.
Lestrade, L., and Weber, M.J. (2006). snoRNA-LBME-db, a comprehensive database of human H/ACA and C/D box snoRNAs. Nucleic Acids Res. *34*, D158-162.
Li, H. (2008). Unveiling substrate RNA binding to H/ACA RNPs: one side fits all. Curr. Opin. Struct. Biol. *18*, 78-85.
Li, L., and Ye, K. (2006). Crystal structure of an H/ACA box ribonucleoprotein particle. Nature *443*, 302-307.
Li, S., Duan, J., Li, D., Ma, S., and Ye, K. (2011a). Structure of the Shq1-Cbf5-Nop10-Gar1 complex and implications for H/ACA RNP biogenesis and dyskeratosis congenita. EMBO J. *30*, 5010-5020.
Li, S., Duan, J., Li, D., Yang, B., Dong, M., and Ye, K. (2011b). Reconstitution and structural analysis of the yeast box H/ACA RNA-guided pseudouridine synthase. Genes Dev. *25*, 2409-2421.
Liang, B., Zhou, J., Kahen, E., Terns, R.M., Terns, M.P., and Li, H. (2009). Structure of a functional ribonucleoprotein pseudouridine synthase bound to a substrate RNA. Nat. Struct. Mol. Biol. *16*, 740-746.
Linger, B.R., and Price, C.M. (2009). Conservation of telomere protein complexes: shuffling through evolution. Crit. Rev. Biochem. Mol. Biol. *44*, 434-446.
Lingner, J., Cech, T.R., Hughes, T.R., and Lundblad, V. (1997a). Three ever shorter telomere (*EST*) genes are dispensable for *in vitro* yeast telomerase activity. Proc. Natl. Acad. Sci. USA *94*, 11190-11195.
Lingner, J., Hughes, T.R., Shevchenko, A., Mann, M., Lundblad, V., and Cech, T.R. (1997b). Reverse transcriptase motifs in the catalytic subunit of telomerase. Science *276*, 561-567.
Livengood, A.J., Zaug, A.J., and Cech, T.R. (2002). Essential regions of *Saccharomyces cerevisiae* telomerase RNA: separate elements for Est1p and Est2p interaction. Mol. Cell. Biol. *22*, 2366-2374.

Ly, H., Xu, L., Rivera, M.A., Parslow, T.G., and Blackburn, E.H. (2003). A role for a novel 'trans-pseudoknot' RNA-RNA interaction in the functional dimerization of human telomerase. Genes Dev. *17*, 1078-1083.

Matera, A.G., and Shpargel, K.B. (2006). Pumping RNA: nuclear bodybuilding along the RNP pipeline. Curr. Opin. Cell Biol. *18*, 317-324.

Matera, A.G., Terns, R.M., and Terns, M.P. (2007). Non-coding RNAs: lessons from the small nuclear and small nucleolar RNAs. Nat. Rev. Mol. Cell Biol. *8*, 209-220.

Meijsing, S.H., Pufall, M.A., So, A.Y., Bates, D.L., Chen, L., and Yamamoto, K.R. (2009). DNA binding site sequence directs glucocorticoid receptor structure and activity. Science *324*, 407-410.

Mihalusova, M., Wu, J.Y., and Zhuang, X. (2011). Functional importance of telomerase pseudoknot revealed by single-molecule analysis. Proc. Natl. Acad. Sci. USA *108*, 20339-20344.

Miller, M.C., and Collins, K. (2002). Telomerase recognizes its template by using an adjacent RNA motif. Proc. Natl. Acad. Sci. USA *99*, 6585-6590.

Min, B., and Collins, K. (2009). An RPA-related sequence-specific DNA-binding subunit of telomerase holoenzyme is required for elongation processivity and telomere maintenance. Mol. Cell *36*, 609-619.

Min, B., and Collins, K. (2010). Multiple mechanisms for elongation processivity within the reconstituted *Tetrahymena* telomerase holoenzyme. J. Biol. Chem. *285*, 16434-16443.

Mitchell, J.R., Cheng, J., and Collins, K. (1999a). A box H/ACA small nucleolar RNA-like domain at the human telomerase RNA 3' end. Mol. Cell. Biol. *19*, 567-576.

Mitchell, J.R., and Collins, K. (2000). Human telomerase activation requires two independent interactions between telomerase RNA and telomerase reverse transcriptase *in vivo* and *in vitro*. Mol. Cell *6*, 361-371.

Mitchell, J.R., Wood, E., and Collins, K. (1999b). A telomerase component is defective in the human disease dyskeratosis congenita. Nature *402*, 551-555.

Mitchell, M., Gillis, A., Futahashi, M., Fujiwara, H., and Skordalakes, E. (2010). Structural basis for telomerase catalytic subunit TERT binding to RNA template and telomeric DNA. Nat. Struct. Mol. Biol. *17*, 513-518.

Mouaikel, J., Verheggen, C., Bertrand, E., Tazi, J., and Bordonne, R. (2002). Hypermethylation of the cap structure of both yeast snRNAs and snoRNAs requires a conserved methyltransferase that is localized to the nucleolus. Mol. Cell *9*, 891-901.

Nakamura, T.M., Morin, G.B., Chapman, K.B., Weinrich, S.L., Andrews, W.H., Lingner, J., Harley, C.B., and Cech, T.R. (1997). Telomerase catalytic subunit homologs from fission yeast and human. Science *277*, 955-959.

Noel, J.F., Larose, S., Abou Elela, S., and Wellinger, R.J. (2012). Budding yeast telomerase RNA transcription termination is dictated by the Nrd1/Nab3 non-coding RNA termination pathway. Nucleic Acids Res. In press.

Nolivos, S., Carpousis, A.J., and Clouet-d'Orval, B. (2005). The K-loop, a general feature of the *Pyrococcus* C/D guide RNAs, is an RNA structural motif related to the K-turn. Nucleic Acids Res. *33*, 6507-6514.

O'Connor, C.M., and Collins, K. (2006). A novel RNA binding domain in *Tetrahymena* telomerase p65 initiates hierarchical assembly of telomerase holoenzyme. Mol. Cell. Biol. *26*, 2029-2036.

O'Sullivan, R.J., and Karlseder, J. (2010). Telomeres: protecting chromosomes against genome instability. Nat. Rev. Mol. Cell Biol. *11*, 171-181.
Osterhage, J.L., Talley, J.M., and Friedman, K.L. (2006). Proteasome-dependent degradation of Est1p regulates the cell cycle-restricted assembly of telomerase in *Saccharomyces cerevisiae*. Nat. Struct. Mol. Biol. *13*, 720-728.
Palm, W., and de Lange, T. (2008). How shelterin protects mammalian telomeres. Annu. Rev. Genet. *42*, 301-334.
Pardue, M.L., and DeBaryshe, P.G. (2011). Retrotransposons that maintain chromosome ends. Proc. Natl. Acad. Sci. USA *108*, 20317-20324.
Pfingsten, J.S., Goodrich, K.J., Taabazuing, C., Ouenzar, F., Chartrand, P., and Cech, T.R. (2012). Mutually exclusive binding of telomerase RNA and DNA by Ku alters telomerase recruitment model. Cell *148*, 922-932.
Podlevsky, J.D., Bley, C.J., Omana, R.V., Qi, X., and Chen, J.J. (2008). The telomerase database. Nucleic Acids Res. *36*, D339-343.
Podlevsky, J.D., and Chen, J.J. (2012). It all comes together at the ends: Telomerase structure, function, and biogenesis. Mutat. Res. *730*, 3-11.
Prathapam, R., Witkin, K.L., O'Connor, C.M., and Collins, K. (2005). A telomerase holoenzyme protein enhances telomerase RNA assembly with telomerase reverse transcriptase. Nat. Struct. Mol. Biol. *12*, 252-257.
Qi, H., and Zakian, V.A. (2000). The *Saccharomyces* telomere-binding protein Cdc13p interacts with both the catalytic subunit of DNA polymerase α and the telomerase-associated Est1 protein. Genes Dev. *14*, 1777-1788.
Qi, X., Xie, M., Brown, A.F., Bley, C.J., Podlevsky, J.D., and Chen, J.J. (2012). RNA/DNA hybrid binding affinity determines telomerase template-translocation efficiency. EMBO J. *31*, 150-161.
Qiao, F., and Cech, T.R. (2008). Triple-helix structure in telomerase RNA contributes to catalysis. Nat. Struct. Mol. Biol. *15*, 634-640.
Reichow, S.L., Hamma, T., Ferre-D'Amare, A.R., and Varani, G. (2007). The structure and function of small nucleolar ribonucleoproteins. Nucleic Acids Res. *35*, 1452-1464.
Ren, X., Gavory, G., Li, H., Ying, L., Klenerman, D., and Balasubramanian, S. (2003). Identification of a new RNA-RNA interaction site for human telomerase RNA (hTR): structural implications for hTR accumulation and a dyskeratosis congenita point mutation. Nucleic Acids Res. *31*, 6509-6515.
Richard, P., Darzacq, X., Bertrand, E., Jády, B.E., Verheggen, C., and Kiss, T. (2003). A common sequence motif determines the Cajal body-specific localization of box H/ACA scaRNAs. EMBO J. *22*, 4283-4293.
Richard, P., Kiss, A.M., Darzacq, X., and Kiss, T. (2006). Cotranscriptional recognition of human intronic box H/ACA snoRNAs occurs in a splicing-independent manner. Mol. Cell. Biol. *26*, 2540-2549.
Richards, R.J., Wu, H., Trantirek, L., O'Connor, C.M., Collins, K., and Feigon, J. (2006). Structural study of elements of *Tetrahymena* telomerase RNA stem-loop IV domain important for function. RNA *12*, 1475-1485.
Riha, K., and Shippen, D.E. (2003). Telomere structure, function and maintenance in *Arabidopsis*. Chromosome Res. *11*, 263-275.
Rivera, M.A., and Blackburn, E.H. (2004). Processive utilization of the human telomerase template: lack of a requirement for template switching. J. Biol. Chem. *279*, 53770-53781.

Robart, A.R., and Collins, K. (2010). Investigation of human telomerase holoenzyme assembly, activity, and processivity using disease-linked subunit variants. J. Biol. Chem. *285*, 4375-4386.

Robart, A.R., and Collins, K. (2011). Human telomerase domain interactions capture DNA for TEN domain-dependent processive elongation. Mol. Cell *42*, 308-318.

Robart, A.R., O'Connor, C.M., and Collins, K. (2010). Ciliate telomerase RNA loop IV nucleotides promote hierarchical RNP assembly and holoenzyme stability. RNA *16*, 563-571.

Savage, S.A., and Alter, B.P. (2008). The role of telomere biology in bone marrow failure and other disorders. Mech. Ageing Dev. *129*, 35-47.

Schnapp, G., Rodi, H.-P., Rettig, W.J., Schnapp, A., and Damm, K. (1998). One-step affinity purification protocol for human telomerase. Nucleic Acids Res. *26*, 3311-3313.

Sekaran, V.G., Soares, J., and Jarstfer, M.B. (2010). Structures of telomerase subunits provide functional insights. Biochim. Biophys. Acta *1804*, 1190-1201.

Seto, A.G., Livengood, A.J., Tzfati, Y., Blackburn, E.H., and Cech, T.R. (2002). A bulged stem tethers Est1p to telomerase RNA in budding yeast. Genes Dev. *16*, 2800-2812.

Seto, A.G., Umansky, K., Tzfati, Y., Zaug, A.J., Blackburn, E.H., and Cech, T.R. (2003). A template-proximal RNA paired element contributes to *Saccharomyces cerevisiae* telomerase activity. RNA *9*, 1323-1332.

Seto, A.G., Zaug, A.J., Sobel, S.G., Wolin, S.L., and Cech, T.R. (1999). *Saccharomyces cerevisiae* telomerase is an Sm small nuclear ribonucleoprotein particle. Nature *401*, 177-180.

Sexton, A.N., and Collins, K. (2011). The 5' guanosine tracts of human telomerase RNA are recognized by the G-quadruplex binding domain of the RNA helicase DHX36 and function to increase RNA accumulation. Mol. Cell. Biol. *31*, 736-743.

Shay, J.W., and Wright, W.E. (2010). Telomeres and telomerase in normal and cancer stem cells. FEBS Lett. *584*, 3819-3825.

Shefer, K., Brown, Y., Gorkovoy, V., Nussbaum, T., Ulyanov, N.B., and Tzfati, Y. (2007). A triple helix within a pseudoknot is a conserved and essential element of telomerase RNA. Mol. Cell. Biol. *27*, 2130-2143.

Steinmetz, E.J., Conrad, N.K., Brow, D.A., and Corden, J.L. (2001). RNA-binding protein Nrd1 directs poly(A)-independent 3'-end formation of RNA polymerase II transcripts. Nature *413*, 327-331.

Stellwagen, A.E., Haimberger, Z.W., Veatch, J.R., and Gottschling, D.E. (2003). Ku interacts with telomerase RNA to promote telomere addition at native and broken chromosome ends. Genes Dev. *17*, 2384-2395.

Stone, M.S., Mihalusova, M., O'Connor, C.M., Prathapam, R., Collins, K., and Zhuang, X. (2007). Stepwise protein-mediated RNA folding directs assembly of telomerase ribonucleoprotein. Nature *446*, 458-461.

Taggart, A.K., Teng, S.C., and Zakian, V.A. (2002). Est1p as a cell cycle-regulated activator of telomere-bound telomerase. Science *297*, 1023-1026.

Talley, J.M., DeZwaan, D.C., Maness, L.D., Freeman, B.C., and Friedman, K.L. (2011). Stimulation of yeast telomerase activity by the ever shorter telomere 3 (Est3) subunit is dependent on direct interaction with the catalytic protein Est2. J. Biol. Chem. *286*, 26431-26439.

Tang, W., Kannan, R., Blanchette, M., and Baumann, P. (2012). Telomerase RNA biogenesis involves sequential binding by Sm and Lsm complexes. Nature *484*, 260-264.
Teixeira, M.T., Forstemann, K., Gasser, S.M., and Lingner, J. (2002). Intracellular trafficking of yeast telomerase components. EMBO Rep. *3*, 652-659.
Teixeira, M.T., and Gilson, E. (2005). Telomere maintenance, function and evolution: the yeast paradigm. Chromosome Res. *13*, 535-548.
Theimer, C.A., Blois, C.A., and Feigon, J. (2005). Structure of the human telomerase RNA pseudoknot reveals conserved tertiary interactions essential for function. Mol. Cell *17*, 671-682.
Theimer, C.A., Jády, B.E., Chim, N., Richard, P., Breece, K.E., Kiss, T., and Feigon, J. (2007). Structural and functional characterization of human telomerase RNA processing and Cajal body localization signals. Mol. Cell *27*, 869-881.
Tomlinson, R.L., Abreu, E.B., Ziegler, T., Ly, H., Counter, C.M., Terns, R.M., and Terns, M.P. (2008). Telomerase reverse transcriptase is required for the localization of telomerase RNA to Cajal bodies and telomeres in human cancer cells. Mol. Biol. Cell *19*, 3793-3800.
Tomlinson, R.L., Ziegler, T.D., Supakorndej, T., Terns, R.M., and Terns, M.P. (2006). Cell cycle-regulated trafficking of human telomerase to telomeres. Mol. Biol. Cell *17*, 955-965.
Trahan, C., and Dragon, F. (2009). Dyskeratosis congenita mutations in the H/ACA domain of human telomerase RNA affect its assembly into a pre-RNP. RNA *15*, 235-243.
Trahan, C., Martel, C., and Dragon, F. (2010). Effects of dyskeratosis congenita mutations in dyskerin, NHP2 and NOP10 on assembly of H/ACA pre-RNPs. Hum. Mol. Genet. *19*, 825-836.
Tycowski, K.T., Shu, M.D., Kukoyi, A., and Steitz, J.A. (2009). A conserved WD40 protein binds the Cajal body localization signal of scaRNP particles. Mol. Cell *34*, 47-57.
Tzfati, Y., Fulton, T.B., Roy, J., and Blackburn, E.H. (2000). Template boundary in a yeast telomerase specified by RNA structure. Science *288*, 863-867.
Tzfati, Y., Knight, Z., Roy, J., and Blackburn, E.H. (2003). A novel pseudoknot element is essential for the action of a yeast telomerase. Genes Dev. *17*, 1779-1788.
Uliel, S., Liang, X.H., Unger, R., and Michaeli, S. (2004). Small nucleolar RNAs that guide modification in trypanosomatids: repertoire, targets, genome organisation, and unique functions. Int. J. Parasitol. *34*, 445-454.
Ulyanov, N.B., Shefer, K., James, T.L., and Tzfati, Y. (2007). Pseudoknot structures with conserved base triples in telomerase RNAs of ciliates. Nucleic Acids Res. *35*, 6150-6160.
Venteicher, A.S., Abreu, E.B., Meng, Z., McCann, K.E., Terns, R.M., Veenstra, T.D., Terns, M.P., and Artandi, S.E. (2009). A human telomerase holoenzyme protein required for Cajal body localization and telomere synthesis. Science *323*, 644-648.
Venteicher, A.S., Meng, Z., Mason, P.J., Veenstra, T.D., and Artandi, S.E. (2008). Identification of ATPases pontin and reptin as telomerase components essential for holoenzyme assembly. Cell *132*, 945-957.
Vulliamy, T., Marrone, A., Goldman, F., Dearlove, A., Bessler, M., Mason, P.J., and Dokal, I. (2001). The RNA component of telomerase is mutated in autosomal dominant dyskeratosis congenita. Nature *413*, 432-435.

Walbott, H., Machado-Pinilla, R., Liger, D., Blaud, M., Rety, S., Grozdanov, P.N., Godin, K., van Tilbeurgh, H., Varani, G., Meier, U.T.*, et al.* (2011). The H/ACA RNP assembly factor SHQ1 functions as an RNA mimic. Genes Dev. *25*, 2398-2408.

Wang, C., and Meier, U.T. (2004). Architecture and assembly of mammalian H/ACA small nucleolar and telomerase ribonucleoproteins. EMBO J. *23*, 1857-1867.

Wang, F., Podell, E.R., Zaug, A.J., Yang, Y., Baciu, P., Cech, T.R., and Lei, M. (2007). The POT1-TPP1 telomere complex is a telomerase processivity factor. Nature *445*, 506-510.

Watkins, N.J., Gottschalk, A., Neubauer, G., Kastner, B., Fabrizio, P., Mann, M., and Lührmann, R. (1998). Cbf5p, a potential pseudouridine synthase, and Nhp2p, a putative RNA-binding protein, are present together with Gar1p in all H BOX/ACA-motif snoRNPs and constitute a common bipartite structure. RNA *4*, 1549-1568.

Watkins, N.J., Lemm, I., Ingelfinger, D., Schneider, C., Hossbach, M., Urlaub, H., and Luhrmann, R. (2004). Assembly and maturation of the U3 snoRNP in the nucleoplasm in a large dynamic multiprotein complex. Mol. Cell *16*, 789-798.

Wenz, C., Enenkel, B., Amacker, M., Kelleher, C., Damm, K., and Lingner, J. (2001). Human telomerase contains two cooperating telomerase RNA molecules. EMBO J. *20*, 3526-3534.

Witkin, K.L., and Collins, K. (2004). Holoenzyme proteins required for the physiological assembly and activity of telomerase. Genes Dev. *18*, 1107-1118.

Wong, J.M., Kyasa, M.J., Hutchins, L., and Collins, K. (2004). Telomerase RNA deficiency in peripheral blood mononuclear cells in X-linked dyskeratosis congenita. Hum. Genet. *115*, 448-455.

Wong, J.M.Y., and Collins, K. (2006). Telomerase RNA level limits telomere maintenance in X-linked dyskeratosis congenita. Genes Dev. *20*, 2848-2858.

Wyatt, H.D., West, S.C., and Beattie, T.L. (2010). InTERTpreting telomerase structure and function. Nucleic Acids Res. *38*, 5609-5622.

Xiao, M., Yang, C., Schattner, P., and Yu, Y.T. (2009). Functionality and substrate specificity of human box H/ACA guide RNAs. RNA *15*, 176-186.

Xie, M., Mosig, A., Qi, X., Li, Y., Stadler, P.F., and Chen, J.J. (2008). Structure and function of the smallest vertebrate telomerase RNA from teleost fish. J. Biol. Chem. *283*, 2049-2059.

Yang, P.K., Hoareau, C., Froment, C., Monsarrat, B., Henry, Y., and Chanfreau, G. (2005). Cotranscriptional recruitment of the pseudouridylsynthetase Cbf5p and of the RNA binding protein Naf1p during H/ACA snoRNP assembly. Mol. Cell. Biol. *25*, 3295-3304.

Yang, Y., Isaac, C., Wang, C., Dragon, F., Pogacic, V., and Meier, U.T. (2000). Conserved composition of mammalian box H/ACA and box C/D small nucleolar ribonucleoprotein particles and their interaction with the common factor Nopp140. Mol. Biol. Cell *11*, 567-577.

Ye, K. (2007). H/ACA guide RNAs, proteins and complexes. Curr. Opin. Struct. Biol. *17*, 287-292.

Yen, W.F., Chico, L., Lei, M., and Lue, N.F. (2011). Telomerase regulatory subunit Est3 in two *Candida* species physically interacts with the TEN domain of TERT and telomeric DNA. Proc. Natl. Acad. Sci. USA *108*, 20370-20375.

Yi, X., Tesmer, V.M., Savre-Train, I., Shay, J.W., and Wright, W.E. (1999). Both transcriptional and posttranscriptional mechanisms regulate human telomerase template RNA levels. Mol. Cell. Biol. *19*, 3989-3997.

Yu, E.Y. (2011). Telomeres and telomerase in *Candida albicans*. Mycoses *55*, e48-e59.

Zappulla, D.C., Goodrich, K., and Cech, T.R. (2005). A miniature yeast telomerase RNA functions *in vivo* and reconstitutes activity *in vitro*. Nat. Struct. Mol. Biol. *12*, 1072-1077.
Zaug, A.J., Podell, E.R., Nandakumar, J., and Cech, T.R. (2010). Functional interaction between telomere protein TPP1 and telomerase. Genes Dev. *24*, 613-622.
Zhang, Q., Kim, N.K., and Feigon, J. (2011). Architecture of human telomerase RNA. Proc. Natl. Acad. Sci. USA *108*, 20325-20332.
Zhong, F., Savage, S.A., Shkreli, M., Giri, N., Jessop, L., Myers, T., Chen, R., Alter, B.P., and Artandi, S.E. (2011). Disruption of telomerase trafficking by TCAB1 mutation causes dyskeratosis congenita. Genes Dev. *25*, 11-16.
Zhu, Y., Tomlinson, R.L., Lukowiak, A.A., Terns, R.M., and Terns, M.P. (2004). Telomerase RNA accumulates in Cajal bodies in human cancer cells. Mol. Biol. Cell *15*, 81-90.